



University of Kentucky
UKnowledge

University of Kentucky Master's Theses

Graduate School

2008

THERMAL DEGRADATION AND AGING OF HIGH TEMPERATURE PIEZOELECTRIC CERAMICS

Sunil W. Gotmare

University of Kentucky, Sunil.Gotmare@uky.edu

[Right click to open a feedback form in a new tab to let us know how this document benefits you.](#)

Recommended Citation

Gotmare, Sunil W., "THERMAL DEGRADATION AND AGING OF HIGH TEMPERATURE PIEZOELECTRIC CERAMICS" (2008). *University of Kentucky Master's Theses*. 564.
https://uknowledge.uky.edu/gradschool_theses/564

This Thesis is brought to you for free and open access by the Graduate School at UKnowledge. It has been accepted for inclusion in University of Kentucky Master's Theses by an authorized administrator of UKnowledge. For more information, please contact UKnowledge@lsv.uky.edu.

ABSTRACT OF THESIS

THERMAL DEGRADATION AND AGING OF HIGH TEMPERATURE PIEZOELECTRIC CERAMICS

Piezoelectric materials have numerous applications like high temperature accelerometers, pressure, flow and NDT transducers, acoustic emission, ultrasonic cleaning, welding, high voltage generators, medical therapy etc. The commonly used piezoelectric material, PZT continues to dominate the commercial market for piezoelectric actuators applications. The primary limitations of PZT are the lower Curie temperature $T_C < 390^\circ\text{C}$ and rapid thermal degradation above 200°C .

Continuing efforts are focused on the development of piezoelectric materials suitable for high temperature applications $> 200^\circ\text{C}$. These materials will be very useful for making sensors for space exploration, oil and geothermal well drilling tools, oil & gas pipeline health monitoring and automotive smart brakes. Recently material based on $(1-x)\text{Bi}(\text{Me})\text{O}_3-x\text{PbTiO}_3$ developed with $T_C \sim 460^\circ\text{C}$, and $d_{33} \sim 500$ pC/N compared to $T_C \sim 390^\circ\text{C}$ and $d_{33} \sim 220$ pC/N of pure PZT. Enhanced room temperature properties and higher transition temperature makes this material interesting for further investigation as a high temperature piezoelectric material.

Reliability of technological piezoelectric devices is a major concern for their applications. Many piezoelectric materials undergo a process of aging, associated with a spontaneous decrease of electromechanical properties. In the current work thermal degradation and aging behavior of high temperature piezoelectric material BSPT was evaluated and compared with the commonly used PZT.

KEYWORDS: Aging, Thermal degradation, BSPT, PZT, High temperature piezoelectric.

(Sunil Gotmare)

Date:

THERMAL DEGRADATION AND AGING OF HIGH TEMPERATURE
PIEZOELECTRIC CERAMICS

By

Sunil W. Gotmare

Director of Thesis

Director of Graduate Studies

Date:

THESIS

Sunil W. Gotmare

The Graduate School
University of Kentucky
2008

THERMAL DEGRADATION AND AGING OF HIGH TEMPERATURE
PIEZOELECTRIC CERAMICS

THESIS

A thesis submitted in partial fulfillment of the
requirements for the degree of Master of Science in
Material Science and Engineering in the
College of Engineering
at the University of Kentucky

By
Sunil W. Gotmare
Lexington, Kentucky

Director: Dr. Richard Eitel, Professor of Chemical and Material Science Engineering
Lexington, Kentucky
2008

Copyright © Sunil W. Gotmare 2008

This work is dedicated to my beloved parent
Mr. Wasudeo Gotmare and Mrs. Vandana Gotmare

ACKNOWLEDGMENTS

The following thesis, while an individual work, benefited from the insight and direction of several people.

I would like to express my deep and sincere gratitude to my thesis Advisor, Dr. Richard Eitel, I thank him also for providing me an opportunity to grow as a engineer in the unique research environment and for his valuable supervision, advice, and technical guidance at every step and for providing me unflinching encouragement and support in various ways.

I wish to thank Dr. John Balk, and Dr. Bruce Hinds, for their advise and constructive comments on this thesis. I am thankful that in the midst of all their activity, they accepted to be members of my thesis committee.

Many thanks to everyone that I have worked with, whose timely technical assistance benefited in assorted ways to the research.

I express my appreciation and feel extraordinarily fortunate in having equally important support from family and friends, my wife, Shivani for her encouragement and persistent confidence in me, her loving support and understanding at every step.

Sincere thanks goes to the faculty and staff of the Chemical and Materials Science Engineering department for the wonderful time in the department. Finally, I wish to thank my research group and colleagues for contributing to a wonderful and memorable graduate school experience at the University of Kentucky.

TABLE OF CONTENTS

Acknowledgements.....	iii
List of Tables	ix
List of Figures	x
Chapter One: Introduction	1
Motivation	1
Organization of thesis	3
Chapter Two: Background for piezoelectric materials and their aging behavior.....	5
Introduction	5
Perovskite Structure	6
Intrinsic and extrinsic contributions	9
Lead zirconate titanate $(1-x)\text{PbZrO}_3\text{-}x\text{PbTiO}_3$	10
High temperature piezoelectric $(1-x)\text{BiScO}_3\text{-}x\text{PbTiO}_3$	12
Properties of piezoelectric materials	14
Ferroelectric Curie temperature (T_C)	15
Piezoelectric constant (d)	16
Dielectric constant (K) and loss (D)	17
Electromechanical coupling coefficient.....	17
Modification of properties by doping	18

Effect of processing on the properties of piezoelectric materials.....	19
Thermal degradation and aging of piezoelectric materials	20
Domain wall clamping by defects	22
Diffusion of defects through domain wall and consequent stabilization of domain wall	22
Presence of space charges at the grain boundaries	23
 Chapter Three: Experimental procedures and methods	 24
Introduction	24
Preparation of piezoelectric ceramics	24
Powder preparation	24
Forming	26
Sintering	27
Electrode application	27
Poling	28
Characterization	28
Structural and physical characterization.....	28
Piezoelectric and dielectric characterization.....	32
Ferroelectric Curie temperature (T_C)	29
Polarization – electric field (P-E) hysteresis loop.....	30
Dielectric constant (K) and dielectric loss (D)	31
Piezoelectric constant (d_{33})	31
Planar coupling coefficient (k_p)	31

Rayleigh analysis for dielectric and piezoelectric response	32
Thermal degradation and aging	33
Chapter Four: Characterization	34
Introduction	34
Physical and structural analysis	34
Unpoled properties	42
Dielectric constant (K) and dielectric loss (D)	42
Ferroelectric Curie temperature (T_C)	42
Polarization – electric field (P-E) hysteresis loop	43
Poled properties	44
Dielectric constant (K) and dielectric loss (D)	44
Piezoelectric constant (d_{33})	49
Planar coupling coefficient (k_p)	49
Rayleigh analysis for dielectric and piezoelectric responses	51
Summary and conclusion	55
Chapter Five: Thermal degradation and aging.....	57
Introduction	57
Aging study	65
Thermal conditioning.....	58
Isothermal aging	58
Results and discussion	59
Thermal conditioning	59

Piezoelectric constant (d_{33})	61
Planar coupling coefficient (k_p)	62
Dielectric coefficient K and dielectric loss D	62
Rayleigh analysis during aging study	67
Summary and conclusion	71
Chapter Six: Summary and future work	72
Summary	72
Thermal degradation and aging study for $(1-x)\text{PbZrO}_3\text{-}x\text{PbTiO}_3$ and $(1-x)\text{BiScO}_3\text{-}x\text{PbTiO}_3$ ceramics	72
Development of methodology for lifetime testing for piezoelectric ceramics	76
Future work	76
Aging study for acceptor doped $(1-x)\text{BiScO}_3\text{-}x\text{PbTiO}_3$	76
Methodology for lifetime testing for piezoelectric ceramics	77
Appendices:	
Appendix A: Particle size and distribution for metal oxides / carbonate powders	79
Appendix B: LOI results for metal oxides / carbonate powder.....	80
Appendix C: XRD scans for PZT and BSPT powders before and after calcination	81
Appendix D: Sintering study for PZT and BSPT (bulk density- for variable time	

& temperature)	82
Appendix E: Dielectric properties of poled sample at various frequencies	83
Appendix F: Details of dielectric properties (1kHz) with the aging time at 250 ⁰ C	84
Appendix G: Details of piezoelectric constant d_{33} after poling and with the aging time at	92
Appendix H: Rayleigh analysis for piezoelectric and dielectric response during aging.....	95
References	101
Vita	105

LIST OF TABLES

Table 2.1. Electromechanical properties of PZT and BSPT materials	15
Table 4.1. Lattice parameters for $(1-x)\text{PbZrO}_3\text{-}x\text{PbTiO}_3$ and $(1-x)\text{BiScO}_3\text{-}x\text{PbTiO}_3$ calculated from XRD scans	37
Table 4.2. Bulk density for $(1-x)\text{PbZrO}_3\text{-}x\text{PbTiO}_3$ and $(1-x)\text{BiScO}_3\text{-}x\text{PbTiO}_3$ after Sintering	40
Table 4.3. Coercive field E_C , remnant polarization P_R and high field d_{33} for unmodified and modified $(1-x)\text{PbZrO}_3\text{-}x\text{PbTiO}_3$ and $(1-x)\text{BiScO}_3\text{-}x\text{PbTiO}_3$	44
Table 4.4. Measured electromechanical properties of poled $(1-x)\text{PbZrO}_3\text{-}x\text{PbTiO}_3$ and $(1-x)\text{BiScO}_3\text{-}x\text{PbTiO}_3$ pellets	50
Table 4.5. Rayleigh parameters for $\text{PbZrO}_3\text{-}x\text{PbTiO}_3$ and $(1-x)\text{BiScO}_3\text{-}x\text{PbTiO}_3$	54
Table 5.1. Electromechanical properties for $(1-x)\text{PbZrO}_3\text{-}x\text{PbTiO}_3$ and $(1-x)\text{BiScO}_3\text{-}x\text{PbTiO}_3$ pellets after thermal conditioning at 250°C for 1 min, compared to poled properties	60
Table 5.2. Aging rate for piezoelectric constant d_{33} , planar coupling coefficient k_p , and dielectric constant K for $(1-x)\text{PbZrO}_3\text{-}x\text{PbTiO}_3$ and $(1-x)\text{BiScO}_3\text{-}x\text{PbTiO}_3$ (at 250°C)	65

LIST OF FIGURES

Figure 2.1,	Charge- field hysteresis loop for ferroelectric materials	5
Figure 2.2,	Schematic for a) Direct and b) Converse piezoelectric effect	7
Figure 2.3,	Perovskite ABO_3 unit cell	8
Figure 2.4,	180° and non- 180° domain walls in a tetragonal unit cell	10
Figure 2.5,	Temperature – composition phase diagram for PZT, a) after Jaffe, et al. 1971 ¹ and b) modified by B. Noheda,2000 ²²	11
Figure 2.6,	Temperature–composition phase diagram for BSPT, Eitel et al. 2004 ¹⁷	13
Figure 2.7,	a) Ferroelectric switching polarization loop, b) Bipolar strain loop, and c) Unipolar strain loop, for PZT and BSPT ceramics	13
Figure 3.1,	Set up for high temperature dielectric measurement	30
Figure 3.2,	Schematic of the circuit used for P-E loop measurement.....	30
Figure 4.1,	Particle size distribution after milling for $(1-x)PbZrO_3-xPbTiO_3$ and $(1-x)BiScO_3-xPbTiO_3$ powder before and after calcinations.....	35
Figure 4.2,	XRD scans after calcination for $(1-x)PbZrO_3-xPbTiO_3$ $x= 0.48$ and $(1-x)BiScO_3-xPbTiO_3$, $x=0.64$ and 0.66	36
Figure 4.3,	XRD scans of crushed pellets after sintering for unmodified and modified $(1-x)PbZrO_3-xPbTiO_3$ $x=0.48$, and $(1-x)BiScO_3-xPbTiO_3$ $x=0.64$ and 0.66	38

Figure 4.4, Microphotographs of the polished and thermally etched pellets for unmodified and Fe-modified $(1-x)\text{PbZrO}_3\text{-}x\text{PbTiO}_3$ $x=0.48$, and unmodified and Mn-modified $(1-x)\text{BiScO}_3\text{-}x\text{PbTiO}_3$ $x=0.64$ and 0.66 41

Figure 4.5a), High temperature dielectric constant K and dielectric loss D for unmodified $(1-x)\text{PbZrO}_3\text{-}x\text{PbTiO}_3$ $x=0.48$, and $(1-x)\text{BiScO}_3\text{-}x\text{PbTiO}_3$ $x=0.64$ and 0.66 45

Figure 4.5b), High temperature dielectric constant K and dielectric loss D for Fe-modified $(1-x)\text{PbZrO}_3\text{-}x\text{PbTiO}_3$ $x=0.48$, and Mn-modified $(1-x)\text{BiScO}_3\text{-}x\text{PbTiO}_3$ $x=0.64$ and 0.66 46

Figure 4.6, Ferroelectric P-E hysteresis loop for unmodified and Fe modified $(1-x)\text{PbZrO}_3\text{-}x\text{PbTiO}_3$ $x=0.48$, and unmodified and Mn-modified $(1-x)\text{BiScO}_3\text{-}x\text{PbTiO}_3$ $x=0.64$ and 0.66 (measured at 50kV/cm , 1 Hz)47

Figure 4.7, Bipolar and unipolar strain loop for unmodified and Fe-modified $(1-x)\text{PbZrO}_3\text{-}x\text{PbTiO}_3$ $x=0.48$, and unmodified and Mn-modified $(1-x)\text{BiScO}_3\text{-}x\text{PbTiO}_3$ $x=0.64$ and 0.66 (measured at 50kV/cm , 1 Hz)48

Figure 4.8, Rayleigh analysis, piezoelectric response as a function of applied electric field for unmodified and modified $(1-x)\text{PbZrO}_3\text{-}x\text{PbTiO}_3$ and $(1-x)\text{BiScO}_3\text{-}x\text{PbTiO}_3$ 52

Figure 4.9, Rayleigh analysis, dielectric responses as a function of applied electric field for unmodified and modified $(1-x)\text{PbZrO}_3\text{-}x\text{PbTiO}_3$ and $(1-x)\text{BiScO}_3 - x\text{PbTiO}_3$	53
Figure 5.1, Aging study at 250°C , piezoelectric constant d_{33} as a function of aging time for unmodified and modified $(1-x)\text{PbZrO}_3\text{-} x\text{PbTiO}_3$ $x=0.48$, and $(1-x)\text{BiScO}_3 - x\text{PbTiO}_3$ $x=0.64$ and 0.66	63
Figure 5.2, Aging study at 250°C , planar coupling coefficient k_p as a function of aging time for unmodified and modified $(1-x)\text{PbZrO}_3\text{-}x\text{PbTiO}_3$ $x=0.48$, and $(1-x)\text{BiScO}_3\text{-}x\text{PbTiO}_3$ $x=0.64$ and 0.66	63
Figure 5.3, Aging study at 250°C , dielectric constant K as a function of aging time for unmodified and modified $(1-x)\text{PbZrO}_3\text{-}x\text{PbTiO}_3$ $x=0.48$, and $(1-x)\text{BiScO}_3\text{-} x\text{PbTiO}_3$ $x=0.64$ and 0.66	66
Figure 5.4, Aging study at 250°C , dielectric loss D as a function of aging time for unmodified and modified $(1-x)\text{PbZrO}_3\text{-}x\text{PbTiO}_3$ $x=0.48$, and $(1-x)\text{BiScO}_3\text{-}x\text{PbTiO}_3$ $x=0.64$ and 0.66	66
Figure 5.5, Aging study at 250°C , Rayleigh analysis for dielectric constant K as a function of aging time for unmodified and modified $(1-x)\text{PbZrO}_3\text{-}x\text{PbTiO}_3$ $x=0.48$, and $(1-x)\text{BiScO}_3\text{-}x\text{PbTiO}_3$ $x=0.64$ and 0.66	68
Figure 5.6, Aging study at 250°C , Rayleigh analysis of α_ϵ (10^{-3} m/V) for dielectric response as a function of aging time for unmodified and modified $(1-x)\text{PbZrO}_3\text{-}x\text{PbTiO}_3$ $x=0.48$, and $(1-x)\text{BiScO}_3\text{-}x\text{PbTiO}_3$ $x=0.64$ and 0.66	69

Figure 5.7, Aging study at 250⁰C, Rayleigh analysis of Piezoelectric constant d_{33} (at 0 kV/cm) as a function of aging time for unmodified and modified (1-x)PbZrO₃-xPbTiO₃ x=0.48, and (1-x)BiScO₃-xPbTiO₃ x=0.64 and 0.66.....70

Figure 5.8, Aging study at 250⁰C, Rayleigh analysis of α_d (10⁻¹⁴ Cm/NV) for piezoelectric response as a function of aging time for unmodified and modified (1-x)PbZrO₃-xPbTiO₃ x=0.48, and (1-x)BiScO₃-xPbTiO₃ x=0.64 and 0.6670

Chapter 1: Introduction

1.1 Motivation

The conversion of mechanical energy in a piezoelectric material into electrical energy and reverse effect is the basis for sensors and actuators. Piezoelectric materials have numerous applications like ultra high temperature accelerometers, pressure, flow and NDT transducers, acoustic emission, ultrasonic cleaning, welding, high voltage generators, medical therapy etc.

Long term reliability is one of the most important requirements for the technologically important piezoelectric devices. Significant work has been done on the development of new piezoelectric materials to meet the requirements of various applications.^{3,52} However there has been less work done on long term degradation and life time analysis of these materials and no widely accepted technique exists for reliability and lifetime testing. Current understanding of the long-term reliability and degradation mechanisms of piezoelectric materials is largely based on empirical evidences. This project will be focused to study thermal degradation and aging of piezoelectric and dielectric properties, and lifetime analysis at high temperature.

Discovery of piezoelectric effect goes back to 19th century. First demonstration of the piezoelectric effect by Currie brothers (Pierre and Jacques) was done in 1880. Since then, lots of work has been done on the development of various piezoelectric materials. The main breakthrough in the field came during early to mid 1940's, with the development of ABO_3 type perovskite structure.²⁰ The most important piezoelectric material lead zirconate titanate $(1-x)PbZrO_3-xPbTiO_3$ (PZT) was developed in 1950's,

and after 50 years it remains the most widely used piezoelectric ceramic.⁴ Large piezoelectric coefficient, large coupling factor and high Curie temperature (T_C) makes this material suitable for a wide range of piezoelectric applications.³ PZT has $T_C \sim 386^\circ\text{C}$ and shows rapid thermal degradation above 200°C .^{3,46} There are several applications where piezoelectric materials are required to operate above this temperature range. Significant work is going on for development of new piezoelectric materials suitable for extreme temperature applications. These materials will be useful for making sensors for space exploration, oil and geothermal well drilling tools, oil & gas pipeline health monitoring and automotive smart brakes.

Recently materials based on $(1-x)\text{BiScO}_3-x\text{PbTiO}_3$ (BSPT) were developed with $T_C \sim 450^\circ\text{C}$, and $d_{33} \sim 460$ pC/N compared to $T_C \sim 386^\circ\text{C}$ and $d_{33} \sim 223$ pC/N for pure PZT.^{3,41} Enhanced room temperature properties and higher transition temperature makes this material more interesting for further investigation as a high temperature piezoelectric material. It was anticipated that due to high T_C these materials are likely to have better resistance against thermal degradation and aging.

In PZT one method of tailoring the performance is doping. Doping can be either by addition of acceptor dopants to create anion vacancies or by addition of donor dopants to create cation vacancies. Acceptor doping is known as “hard” doping and donor doping is called “soft” doping. The point defects created by intrinsic and dopant reactions are believed to impact its domain structure and domain wall stability on microscopic level. In acceptor doped piezoelectric ceramics, alignment of defect dipoles in the direction of polarization vector tend to stabilize the domain structure and increase coercive field E_C to

make these materials hard for poling and depoling.¹⁵ For the current work “hard” doping will be studied in order to improve aging behavior of PZT and BSPT.

Goal of this work is to conduct the thermal degradation and aging study for the high temperature piezoelectric ceramic BSPT and comparing it with PZT. Unmodified and doped BSPT and PZT ceramics will be synthesized using conventional mixed oxide method and thermal degradation and aging study will be conducted at 250⁰C for 1000 hrs. Piezoelectric and dielectric characterizations will be done at predetermined intervals throughout the aging period. Changes in the properties will be compared with the initial and conditioned properties of these materials to establish the aging rates.

1.2 Organization of Thesis

This thesis is formatted to provide comprehensive review of the work performed for the thermal degradation and aging study of high temperature piezoelectric ceramic (1-x)BiScO₃-xPbTiO₃ to evaluate suitability of this material for high temperature remote sensing applications. This thesis consists of six chapters.

The Chapter 2 consists of literature review and classical background related to piezoelectric materials and their aging behaviors. It also covers brief introduction about the two important piezoelectric systems PZT and BSPT selected for thermal degradation and aging study and summary of their important properties. Chapter 3, details the experimental procedures and methods used for the processing of above ceramics by solid state route, structural and physical characterization of the processed ceramics, and thermal degradation and aging study. Piezoelectric and dielectric characterization of virgin and poled pellets is covered in Chapter 4 including sintering study, phase

identification, microstructure analysis and grain size measurement, summary of the initial piezoelectric and dielectric properties along with ferroelectric Curie temperature, high temperature dielectric measurements, P-E hysteresis loops, bipolar and unipolar strain loops and Rayleigh analysis for piezoelectric and dielectric response. Chapter 5, presents the details of thermal degradation and aging study, change in piezoelectric constant d_{33} , planar coupling coefficient k_p , dielectric constant K , dielectric loss D , and Rayleigh analysis for piezoelectric and dielectric responses as a function of aging time. Chapter 6 summarizes the work done for thermal degradation and aging study for BSPT system and roadmap for future studies.

Chapter 2: Background for piezoelectric materials and their aging behavior

2.1 Introduction:

Ferroelectric materials possess a local spontaneous polarization which can be reoriented between two or more equivalent crystallographic directions under application of a DC electric field. Ferroelectric ceramics can be made piezoelectric (poled) below Curie temperature (T_C) by application of electrical field (E) greater than Coercive field (E_C). Poling process aligns domains in the direction of the applied field yielding a net remnant polarization (P_R). Piezoelectric materials can be polarized by application of an electric field and also by application of mechanical stresses.

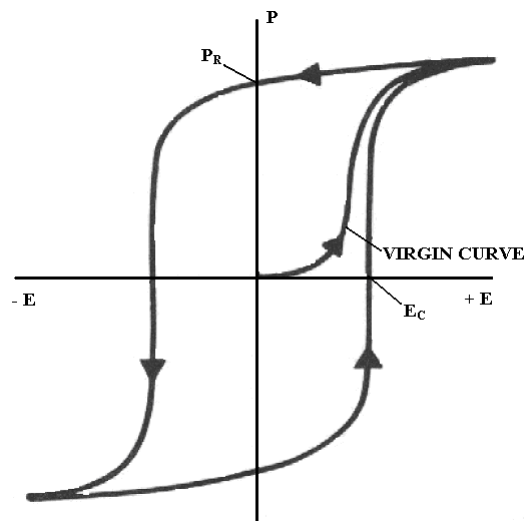


Figure 2.1. Charge- field hysteresis loop for ferroelectric materials

Ferroelectricity can be verified through polarization of the material by application of electric field. The most important characteristic of ferroelectric material is switching of

polarization. Figure 2.1 shows the typical charge – field hysteresis loop for ferroelectric materials. With the application of increasing field domains start orienting in the direction of field, extreme ends of the hysteresis loop (tail) represent the saturation where most of the domains are aligned in the direction of the applied field. Even after decreasing the field strength to zero all domains will not go back to original position, some domains will remain aligned in the positive direction. That is called as remnant polarization (P_R). When the field is applied in opposite direction, the dipoles reverse their orientation and then saturate in other direction. Field in negative direction when all domains are back to original position (zero polarization) is called coercive field (E_C). The relation between polarization (P) and electric field (E) is represented by hysteresis loop. Experimentally ferroelectric hysteresis loop can be observed using Sawyer-Tower circuit.¹¹

The piezoelectric effect includes two types of responses; direct and converse. Production of electric charge when stress is applied is known as direct piezoelectric effect whereas the production of stress and/or strain when an electric field is applied is known as converse piezoelectric effect. Figure 2.2 shows the schematic illustration for direct and converse piezoelectric effect. The mathematical equation for these effects are discussed in section 2.5.2.

2.2 Perovskite Structure

Crystal structure is very important for the performance of piezoelectric ceramics. Piezoelectricity is related to lack of a center of symmetry. Crystal structures can be divided into 32 point groups, 21 of them are noncentrosymmetric and 20 are piezoelectric. Under the application of homogeneous stress materials which lack a center

of symmetry observe a net movement of positive and negative ions with respect to each other developing an electrical polarization proportional to an applied stress.

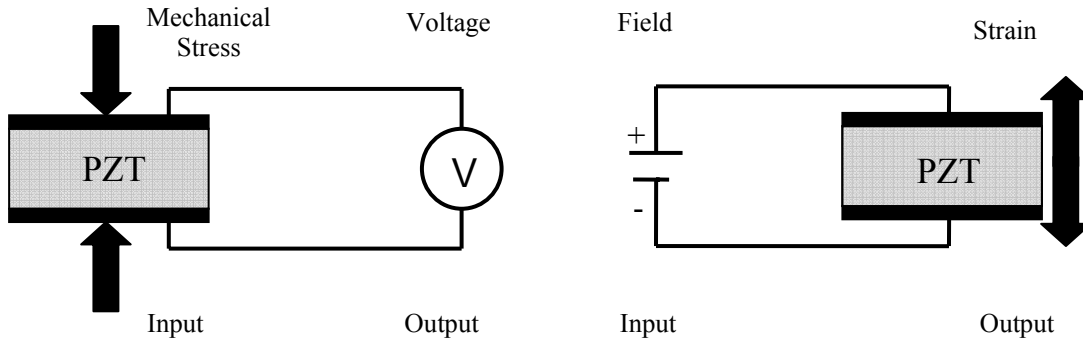


Figure 2.2. Schematic for a) Direct and b) Converse piezoelectric effect

Discovery of the piezoelectric effect goes back to 19th century. Since the discovery of piezoelectric effect, lots of work has been done on development of various ferroelectric materials. The main breakthrough in the field came in the mid 1900's with the synthesis and characterization of materials with perovskite structure.²⁰ Large numbers of technologically important piezoelectric materials crystallize in the perovskite structure. Two of the most interesting piezoelectric materials selected for aging study are lead zirconate titanate $(1-X)\text{PbZrO}_3-x\text{PbTiO}_3$ or PZT and Bismuth scandium – lead titanate $(1-x)\text{BiScO}_3-x\text{PbTiO}_3$ or BSPT belong to perovskite family.

The perovskite structure applies to series of compounds with three types of atoms with general formula ABO_3 described by a simple cubic unit cell with oxygen atoms at the face centers, larger cations at the cube corners (A sites) and smaller cations in body center (B sites). Typical perovskite ABO_3 unit cell is shown in Figure 2.3.³² There are

many complex perovskites which can be describe with the formula $(A', A'')^{xII}(B', B'')^{yVI}O_3$, where XII and VI represent coordination numbers. In PZT, Pb^{2+} ions are situated at the corner of the unit cell (A sites), Zr^{4+} or Ti^{4+} at body center positions (B site). In BSPT, Pb^{2+} and Bi^{3+} share the A sites whereas Ti^{4+} and Sc^{3+} share the B sites. In both material O^{2-} is situated at face center position forming octahedra around the B site (BO_6).

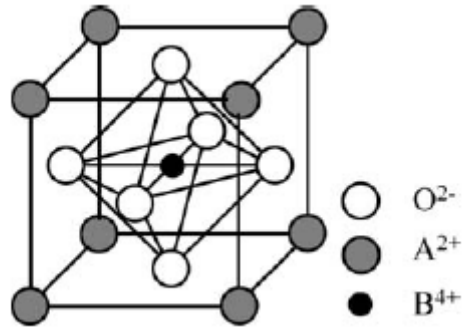


Figure 2.3. Perovskite ABO_3 unit cell.¹³

Ideal perovskite structure is simple cubic lattice. Depending on the ionic radii of cations and anions the perovskite unit cell may be distorted to rhombohedral or tetragonal symmetry. Type of the perovskite crystal structure can be predicted using Goldschmidt tolerance factor (t), given in equation (2.1).³

$$t = (R_A + R_O) / \sqrt{2} (R_B + R_O) \quad (2.1)^3$$

where R_A , R_B , and R_O are the ionic radius of large cation, small cation, and anion respectively. In general it is observed that perovskite structures with $t = 0.95 - 1.0$ are cubic, $t < 0.95$ - rhombohedral or monoclinic, and $t > 1.0$ - tetragonal. Polarization direction for rhombohedral is $\langle 111 \rangle$, for tetragonal $\langle 001 \rangle$, and for monoclinic phase it contained in monoclinic plane between $[001]$ and $[111]$.⁶ This provide 8 equivalent

polarization states for rhombohedral and 6 for tetragonal. In the case of a monoclinic ferroelectric phase the polarization may continuously rotate between up to 24 different states.

2.3 Intrinsic and extrinsic contributions

In polycrystalline ceramics piezoelectric and dielectric properties are depend on both intrinsic and extrinsic mechanisms. Intrinsic contributions are due to relative shift between cation and anion.⁹ When a voltage is applied to the perovskite unit cells one or more of the cations move due to the local field. Displacement of the cations with respect to oxygen octahedra causes distortion of the individual unit cell resulting strain in the piezoelectric material. This strain is typically $\sim 0.2\%$ for high performing polycrystalline ceramics whereas single crystals may strain $>1\%$. Displacement of the central atoms can only occur in certain crystallographic directions depending on the type of structure i.e. tetragonal or rhombohedral.

Extrinsic contributions are mainly due to presence of domain walls and defect dipoles and those are thermally activated.⁹ Depending on the relative orientation between polarization directions in neighboring domains there 180° and non- 180° domain walls. A schematic representation of 180° and non- 180° domain walls is shown in Figure 2.4. Ferroelectric domain walls may move under weak or moderate fields. The movement of domain walls due to external field affects the polarization and influences the piezoelectric and dielectric properties of ferroelectric materials. Both 180° and non- 180° domain wall motion influences the changes in polarization, while only non- 180° domain wall motion

influences the strain output. The real ferroelectric ceramics always contain imperfections, electrical and elastic defects. These imperfections and defects may cause pinning and clamping of domain walls.¹⁵

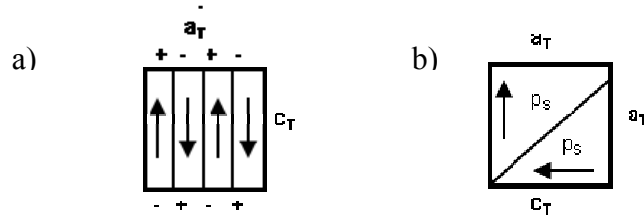


Figure 2.4. 180° a) and non-180° b) domain walls in a tetragonal unit cell.¹⁵

2.4 Lead Zirconate Titanate (1-x)PbZrO₃-xPbTiO₃

The most important piezoelectric material lead zirconate titanate (1-x)PbZrO₃-xPbTiO₃ or PZT was developed in 1950's, since then it is been the dominant piezoelectric ceramic in the commercial market.^{3,4} The high electromechanical properties, and Curie temperature and ability to tailor properties make this material suitable for wide range of applications. Commonly used PZT 5A has Curie temperature $T_C \sim 365^\circ\text{C}$ and piezoelectric coefficient $d_{33} \sim 375 \text{ pC/N}$.⁵²

In PZT depending on the % of Zr^{+4} or Ti^{+4} the crystal structure is either rhombohedral or tetragonal. Figure 2.5, shows the temperature–composition phase diagrams for PZT system.^{3,7} At room temperature Zr rich region has rhombohedral structure (F_R) with two space groups $R3m$ and $R3c$, and Ti rich region has tetragonal structure (F_T) with space group $P4mm$.³ In rhombohedral phase the polarization is along the body diagonal of unit cells which gives eight equivalent state of polarization whereas

in tetragonal phase polarization is parallel to the edges of the unit cell and has six equivalent state of polarization. The line separating two regions called morphotropic phase boundary (MPB) which is about $x \sim 0.48$. PZT has nearly vertical MPB. Traditional understanding is that compositions near the MPB have coexistence of rhombohedral and tetragonal phases to give 14 possible polarization directions to optimize crystallographic orientation and resulting high dielectric and piezoelectric properties.³

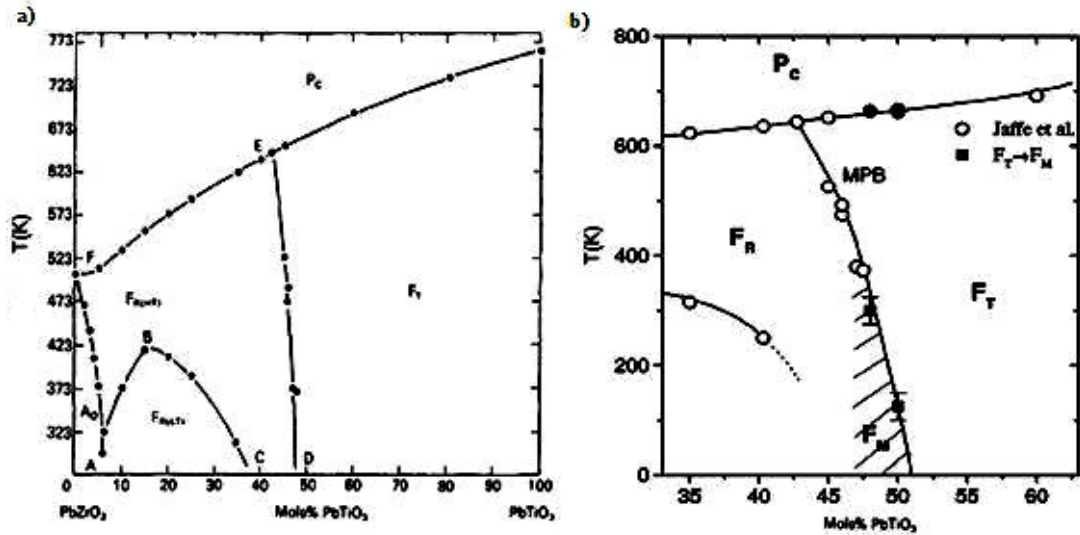


Figure 2.5. Temperature – composition phase diagram for PZT
a) after Jaffe et al. 1971³ and b) modified by B. Noheda,2000⁷

Recently Noheda et al. 2002 reported the presence of the monoclinic structure (F_M) with space group Pc at the MPB.⁶ PZT has the cubic structure at high temperatures; the cubic to tetragonal phase transformation takes place at 660 K for MPB composition. The tetragonal to monoclinic phase transformation was discovered at ~ 300 K.⁶ The monoclinic unit cell is rotated 45° about c axis with respect to tetragonal cell, a_m and b_m

lie along the tetragonal face diagonals $[\bar{1}\bar{1}0]$ and $[1\bar{1}0]$ directions and c_m deviates slightly from $[001]$ direction.

2.5 High temperature piezoelectric $(1-x)\text{BiScO}_3\text{-}x\text{PbTiO}_3$

PZT with the MPB composition has $T_C \sim 386^\circ\text{C}$ and shows rapid thermal degradation above 200°C .^{3,46} There are several applications where piezoelectric materials are required to operate above this temperature range. Lots of work is going on in the development of new piezoelectric materials suitable for extreme temperature applications. These materials will be very useful for making sensors for space exploration, oil and geothermal well drilling tools, oil & gas pipeline health monitoring and automotive smart brakes.

Materials based on $(1-x)\text{BiScO}_3\text{-}x\text{PbTiO}_3$ (BSPT) have a $T_C \sim 450^\circ\text{C}$ and $d_{33} \sim 460$ pC/N; compared to $T_C \sim 386^\circ\text{C}$ and $d_{33} \sim 223$ pC/N for pure PZT.^{3,41} Enhanced room temperature properties and higher transition temperature makes this material interesting for high temperature application above 200°C . Figure 2.6 shows the temperature - composition phase diagram for BSPT system.⁴² It is clear from the below phase diagram that near the MPB region phase transition temperature from the tetragonal and rhombohedral phase to the paraelectric - cubic phase is about 450°C and increases with mol% of PbTiO_3 .

Figure 2.7 shows ferroelectric switching polarization loop (a), bipolar strain loop (b), and unipolar strain loop (c) for PZT and BSPT ceramics with the MPB compositions which compare the behavior of these two important piezoelectric systems.

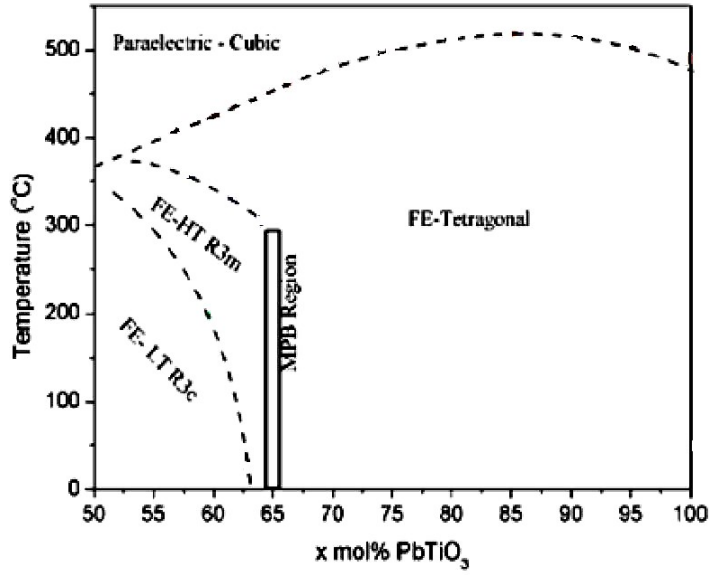


Figure 2.6. Temperature–composition phase diagram for BSPT (Eitel et al. 2004)⁴²

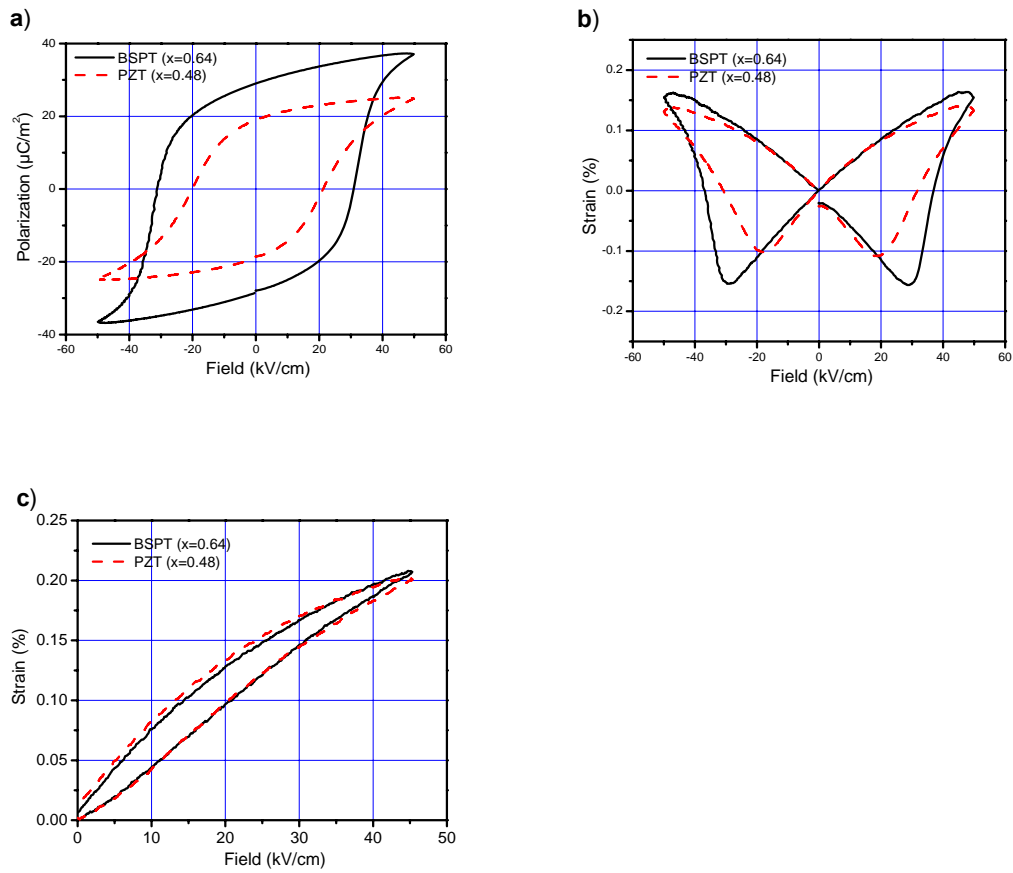


Figure 2.7. a) Ferroelectric switching polarization loop, b) Bipolar strain loop, and c) Unipolar strain loop for PZT and BSPT ceramics

2.6 Properties of piezoelectric materials

The performance of piezoelectric devices depends on various electromechanical properties. Some of the important properties of piezoelectric materials are ferroelectric Curie temperature (T_C), piezoelectric constant (d), dielectric constant (K) and loss (D or $\tan\delta$) and electromechanical coupling coefficient (k). Typical properties for various PZT and BSPT materials are given in Table 2.1. ShROUT et al. 2007 showed that general piezoelectric properties of a ferroelectric ceramic can be expressed with a simple mathematical equation (2.2),

$$d_{ij} \sim 2 Q_{ij} K \epsilon_0 P_i \quad (2.2)^{52}$$

where d_{ij} is the piezoelectric constant, P_i the remnant polarization, K the dielectric constant, ϵ_0 the permittivity of free space, and Q_{ij} the electrostrictive coefficient.⁵² Since Q_{ij} exhibit little temperature dependant below Curie temperature T_C , the perovskite ferroelectric ceramics with high piezoelectric constant d_{ij} also exhibits high dielectric constant K .⁵² Within the lead base piezoelectric family, materials with low ferroelectric Curie temperature T_C exhibit high piezoelectric and dielectric properties. The reduction of ferroelectric Curie temperature is also associated with high thermal dependence of properties, and high aging rates. As a thumb rule piezoelectric ceramics can be used safely to $\sim \frac{1}{2} T_C$ ($^{\circ}\text{C}$) without much change in piezoelectric properties.⁵² Hence engineering of piezoelectric ceramics is always an optimization of piezoelectric and dielectric properties and also ferroelectric Curie temperature T_C .

2.6.1 Ferroelectric Curie temperature (T_C)

Ferroelectric materials possess a local spontaneous polarization and shows hysteresis relation between polarization and applied electric field. This behavior is observed in certain temperature region which depends on the transition of ferroelectric phase to paraelectric phase. Temperature above which the material loses its spontaneous polarization and piezoelectric characteristics is known as ferroelectric Curie temperature (T_C).

Depending on composition PZT has rhombohedral, tetragonal or mixed perovskite structure below T_C and shows net dipole moment due to displaced central cation (Zr^{4+} or Ti^{4+}). Above T_C the material is cubic and the central cation is no longer displaced from the centre of the unit cell, leaving no net dipole moment and no spontaneous polarization.

Table 2.1. Electromechanical properties of PZT and BSPT materials.

Material	Curie point ($^{\circ}C$) T_C	Dielectric Constant (1Khz) K	Dielectric loss (1Khz) D	Piezoelectric constant (10^{-12} C/N) d_{33}	Electromechanical coupling coefficient k_{33}
Pb($Zr_{0.52}Ti_{0.48}$)O ₃ ³	386	730	0.004	223	0.67
Hard PZT – 5H ⁵²	190	3400	0.02	590	0.75
Hard PZT- 8 ⁵²	300	1000	0.004	225	0.64
Hard PZT- 4 ⁵²	328	1300	0.004	290	0.70
Hard PZT PCM-40 ³³	325	1250	0.003	290	0.67
Hard PZT PIC 181 ³⁴	330	1200	0.003	265	0.66
Soft PZT- 5A ⁵²	365	1700	0.02	375	0.71
Soft PZT PCM-51 ³³	340	1850	0.019	405	0.74
Soft PZT PIC 151 ³⁴	250	2400	0.02	500	0.69
BSPT 64 ^{41,50}	450	2010	0.05	460	0.56
BSPT 66 ⁴¹	460	1370	0.03	260	0.43
BSPT 64 + Mn ⁴⁸	445	1540	0.01	390	0.69
BSPT 66 + Mn ⁴⁸	468	1112	0.01	270	0.65

As the temperature is increased, near T_C the dipoles have the tendency to revert back to random orientation. Degradation of piezoelectric properties due to loss of polarization is called thermally activated aging. In order to minimize the aging effect, maximum applications of materials are restricted to $\sim \frac{1}{2}T_C$.⁵² PZT has $T_C \sim 386^\circ\text{C}$ and shows rapid degradation above 200°C .³ Recently developed BSPT system has $T_C \sim 450^\circ\text{C}$ and are much more stable at temperature higher than 200°C .^{41,46}

2.6.2 Piezoelectric constant (d)

As discussed in section 2.1, the piezoelectric effects include two types of responses; direct and converse. The basic mathematical equations (2.3) and (2.4) describe the above two types of piezoelectric effects are,

$$D = d \cdot T \quad (\text{Direct piezoelectric effect}) \quad (2.3)$$

$$S = d \cdot E \quad (\text{Converse piezoelectric effect}) \quad (2.4)$$

where D is the dielectric displacement, T the stress, S the mechanical strain, E the electric field, and d the piezoelectric constant which is numerically constant for both effects.³ Piezoelectric properties are also anisotropic and vary with direction of polarization axis and strain, hence may be specified in tensor form as in equation (2.5) to indicate directionality.

$$D_i = d_{ijk} \cdot T_{jk} \quad \text{and} \quad S_{jk} = d_{ijk} \cdot E_i \quad (2.5)$$

Depending on the application, piezoelectric devices may use one of the above piezoelectric effects. High d is desirable for actuator applications like ultrasonic cleaner transducers, where materials are intended to develop motion or vibrations.

Another frequently used piezoelectric constant is g_{ij} which is related to d by equation (2.5).³

$$g = d / \varepsilon = d / K \varepsilon_0 \quad (2.5)$$

where ε the dielectric permittivity of material, and ε_0 the dielectric permittivity of vacuum. High g is desirable for sensors applications like pressure sensors, where materials are intended to generate voltage in response to mechanical stress.

2.6.3 Dielectric constant (K) and loss (D)

The relative dielectric constant K is the ratio of the complex permittivity ε of the material and the permittivity of free space ε_0 (8.85×10^{-12} F/m). Piezoelectric ceramics generally have a higher dielectric constant K , typical values for PZT and BSPT systems are 800 and as high as 2000 respectively.^{3,41}

$$K = \varepsilon / \varepsilon_0 \quad (2.7)$$

When an alternating voltage is applied to dielectric materials induced dielectric moment has both real and imaginary components, which is due to resistive leakage or dielectric absorption. The loss factor D is the ratio of imaginary component to the real component and expressed as equation (2.8),

$$D (\tan \delta) = \varepsilon'' / \varepsilon' = k'' / k' \quad (2.8)$$

2.6.4 Electromechanical coupling coefficient

Input energy to piezoelectric devices can be either in mechanical stress or electrical charge. The electromechanical coupling factor (k) is square root of the fraction

of mechanical energy converted to electrical energy or vice versa.³ k is the material constant for piezoelectric crystals and it depends on degree of poling for ceramics.

$$k = \sqrt{\frac{\text{Energy converted (mechanical or electrical)}}{\text{Energy applied (mechanical or electrical)}}} \quad (2.9)$$

Typical value of electromechanical factor for PZT and BSPT is in the range from 0.45 to 0.70.^{3,41}

2.7 Modification of properties by doping

The electromechanical properties of piezoelectric ceramics can be tailored through compositional modification to make them suitable for different applications. Lead volatility in Pb-based perovskites produces Pb vacancies (V_{Pb}'') which are naturally compensated by oxygen vacancies (V_O'') lead to acceptor (p-type) characteristics. Doping can be either “hard” by addition of acceptor dopants (Mg^{2+} , Fe^{3+} , Na^+) creating anion vacancies or “soft” by addition of donor dopants (Nb^{5+} , Sb^{5+} , La^{3+}) eliminating V_O'' . Point defects created by intrinsic and dopant reaction are believed to impact domain structure and domain wall stability in piezoelectric materials.

In acceptor doped materials mobility of point defects is relatively high due to large numbers of anion vacancies.¹⁵ This allows alignment of paired defect dipoles in the direction of polarization vector stabilizing the domain structure. Stability of domain wall structure increases the coercive field E_C to make this material “hard” and reduces the piezoelectric constant d_{33} and dielectric loss D . In donor doped materials anion vacancies are reduced and these piezoelectric materials exhibits low E_C , and D .

Berlincourt et al. 1992 reported effects of two types of dopants on properties of PZT.¹³ Addition of donor substitution to PZT improved piezoelectric coupling factor and dielectric permittivity. Also donor doped PZT shows reduction in aging due to relaxation of internal stresses with less strain accommodation by Pb^{2+} vacancies. On the other hand additions of acceptor dopants create vacancies on oxygen sites and help to reduce the dielectric losses and improve mechanical and electrical quality factors.

2.8 Effect of processing on the properties of piezoelectric materials

Processing of the ceramic has great impact on its properties and performance of piezoelectric ceramics. Processing of ceramics mainly consist of forming a green body by mixing of metal oxide powders and then producing dense structure by sintering. The two most widely used methods for piezoelectric ceramics are sol gel processing and solid state synthesis. Sol gel process is expensive; it produces very fine high purity powders which can sinter at much lower temperatures to achieve densities close to theoretical value. Solid state synthesis is more common due to its lower cost.

Density is very important to achieve good piezoelectric and dielectric properties in a piezoelectric ceramic. In general bulk density of the ceramic after sintering should be more than 95% of theoretical densities. Processing parameters like milling time of the powders before and after calcinations and sintering time and temperature plays vital role in producing high density materials.

Microstructure of the piezoelectric ceramic mainly depends on composition, primary particle size, sintering temperature and time. In the past various studies been carried out by several researchers to investigate effect of grain size on the properties of

piezoelectric ceramics. General understanding was that, fine grain microstructure leads to significantly higher dielectric constant and remnant polarization and a much lower coercive field with slight improvement in piezoelectric constant. Recently Randall et al. 1998 studied the effect of grain size on the dielectric and piezoelectric properties of PZT.⁹ Results show that ferroelectric transition temperature is almost independent of grain size, dielectric constant K , piezoelectric coefficient d_{33} and d_{31} and electromechanical coupling coefficient k_p and k_{31} , remnant polarization P_R decreases and coercive field E_C increases with decrease in grain size.

2.9 Thermal degradation and aging of piezoelectric materials

Piezoelectric ceramics suffer from loss of polarization as dipoles have a tendency to revert back to random orientation at high temperature; this loss of polarization is called thermal degradation. The thermal degradation is associated with an external influence and usually implies a large detrimental change to a property of a material. In order to minimize the thermal degradation, maximum application of piezoelectric materials is generally restricted to $\sim 1/2 T_c$.^{52,46}

Aging should be considered separately to thermal degradation. Aging is a process for a system to reach to an equilibrium state from a non-equilibrium state. More precisely aging can be defined as the spontaneous change of a material property with time, under zero external stress and constant temperature.⁵⁶ Like other characteristics of piezoelectric materials, aging depends on material type, processing and poling condition. Aging can be characterized as thermally activated process as aging rate increases with increase in the temperature.¹ Change in property due to aging may be on either side, increase or

decrease. In the ferroelectrics and related materials aging can be reversed or set back to initial property by long thermal cycle above ferroelectric Curie temperature T_C .

In the past, many researchers worked on aging studies of dielectrics and compressive review of these studies was presented by Schulze et al. 1988.⁵⁶ Investigation of BaTiO₃ capacitors shows that aging of dielectric constant or capacitance follows a linear logarithmic relation with the time. It was also observed that polarization-field hysteresis loop of aged specimen acquires a pinched or propeller shape, which reflect buildup of an internal field due to migration of defects and also preferential location of electron trapping sites.

The main characteristics of aging process can be summarized as below; aged samples show lower dielectric constant, $\tan\delta$, and electromechanical coupling factor, when mechanical quality factor and resonance frequency become higher; polarization-field hysteresis loop becomes constricted into a pinched or propeller shape with time; aging can be completely reversed by heating the dielectric above Curie temperature and holding in the paraelectric phase; aging rate decreases with increase in tetragonal distortion of perovskite cell but is not observed in paraelectric phase.⁵⁶

Robel et al. 1993 reported aging study of acceptor doped BaTiO₃ and PZT ceramics and proposed the quantitative model based on reorientation of defects with the time which causes clamping of domain walls and results in decrease of material properties during aging.⁵⁵ Orientation of defects caused by slow diffusion of oxygen vacancies was attributed to splitting of energy due to electric and elastic dipoles. Stabilization of domains due to orientation of defects results an increase in the force constant for the 90° domain wall displacement.

The basic modification happening in the piezoelectric material over a period of time due to aging is alignment of defect or space charge, development of internal bias field and stabilization domain structure.¹⁵ In the past many authors have investigated the aging behaviors and several plausible models have been developed to interpret aging in the normal ferroelectric materials. Broadly those can be classified as relocation of the charges, reorientation of defect dipole, domain wall mobility and intrinsic dielectric response.¹

2.9.1 Domain wall clamping by defects

This mechanism is related to volumetric defect. Initially all elastic and electric defects are randomly oriented. With the time all these defect start relocating to energetically favorable position which is related to direction of polarization. Reorientation of polarization and displacement of domain walls by external field become more difficult once these defects are aligned.

2.9.2 Diffusion of defects through domain wall and consequent stabilization of domain wall

The driving force for migration of defects is likely to be relaxation of stresses or compensation of electric charges in the wall region. The defects act as pinning centers to restrict the wall motion hence contribution of domain wall to the properties get reduced.

2.9.3 Presence of space charges at the grain boundaries

Grain boundaries are always higher energy location compared to grains hence it is more energy favorable location for segregation of dopants or secondary phases. These heterogeneous space charges may require long time to reach to equilibrium positions. After reaching equilibrium positions, the local electric field created by space charges stabilize the domain wall configuration and whole grain become biased in certain directions.

Recently Chen et al. 2006 reported the thermal depoling study for high temperature piezoelectric ceramic $(1-x)\text{BiScO}_3\text{-}x\text{PbTiO}_3$ with rhombohedral, MPB and tetragonal compositions.⁴⁶ Study reveals that tetragonal compositions of $(1-x)\text{BiScO}_3\text{-}x\text{PbTiO}_3$ showed good resistance to thermal depoling up to the temperature close to their ferroelectric Curie temperature $T_C \sim 445^\circ\text{C}$. Rhombohedral and MPB compositions started to depole at $\sim 300^\circ\text{C}$, which is far below their ferroelectric Curie temperature. Compared to the MPB composition the tetragonal materials have lower piezoelectric constant d_{33} and planar coupling coefficient k_p but they showed excellent thermal stability which make them better choice for high temperature applications. One of the most important requirements for any material or devices in the service is long term reliability. 1000 hr aging study was conducted for $(1-x)\text{BiScO}_3\text{-}x\text{PbTiO}_3$ and results were compared with $(1-x)\text{PbZrO}_3\text{-}x\text{PbTiO}_3$. Details of the processing, characterization and aging study are presented in the following chapters.

Chapter 3: Experimental procedures and methods

3.1 Introduction

Processing of piezoelectric ceramics consists of reacting metal oxide powders to achieve the desired phase, compaction of powder to form a green body and then sintering to produce dense structure. The two most widely used methods to produce piezoelectric ceramic powders are sol gel processing and solid state synthesis. Sol gel process is expensive; it produces very fine high purity powders which can sinter at much lower temperatures to achieve densities close to theoretical value. Solid state synthesis is more common due to its lower cost. For the current work $(1-x)\text{PbZrO}_3-x\text{PbTiO}_3$ and $(1-x)\text{BiScO}_3-x\text{PbTiO}_3$ were synthesized by solid state mixed oxides method. Piezoelectric and dielectric properties were evaluated for the set of virgin poled pellets. Poled pellets were kept in oven at 250°C for 1000 hrs. Measurement of piezoelectric and dielectric properties was done at predetermined intervals to analyze the thermal degradation of properties as a function of time.

3.2 Preparation of piezoelectric ceramics

3.2.1 Powder preparation

The conventional mixed oxide (solid state) route was used to synthesize $(1-x)\text{PbZrO}_3-x\text{PbTiO}_3$ and $(1-x)\text{BiScO}_3-x\text{PbTiO}_3$ ceramics of the MPB and tetragonal composition with and without acceptor doping. Commercially available reagent grade metal oxides and carbonates including PbCO_3 (white lead A, Halstab), ZrO_2 (99.5%, Alfa

Aesar), TiO₂ (99.9%, Ishihara), Bi₂O₃ (99.975%, Alfa Aesar), Sc₂O₃ (99.95%, PIDC), MnO₂ (99.9%, Alfa Aesar), and Fe₂O₃ (99.5%, Alfa Aesar), were used as starting materials. Powder preparation is important for adequate control of microstructure and properties of the final product. Important characteristics of the powders that have a great impact on final product properties are chemical composition, purity, particle size, and size distribution, shape of powders, and degree of agglomeration, surface area, density, and porosity. Loss on ignition (LOI) was carried out for starting metal oxide powders to improve accuracy of the batching by compensating for hydration and ignition losses. Particle size analysis of metal oxide powders was done by light scattering technique. Mean particle size of starting powders was in the range of 1 to 10 μm.

For the MPB type of piezoelectric ceramics it is well known that compositions near the MPB have enhanced piezoelectric and dielectric properties, while the tetragonal compositions are anticipated to have high curie temperatures and resistance against aging.^{3,41,59} An acceptor dopant reduces dielectric losses and should improve resistance to aging. For the current work the MPB and tetragonal compositions for (1-x)BiScO₃-xPbTiO₃ and the MPB composition for (1-x)PbZrO₃-xPbTiO₃ with and without addition of acceptor dopant were selected for thermal degradation and aging study. The metal oxide powders were mixed in stoichiometric ratio in the batches of ~80 g considering hydration and ignition losses to form the intended compositions (1-x)PbZrO₃-xPbTiO₃ x =0.48 and (1-x)BiScO₃-xPbTiO₃ x=0.64 and 0.66. In solid state synthesis, larger surface area is required to accelerate diffusion between various oxide particles to form uniform phase in the calcination. This can be achieved by reducing particle size of the powder mixture in milling. To make milling more effective, highly concentrated aqueous

suspension of powders was prepared by addition of ammonium polyacrylate (Darvan 821™, R.T. Vanderbilt Company Inc.) as a dispersant and controlling its PH. Suspensions were vibratory milled for 24 hrs using ϕ 5mm spherical yttrium stabilized zirconia media (Nikkato, Japan). The milled slurry was dried for 12 hours at 120°C.

Calcination of milled and dried (1-x)PbZrO₃-xPbTiO₃ and (1-x)BiScO₃-xPbTiO₃ powders was done for 6 hours at 850°C and 750°C respectively. The calcination process was repeated to get uniform perovskite phase with very little impurity level. Each calcination was followed by 24 hrs vibratory milling and drying as above to improve homogeneity and to expose new surfaces to improve diffusion in thermal treatment. The perovskite phase development after calcination was evaluated by X-ray diffraction (XRD). Modified (1-x)PbZrO₃-xPbTiO₃ and (1-x)BiScO₃-xPbTiO₃ were prepared using Fe₂O₃ and MnO₂ as acceptor dopants respectively. These dopants were added in the calcined powders before final milling. Acrylic copolymer (R.E. Mistler) ~ 3- 4% wt was added to ceramic powders to provide the necessary plasticity for forming and green strength to facilitate handling of pellets after compaction. Powder binder mixed were dried at 120°C and crushed using mortar and pestle and passed through 80 mesh sieve.

3.2.2 Forming

Forming is the consolidation of loose calcined powders to a homogeneously packed green body prior to densification. For the current work, circular pellets of ~ Φ 13mm x 1 mm thickness were uniaxially pressed at 8000 psi in a hydraulic press using rigid steel die. Binder was burnt out by slow heating of the pellets to 500°C (1°C/min) for 2 hrs in the box furnace prior to sintering.

3.2.3 Sintering

Densification of the powders into a pore-free, high quality final product is achieved through the sintering. The two most commonly used densification methods are hot pressing and conventional sintering process. For the current work conventional sintering process was utilized. Sintering for pressed pellets was done in the tube furnaces for 1 hr at the temperature range from 1200⁰C to 1300⁰C for unmodified (1-x)PbZrO₃-xPbTiO₃ and 1050⁰C to 1250⁰C for Fe-modified (1-x)PbZrO₃-xPbTiO₃. Sintering of unmodified and Mn-modified (1-x)BiScO₃-xPbTiO₃ pellets was done in box furnace at the temperature range from 1000⁰C to 1100⁰C for 1 hr. Volatilization losses were controlled by using source powder and sealed crucibles. Pb_{1.1}ZrO_{3.1} and (1-x)BiScO₃-xPbTiO₃ x= 0.64 with ~ 5% excess Pb and Bi were used as source powder for sintering of (1-x)PbZrO₃-xPbTiO₃ and (1-x)BiScO₃-xPbTiO₃ pellets respectively. Sintering parameters were optimized to achieve high density, low porosity and uniform microstructure with average grain size ~10μm and to achieve good piezoelectric and dielectric properties in the sintered pellets. After optimizing the sintering parameters, sets of 15 pellets for each composition were prepared for thermal degradation analysis. Final batches of unmodified and Mn-modified (1-x)BiScO₃-xPbTiO₃ were sintered at 1100⁰C for 1 hr. Unmodified (1-x)PbZrO₃-xPbTiO₃ pellets were sintered at 1200⁰C for 1 hr whereas Fe-modified (1-x)PbZrO₃-xPbTiO₃ pellets were sintered at 1100⁰C for 1 hr.

3.2.4 Electrode application

Sintered pellets were ground parallel to ~0.5mm using 280 and 600 grit abrasive paper disk. Ground pellets were cleaned ultrasonically with methanol and dried at 120⁰C

for 12 hrs to remove moisture from the pellets prior to electrode application. Conductive Ag electrode paste (DuPont 6160) was applied and dried at 160⁰C for 15min and then fired at 850⁰C after cleaning the edges.

3.2.5 Poling

Electroded pellets were poled in an oil bath at 100⁰C under 40kV/cm DC field for 15 min. Dielectric and piezoelectric properties of poled pellets were measured after 24 hr of the poling.

3.3 Characterization

3.3.1 Structural and physical characterization

The properties of piezoelectric ceramics are mainly dependant on the phases present in the structure. X ray diffraction (XRD) of calcined powders and crushed sintered pellets was done for phase determination using θ -2 θ diffractometer (Model-D500, Siemens) with $CuK\alpha 1$ radiation (1.5418 Å). Lattice parameters, c/a ratio, and theoretical density of the ceramics were calculated by indexing peaks from XRD scan.

The densities of sintered pellets were measured in water using Archimedes method. Bulk density, apparent density and porosity were calculated from the measured data. Pellets with bulk density more than 95% theoretical value were used for characterization of piezoelectric and dielectric properties.

Sintered pellets were polished and thermally etched at 900⁰C for 15 minutes. Grain size of the sintered pellets for all compositions except Fe-modified (1-x)PbZrO₃-xPbTiO₃ was determined from the microphotographs taken by optical microscope

(Model- LV100POL, Nikon) with digital camera (Model-DXM 1200C, Nikon). Grain size for Fe-modified $(1-x)\text{PbZrO}_3-x\text{PbTiO}_3$ was determined from the microphotographs taken by scanning electron microscope SEM (Model-S3200-N, Hitachi). Average grain size was calculated using lineal intercept technique.²⁸

3.3.2 Piezoelectric and dielectric characterization

3.3.2.1 Ferroelectric Curie temperature (T_C)

As the temperature is increased, near T_C the dipoles have the tendency to revert back to random orientation. The temperature above which the material loses its spontaneous polarization and piezoelectric characteristics is known as Curie temperature. High temperature dielectric measurement was done up to 600°C for unpoled pellets in a vertical tube furnace (Model-F21130, Barnstead) using computerized control LCR meter (Model-E4980A, Agilent) and data acquisition. The set up used for high temperature dielectric measurement is shown in Figure 3.1. Dielectric constant increases with increasing temperature, reaches to the peak value and then decreases. This peak corresponds to ferroelectric Curie temperature.

3.3.2.2 Polarization – electric field (P-E) hysteresis loop

The most important characteristic of ferroelectric materials is the switching of polarization. Ferroelectric properties such as coercive field E_C , remnant polarization P_R , and spontaneous polarization P_S are determined through P-E hysteresis loops.

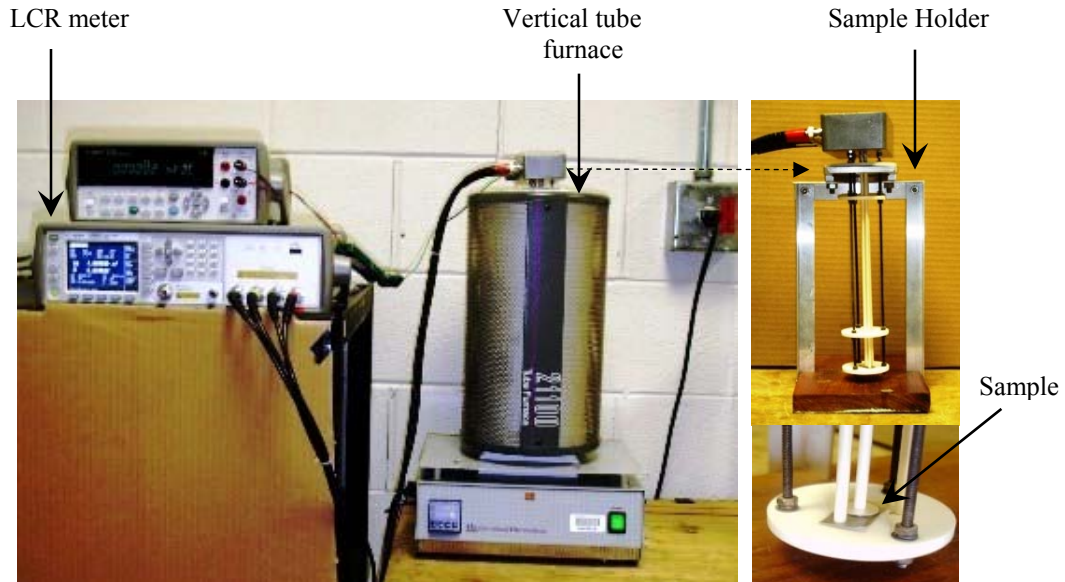


Figure 3.1. Set up for high temperature dielectric measurement

Ferroelectric hysteresis loops, bipolar and unipolar strain loops, were measured at an electric field of 50kV/cm and frequency 1 Hz using a Sawyer-Tower circuit with a linear variable differential transducer (LVDT), high voltage power supply (Model- 610B, TReK), and computerized control and data acquisition. Schematic for the Sawyer-Tower circuit used for P-E loop measurement is shown in Figure 3.2.³

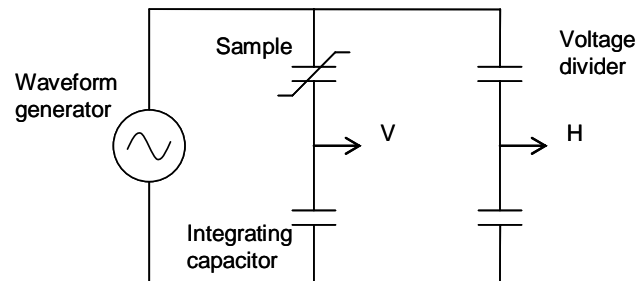


Figure 3.2. Schematic of the circuit used for P-E loop measurement.³

3.3.2.3 Dielectric constant (K) and dielectric loss (D)

The relative dielectric constant K is the ratio of the permittivity ϵ of the material and the permittivity of free space ϵ_0 (8.85×10^{-12} F/m).³ Room temperature capacitance C_p and dielectric loss D were measured using multi frequency LCR meter (Model- 4274A, Hewlett Packard). Dielectric constant K was calculated from the measured capacitance using equation (3.1). Room temperature dielectric measurements were done for the electroded pellets before and after poling.

$$K = \epsilon / \epsilon_0 \text{ and } \epsilon = C_p \times (t/A) \quad (3.1)$$

where ϵ is the permittivity of the material, ϵ_0 the permittivity of free space, C_p the capacitance, t the thickness, and A the area of pellets.

Dielectric permittivity is a complex value, under the application of alternating voltage it has both real (in phase) and imaginary (out of phase) components $\epsilon = \epsilon' + i\epsilon''$. Dielectric loss (D or $\tan\delta$) is the ratio of imaginary and real components, and expressed by simple mathematical equation (3.2)

$$\tan\delta = \epsilon'' / \epsilon' \quad (3.2)$$

3.3.2.4 Piezoelectric constant (d_{33})

Piezoelectric constant d_{33} was measured using Berlincourt type d_{33} meter (Model- YE2730A, APC International Ltd.). This method gives direct reading for d_{33} .

3.3.2.5 Planar coupling coefficient (k_p)

Planar coupling coefficient k_p was measured using Impedance / Gain- phase analyzer (Model- 4194A, Hewlett Packard). The parallel resonance frequency f_p and the

series resonance frequency f_s were obtained from the measurements and k_p was calculated from using the equation (3.3).³

$$\frac{k_p^2}{1-k_p^2} = \frac{(1-\sigma^E)J_1[\eta_1(1+\Delta f/f_s)] - \eta_1(1+\Delta f/f_s)J_0[\eta_1(1+\Delta f/f_s)]}{(1+\sigma^E)J_1[\eta_1(1+\Delta f/f_s)]} \quad (3.3)^3$$

where J_0 is the Bessel function of first kind and zero order, J_1 the Bessel function of first kind and first order, η_1 the lowest positive root of $(1-\sigma^E)J_1(\eta_1)$, and σ^E the Poisson's cross contraction ratio.

3.3.2.6 Rayleigh analysis for dielectric and piezoelectric response

Rayleigh law was used originally to describe the dependence of magnetization and magnetic permeability in ferromagnetic materials.^{12,16-18} Same approach is being used in piezoelectric materials to quantify irreversible and reversible piezoelectric response. Rayleigh law is suitable in low field region where density and domain wall structure remain unchanged. Rayleigh law indicates a linear dependence on the piezoelectric constant and dielectric constant with increasing field.

Piezoelectric response in ferroelectric material contains both intrinsic and extrinsic contribution. Intrinsic contributions are mainly due to strain in crystal lattice, in general those are reversible and with no loss. Extrinsic contribution is mainly due to motion of non-180° domain walls. Extrinsic contribution are generally non linear and lossy and varies as a function of time, frequency, and field.^{12,16-18}

Rayleigh measurement for dielectric and piezoelectric response were made using a Sawyer-Tower circuit with a linear variable differential transducer (LVDT), high voltage power supply, and computerized control and data acquisition. Two poled pellets

were evaluated for dielectric and piezoelectric responses at low field for unmodified and modified compositions of $(1-x)\text{PbZrO}_3\text{-}x\text{PbTiO}_3$ and $(1-x)\text{BiScO}_3\text{-}x\text{PbTiO}_3$.

3.4 Thermal degradation and aging

Sets of 15 pellets for each composition were prepared for thermal degradation and aging study. Poled pellets were characterized for dielectric constant K , dielectric loss D , piezoelectric constant d_{33} , and electromechanical coupling coefficient k_p and Rayleigh measurement for piezoelectric and dielectric response. Pellets with the maximum 10% variation from mean value of the above properties were used for the thermal degradation and aging study. The sets of poled pellets were loaded at 250°C in the oven for 1 min for thermal conditioning treatment. Samples were reloaded after characterization for 1000 h. Changes in the above properties were evaluated at predetermined interval of 1 h, 10 h, 100 h, 200h, 400h, 700h and 1000h. The results were evaluated to find out aging rate for piezoelectric and dielectric properties. Standard statistical methods were used to evaluate errors, variability and standard deviations for the above measurements.

For piezoelectric materials, aging of the piezoelectric and dielectric properties (d_{33} , k_p , and K) can be describe as a function of time (t). It shows the linear relation with t on logarithmic scale, which can be describe with the general equation (3.4)

$$p(t) = p(t_0) + A \log(t) \quad (3.4)$$

where p is the material property, t_0 is the starting time for the measurements, and A is the aging rate (constant) which can be either positive or negative.

Chapter 4: Characterization

4.1 Introduction

For the thermal degradation and aging study one of the important step is the characterization of the processed materials to evaluate their properties in comparison with the studies done in past. Additionally measured properties provide the basis for further study to evaluate the degradation and calculate the aging rates. Unmodified and Fe-modified $(1-x)\text{PbZrO}_3-x\text{PbTiO}_3$ $x=0.48$ and unmodified and Mn-modified $(1-x)\text{BiScO}_3-x\text{PbTiO}_3$ $x=0.64$ and 0.66 ceramics were prepared using solid state route as discussed in Chapter 3. This chapter details the characterization for phase identification, microstructure and grain size for sintered ceramics in addition to piezoelectric and dielectric characterization for ferroelectric Curie temperature T_C , P-E hysteresis, bipolar and unipolar strain loops, piezoelectric constant d_{33} , planar coupling coefficient k_p , dielectric constant K , dielectric loss D and Rayleigh analysis for piezoelectric and dielectric response. Measurement procedures and methods used for these characterizations are discussed in previous chapter.

4.2 Physical and structural analysis

Analysis of starting metal oxide and carbonate powders was done for mean particle size, particle size distribution and LOI. Particle size of the starting powders found in the range of 1 to 10 μm . Appendix-A, shows the plots of particle size distribution and Appendix-B summaries LOI results for starting powders used for synthesis of $(1-x)\text{PbZrO}_3-x\text{PbTiO}_3$ and $(1-x)\text{BiScO}_3-x\text{PbTiO}_3$. Particle size less than $1\mu\text{m}$ were aimed

for satisfactory processing of these ceramics. Particle size analysis was done after each 24 hr milling; mean particle size after post calcination milling was found less than 0.5 μm . Figure 4.1, shows the distribution of particle size after 24 hrs milling for mixture of raw powders, after first, and second calcination for $(1-x)\text{PbZrO}_3-x\text{PbTiO}_3$ and $(1-x)\text{BiScO}_3-x\text{PbTiO}_3$.

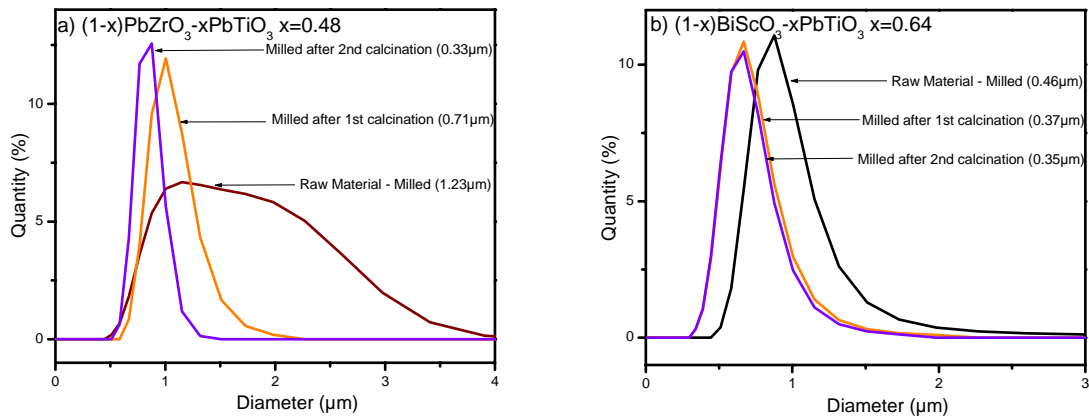


Figure 4.1. Particle size distribution after milling for $(1-x)\text{PbZrO}_3-x\text{PbTiO}_3$ and $(1-x)\text{BiScO}_3-x\text{PbTiO}_3$ powder before and after calcinations.

The development of perovskite phase after calcination was evaluated by θ -2 θ XRD using 1.5418\AA $\text{CuK}\alpha 1$ radiation. Figure 4.2, shows the XRD scans for powders after calcination. XRD scans for $(1-x)\text{PbZrO}_3-x\text{PbTiO}_3$ $x=0.48$ shows well defined single phase perovskite peaks. XRD scans for $(1-x)\text{BiScO}_3-x\text{PbTiO}_3$ $x=0.64$ and 0.66 shows small peak between $\{100\}$ and $\{110\}$ peaks which corresponds little impurity phase which was reacted completely in the sintering process.

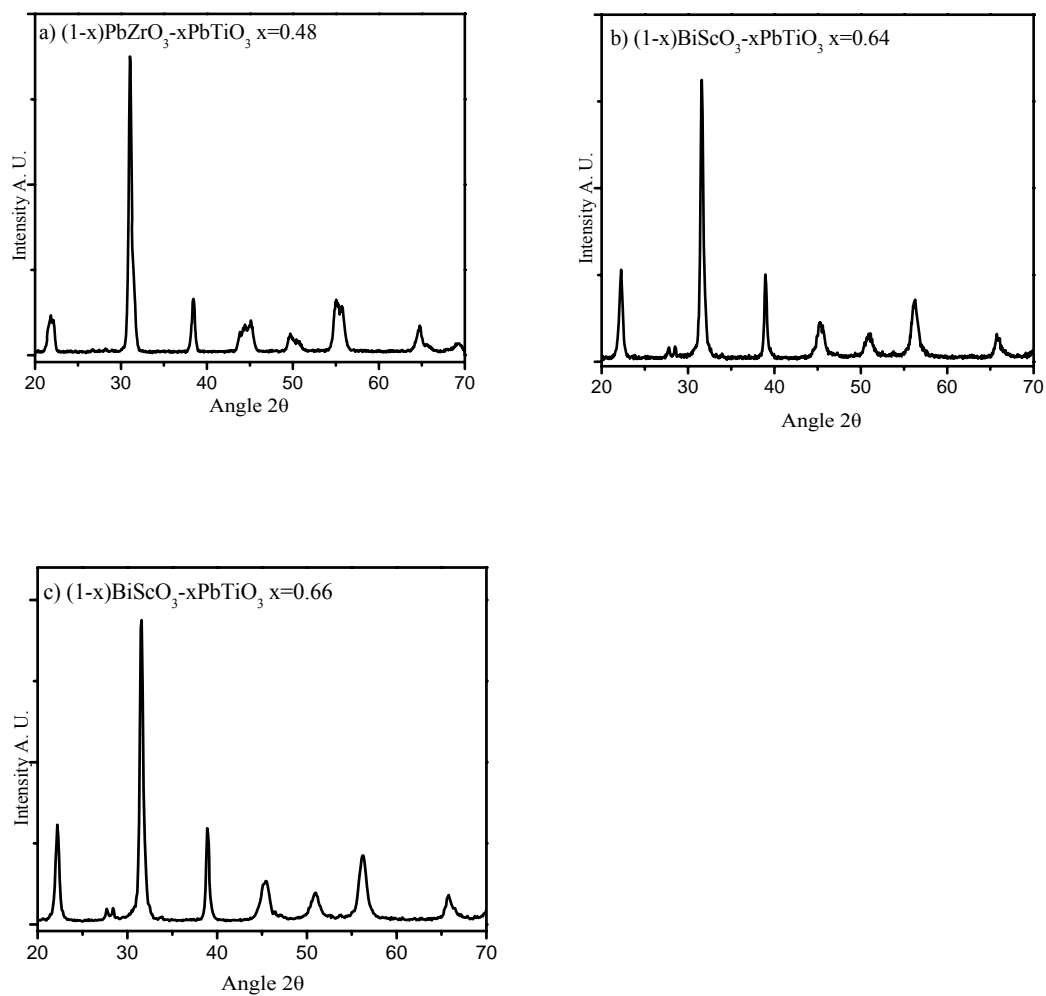


Figure 4.2. XRD scans after calcination for $(1-x)\text{PbZrO}_3-x\text{PbTiO}_3$ $x= 0.48$ and $(1-x)\text{BiScO}_3-x\text{PbTiO}_3$, $x=0.64$ and 0.66

XRD scans for crushed sintered pellets were done to analyze the crystal structure as shown in Figure 4.3. The MPB region corresponds to a mixed phase region. XRD scans for the MPB compositions of $(1-x)\text{PbZrO}_3\text{-}x\text{PbTiO}_3$ ($x=0.48$) and $(1-x)\text{BiScO}_3\text{-}x\text{PbTiO}_3$ ($x=0.64$) showed splitting of $\{100\}$ and $\{110\}$ peaks which indicate presence tetragonal phase along with rhombohedral phase. XRD scans for $(1-x)\text{BiScO}_3\text{-}x\text{PbTiO}_3$ ($x=0.66$) showed more splitting of these peaks which suggest more tetragonality. XRD scan for Fe-modified $(1-x)\text{PbZrO}_3\text{-}x\text{PbTiO}_3$ ($x=0.48$) is almost similar to unmodified composition whereas for Mn-modified $(1-x)\text{BiScO}_3\text{-}x\text{PbTiO}_3$ ($x=0.64$ and 0.66) intensity of all peaks was suppressed compared to unmodified compositions. The lattice parameters were calculated from the peak position in the XRD scans. Table 4.1, summarizes lattice parameters, and c/a ratio. Calculated c/a ratio for the $\text{BiScO}_3\text{-}x\text{PbTiO}_3$ $x=0.64$ and 0.66 were 1.023 and 1.028 respectively whereas for $(1-x)\text{PbZrO}_3\text{-}x\text{PbTiO}_3$ $x=0.48$ it was 1.026 .

Table 4.1, Lattice parameters for $(1-x)\text{PbZrO}_3\text{-}x\text{PbTiO}_3$ and $(1-x)\text{BiScO}_3\text{-}x\text{PbTiO}_3$ calculated from XRD scans.

Material		a (\AA)	c (\AA)	c/a
$(1-x)\text{PbZrO}_3\text{-}x\text{PbTiO}_3$ $x=0.48$	Unmodified	4.0333	4.1382	1.026
	Fe-modified	4.0290	4.1338	1.026
$(1-x)\text{BiScO}_3\text{-}x\text{PbTiO}_3$ $x=0.64$	Unmodified	3.9872	4.0800	1.023
	Mn-modified	3.9788	4.0676	1.022
$(1-x)\text{BiScO}_3\text{-}x\text{PbTiO}_3$ $x=0.66$	Unmodified	3.9735	4.0852	1.028
	Mn-modified	3.9747	4.0850	1.028

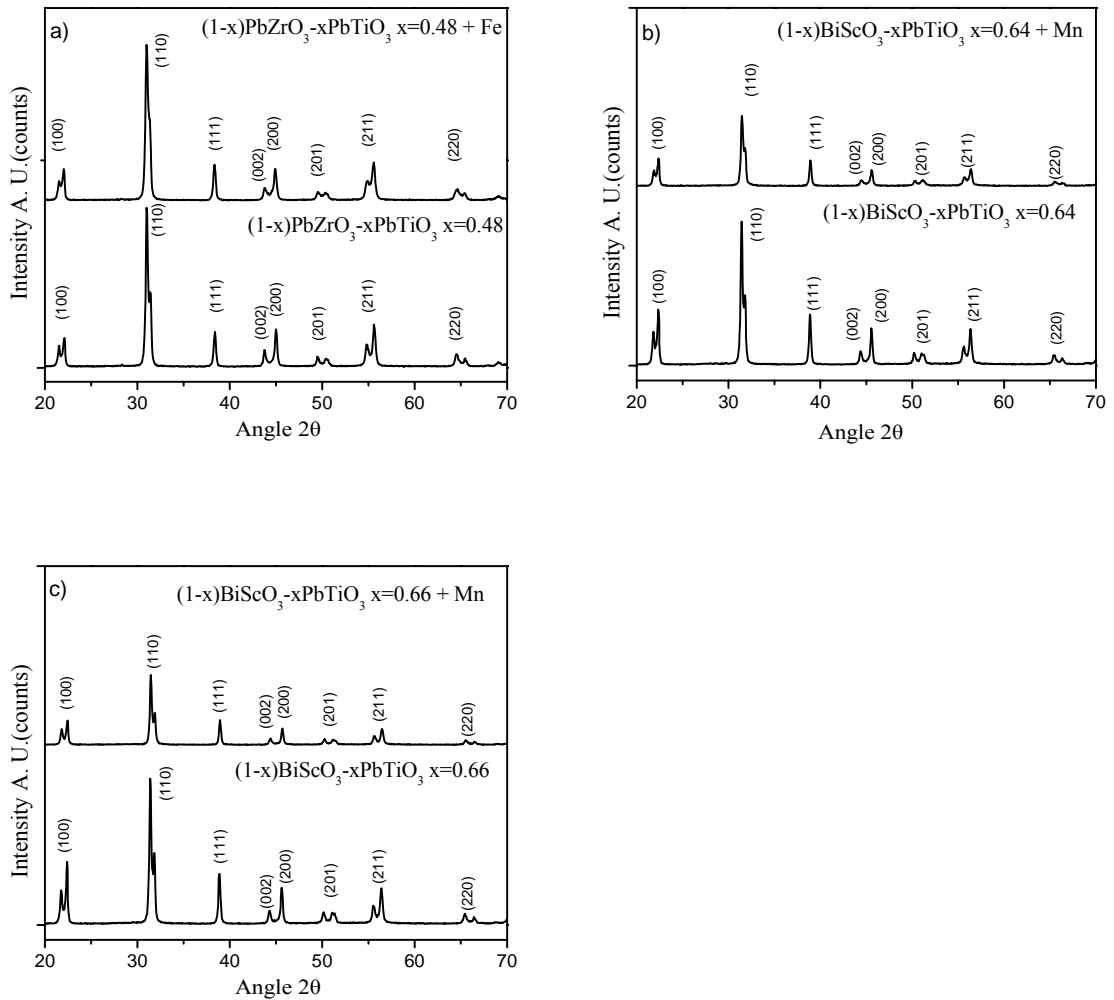


Figure 4.3. XRD scans of crushed pellets after sintering for unmodified and modified $(1-x)\text{PbZrO}_3\text{-}x\text{PbTiO}_3$ $x=0.48$, and $(1-x)\text{BiScO}_3\text{-}x\text{PbTiO}_3$ $x=0.64$ and 0.66 .

The detail sintering study was carried out to achieve maximum possible density and minimum volatilization loss of lead (Pb) in $(1-x)\text{PbZrO}_3\text{-}x\text{PbTiO}_3$ and Bismuth (Bi) and Pb in $(1-x)\text{BiScO}_3\text{-}x\text{PbTiO}_3$ system. Physical characterization of sintered pellets were carried out to evaluate density, microstructure and grain size using methods and procedures as described in previous chapter. Results of sintering studies for

(1-x)PbZrO₃-xPbTiO₃ and (1-x)BiScO₃-xPbTiO₃ are summarized in Table 4.2. Best densification of unmodified (1-x)PbZrO₃-xPbTiO₃ x=0.48 was achieved at 1200⁰C and addition of acceptor dopant Fe₂O₃ to it assisted to lower the sintering temperature to 1100⁰C, whereas in case of (1-x)BiScO₃-xPbTiO₃ doping with MnO₂ did not act as sintering aid. Sintering for unmodified and Mn-modified (1-x)BiScO₃-xPbTiO₃ was done at temperature 1100⁰C. Measured bulk density of sintered pellets decreases with increase in sintering temperature. Reduction in bulk density at high temperature is associated with higher weight loss due to volatilization.

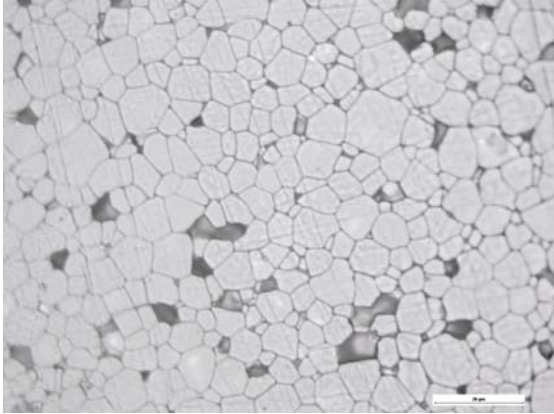
Average grain size was targeted ~10 μm for each composition to neutralize the grain size effect on aging study. Microphotographs were taken using either optical microscope or SEM, depending on the grain size. Figure 4.4 shows the microphotographs for unmodified and modified (1-x)PbZrO₃-xPbTiO₃ and (1-x)BiScO₃-xPbTiO₃. Microstructure for all the compositions shows equiaxed grains with scattered porosity and some grain pull out due to polishing of pellets. Microstructures do not show any abnormal grain growth.

Average grain size determined were 11 μm and 3 μm for unmodified and Fe-modified (1-x)PbZrO₃-xPbTiO₃ x=0.48, 10 μm and 12 μm for unmodified and Mn-modified (1-x)BiScO₃-xPbTiO₃ x=0.64, 8 μm and 11 μm for unmodified and Mn-modified (1-x)BiScO₃-xPbTiO₃ x=0.66. Average grain size for Fe-modified (1-x)PbZrO₃-xPbTiO₃ x=0.48 was smaller than the targeted value but high sintering temperature were resulting low resistivity for the sintered pellets.

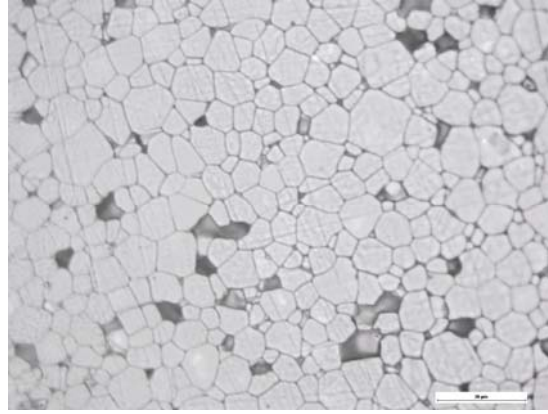
Table 4.2. Bulk density for (1-x)PbZrO₃-xPbTiO₃ and (1-x)BiScO₃-xPbTiO₃ after sintering.

Composition	Sintering Temperature °C	Bulk density (gm/cm ³)	% Theoretical density	% Weight loss
(1-x)PbZrO ₃ -xPbTiO ₃ x=0.48	1200	7.71	96.0	- 0.29
	1225	7.69	95.8	-0.22
	1250	7.65	95.3	-0.13
(1-x)PbZrO ₃ -xPbTiO ₃ x=0.48 + Fe	1050	7.69	95.5	0.01
	1100	7.81	96.9	0.09
	1200	7.83	97.1	0.24
	1250	7.67	95.2	0.42
(1-x)BiScO ₃ -xPbTiO ₃ x=0.64	1000	7.50	96.8	0.12
	1050	7.42	95.8	0.15
	1100	7.39	95.4	0.31
(1-x)BiScO ₃ -xPbTiO ₃ x=0.64 + Mn	1000	7.53	96.4	0.06
	1050	7.53	96.4	0.02
	1100	7.48	95.8	0.21
(1-x)BiScO ₃ -xPbTiO ₃ x=0.66	1000	7.54	96.7	0.14
	1050	7.47	95.9	0.14
	1100	7.42	95.2	0.37
(1-x)BiScO ₃ -xPbTiO ₃ x=0.66 + Mn	1000	7.54	96.8	0.27
	1050	7.52	96.6	0.31
	1100	7.46	95.7	0.36

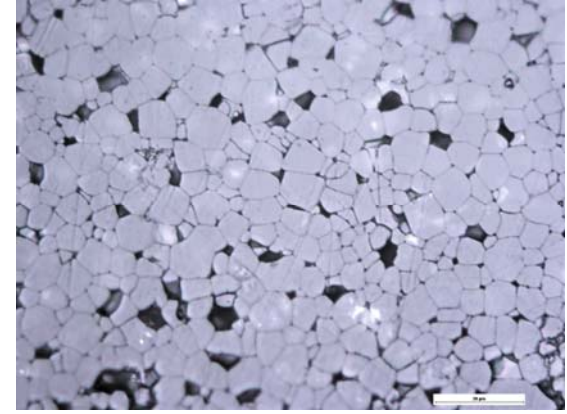
$(1-x)\text{PbZrO}_3-x\text{PbTiO}_3$ $x=0.48$



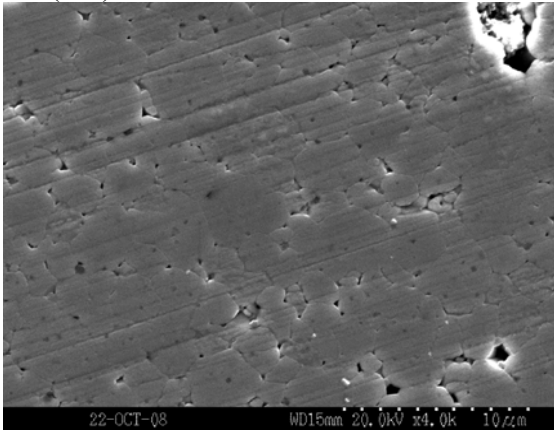
$(1-x)\text{BiScO}_3-x\text{PbTiO}_3$ $x=0.64$



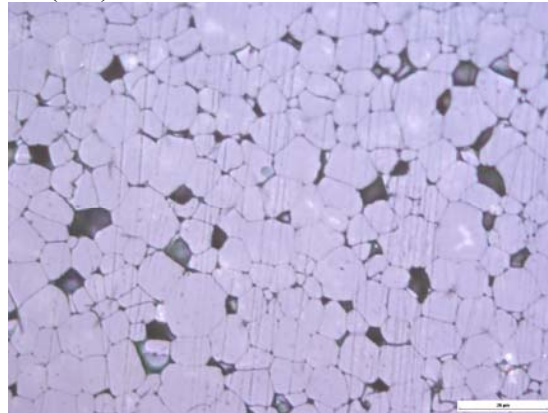
$(1-x)\text{BiScO}_3-x\text{PbTiO}_3$ $x=0.66$



$(1-x)\text{PbZrO}_3-x\text{PbTiO}_3$ $x=0.48 + \text{Fe}$



$(1-x)\text{BiScO}_3-x\text{PbTiO}_3$ $x=0.64 + \text{Mn}$



$(1-x)\text{BiScO}_3-x\text{PbTiO}_3$ $x=0.66 + \text{Mn}$

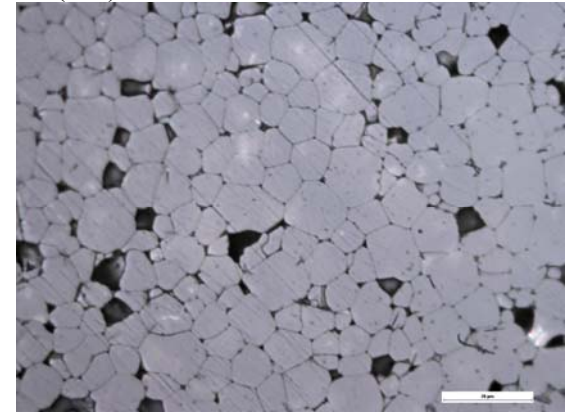


Figure 4.4. Microphotograph of the polished and thermally etched pellets for unmodified and Fe-modified $(1-x)\text{PbZrO}_3-x\text{PbTiO}_3$ $x=0.48$, and unmodified and Mn-modified $(1-x)\text{BiScO}_3-x\text{PbTiO}_3$ $x=0.64$ and 0.66 .

4.3 Unpoled properties

4.3.1 Dielectric constant (K) and dielectric loss (D)

Dielectric constant K and dielectric loss D were measured on virgin pellets prior to poling. The measured K and D were ~ 1050 and 0.015 for $(1-x)\text{PbZrO}_3-x\text{PbTiO}_3$ $x=0.48$, 950 and 0.008 for Fe-modified $(1-x)\text{PbZrO}_3-x\text{PbTiO}_3$ $x=0.48$, 1250 and 0.06 for $(1-x)\text{BiScO}_3-x\text{PbTiO}_3$ $x=0.64$, 1100 and 0.04 for Mn-modified $(1-x)\text{BiScO}_3-x\text{PbTiO}_3$ $x=0.64$, 1040 and 0.05 for $(1-x)\text{BiScO}_3-x\text{PbTiO}_3$ $x=0.66$, 1070 and 0.03 for Mn-modified $(1-x)\text{BiScO}_3-x\text{PbTiO}_3$ $x=0.66$. $(1-x)\text{PbZrO}_3-x\text{PbTiO}_3$ $x=0.48$ showed reduction in K after poling whereas $(1-x)\text{BiScO}_3-x\text{PbTiO}_3$ $x=0.64$ and 0.66 showed improvement which distinguish behavior of these two systems.

4.3.2 Ferroelectric Curie temperature (T_C)

The high temperature dielectric measurements were done on unpoled pellets at various frequencies from 1 KHz to 1 MHz. Relative permittivity K and dielectric losses D were measured as a function of temperature as shown in Figure 4.5(a & b). Ferroelectric Curie temperature T_C measured at the frequency 10 KHz are summarized in Table 4.4. T_C for unmodified and Fe-modified $(1-x)\text{PbZrO}_3-x\text{PbTiO}_3$ $x=0.48$ was 386°C and 388°C respectively. $(1-x)\text{BiScO}_3-x\text{PbTiO}_3$ $x=0.64$ and 0.66 showed T_C of 436°C and 446°C , whereas modification with Mn for these compositions increased their T_C to 438°C and 448°C respectively.

4.3.3 Polarization – electric field (P-E) hysteresis loop

Ferroelectric P-E hysteresis loops were measured at an electric field of 50kV/cm and frequency 1 Hz as shown in Figure 4.6. Coercive field E_C and remnant polarization P_R were extracted from P-E loops as summarized in Table 4.3. E_C for unmodified $(1-x)\text{PbZrO}_3\text{-xPbTiO}_3$ $x=0.48$ and $(1-x)\text{BiScO}_3\text{-xPbTiO}_3$ $x=0.64$, and 0.66 was 20kV/cm, 31kV/cm and 33 kV/cm respectively. P_R was $29 \mu\text{C}/\text{cm}^2$ for $(1-x)\text{BiScO}_3\text{-xPbTiO}_3$ $x=0.64$ and $33 \mu\text{C}/\text{cm}^2$ for $(1-x)\text{BiScO}_3\text{-xPbTiO}_3$ $x=0.66$. P-E hysteresis loop for Fe-modified $(1-x)\text{PbZrO}_3\text{-xPbTiO}_3$ $x=0.48$ shows pinching effect which indicate the instantaneous aging at ambient temperature for this material. P-E hysteresis loops for Mn modified $(1-x)\text{BiScO}_3\text{-xPbTiO}_3$ $x=0.64$, and 0.66 looks like soft piezoelectric material but those were hard for poling and this shape is likely to be due to low frequency used for the measurement.

Bipolar strain loops as shown in Figure 4.7(a, b, and c) have the symmetrical butterfly shape. Unipolar strain loops were measured on poled pellets as shown in Figure 4.7(d, e, and f). Substantial reduction in measured strain was observed for acceptor doped materials compared to unmodified compositions. High field d_{33} were obtained from the unipolar strain loops as summarized in Table 4.3. The MPB compositions $(1-x)\text{PbZrO}_3\text{-xPbTiO}_3$ $x=0.48$ and $(1-x)\text{BiScO}_3\text{-xPbTiO}_3$ $x=0.64$ shows high field $d_{33} = 489 \text{ pC}/\text{N}$ and $488 \text{ pC}/\text{N}$ respectively.

Table 4.3. Coercive field E_C , remnant polarization P_R and high field d_{33} for unmodified and modified $(1-x)\text{PbZrO}_3-x\text{PbTiO}_3$ and $(1-x)\text{BiScO}_3-x\text{PbTiO}_3$.

Material		Coercive field E_C (kV/cm)	Remnant polarization P_R ($\mu\text{C}/\text{cm}^2$)	High field d_{33} (10^{-12} C/N)
$(1-x)\text{PbZrO}_3-x\text{PbTiO}_3$ $x=0.48$	Unmodified	21	18	489
	Fe-modified	-	-	208
$(1-x)\text{BiScO}_3-x\text{PbTiO}_3$ $x=0.64$	Unmodified	31	29	488
	Mn-modified	18	15	360
$(1-x)\text{BiScO}_3-x\text{PbTiO}_3$ $x=0.66$	Unmodified	33	33	362
	Mn-modified	20	11	245

4.4 Poled properties

4.4.1 Dielectric constant (K) and dielectric loss (D)

Dielectric constant K and dielectric loss D were measured for the sets of 15 poled pellets for each composition. The average K and D were 766 and 0.011 for $(1-x)\text{PbZrO}_3-x\text{PbTiO}_3$ $x=0.48$ and Fe-modification improved K to 885 and reduced D to 0.006. $(1-x)\text{BiScO}_3-x\text{PbTiO}_3$ $x=0.64$ and 0.66, showed average K= 1678 and 1276 and average D = 0.025 and 0.016 respectively. Addition of acceptor dopants to $(1-x)\text{PbZrO}_3-x\text{PbTiO}_3$ and $(1-x)\text{BiScO}_3-x\text{PbTiO}_3$ both shows substantial reduction in dielectric losses D. Mn-modification reduced the dielectric losses to 0.006 for $\text{BiScO}_3-x\text{PbTiO}_3$ $x=0.66$. Results for K and D measured at 1 kHz are summarized in Table 4.4. Refer APPENDIX-E for the details of dielectric measurement done at frequency 100Hz, 1 kHz, 10 kHz and 100 kHz for individual samples.

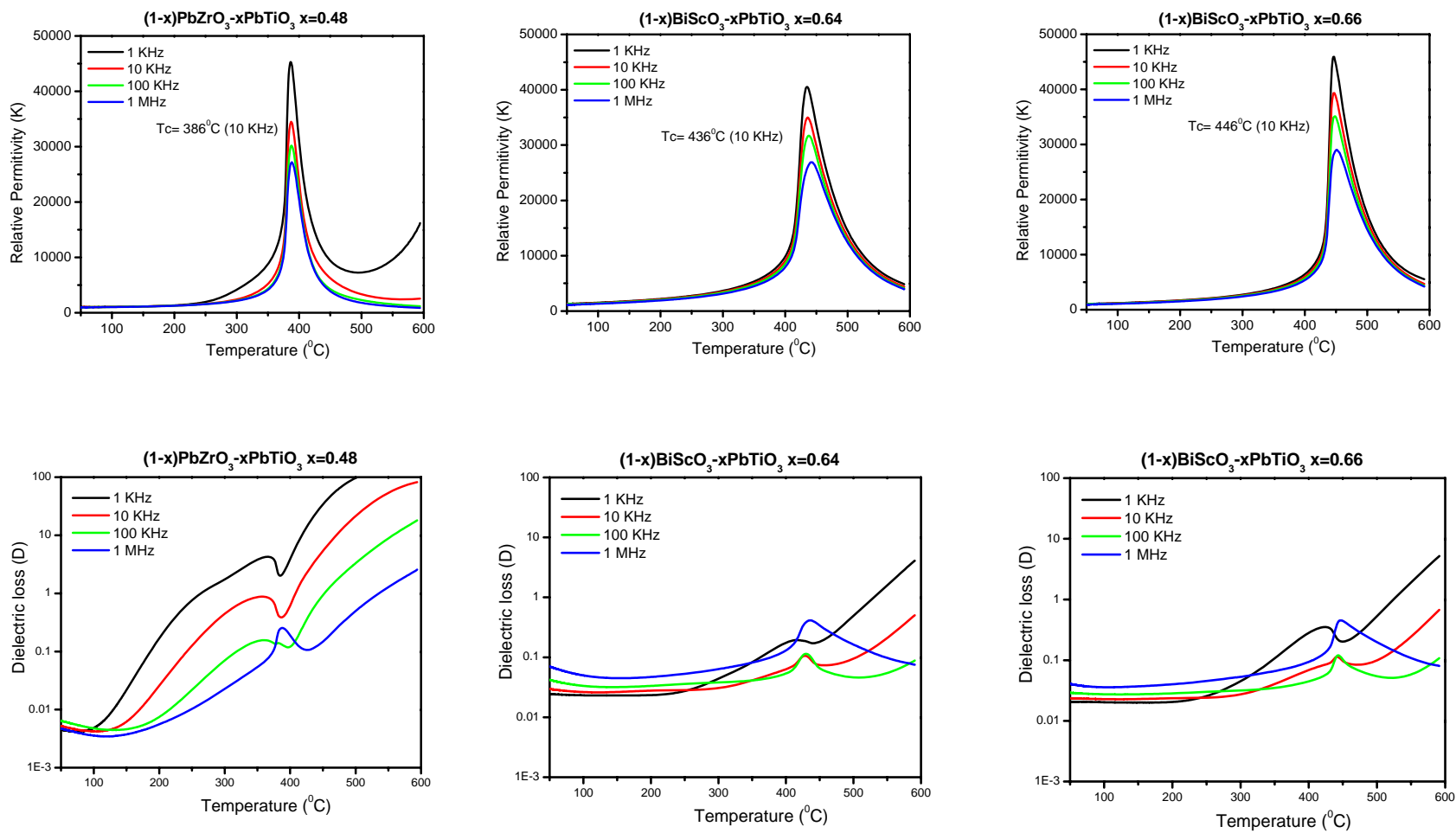


Figure 4.5 a). High temperature dielectric constant K and dielectric loss D for unmodified $(1-x)\text{PbZrO}_3-x\text{PbTiO}_3$ $x=0.48$ and $(1-x)\text{BiScO}_3-x\text{PbTiO}_3$ $x=0.64$ and 0.66 .

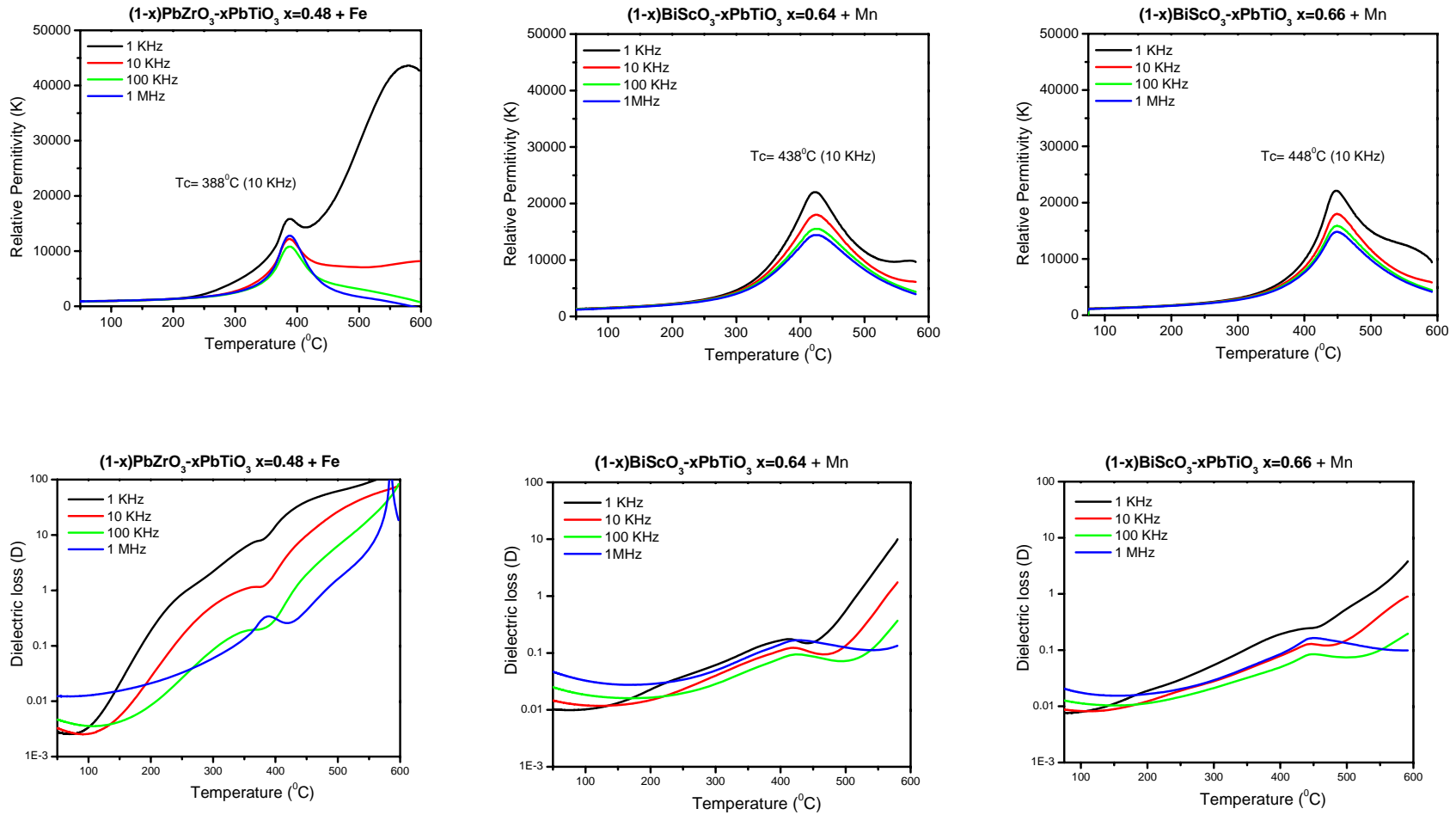


Figure 4.5 b). High temperature dielectric constant K and dielectric loss D for Fe-modified $(1-x)\text{PbZrO}_3-x\text{PbTiO}_3$ $x=0.48$, and Mn-modified $(1-x)\text{BiScO}_3-x\text{PbTiO}_3$ $x=0.64$ and 0.66 .

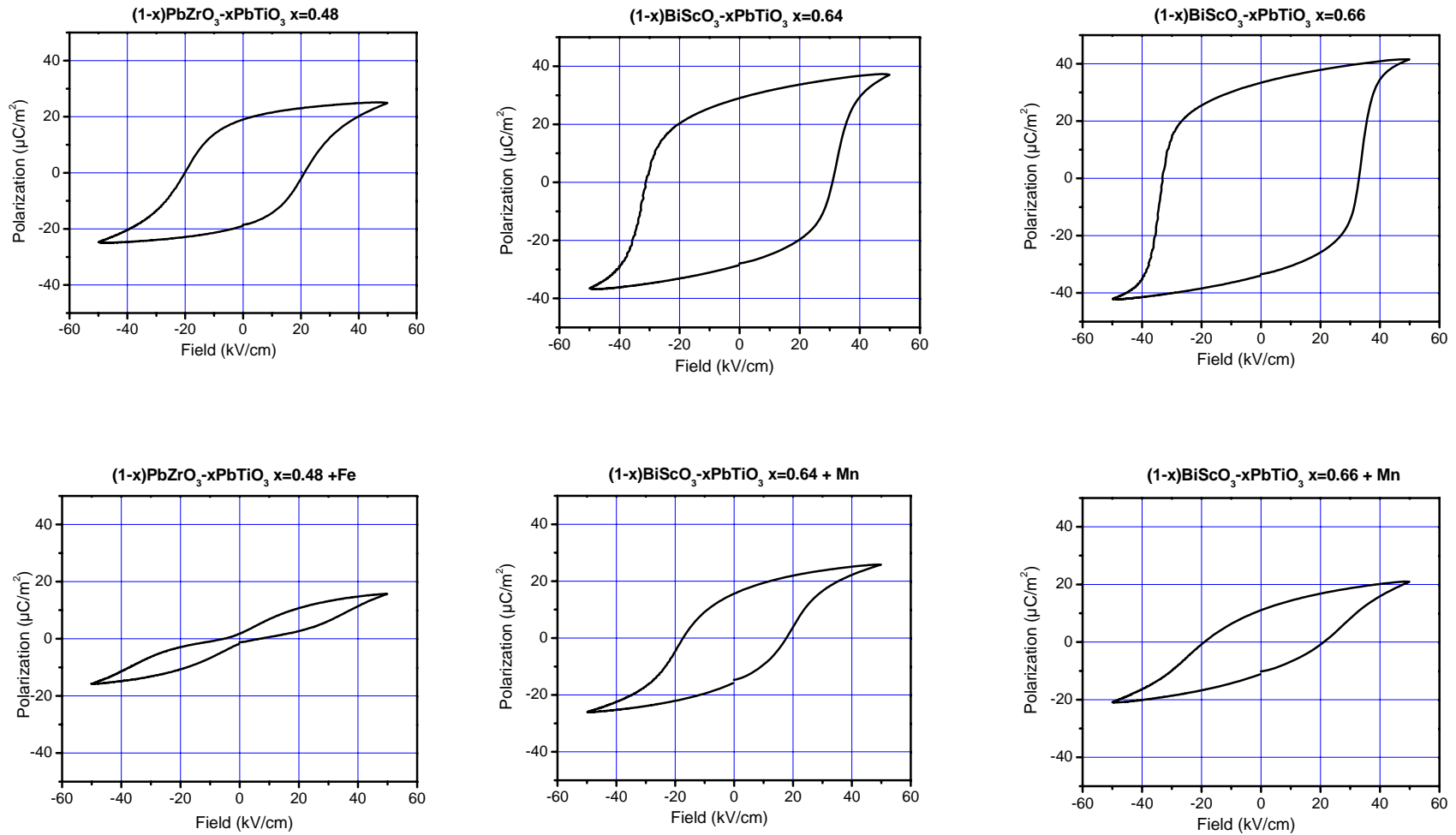


Figure 4.6 Ferroelectric P-E hysteresis loop for unmodified and Fe-modified $(1-x)\text{PbZrO}_3-x\text{PbTiO}_3$ $x=0.48$, and unmodified and Mn-modified $(1-x)\text{BiScO}_3-x\text{PbTiO}_3$ $x=0.64$ and 0.66 (measured at $50\text{kV}/\text{cm}$, 1 Hz)

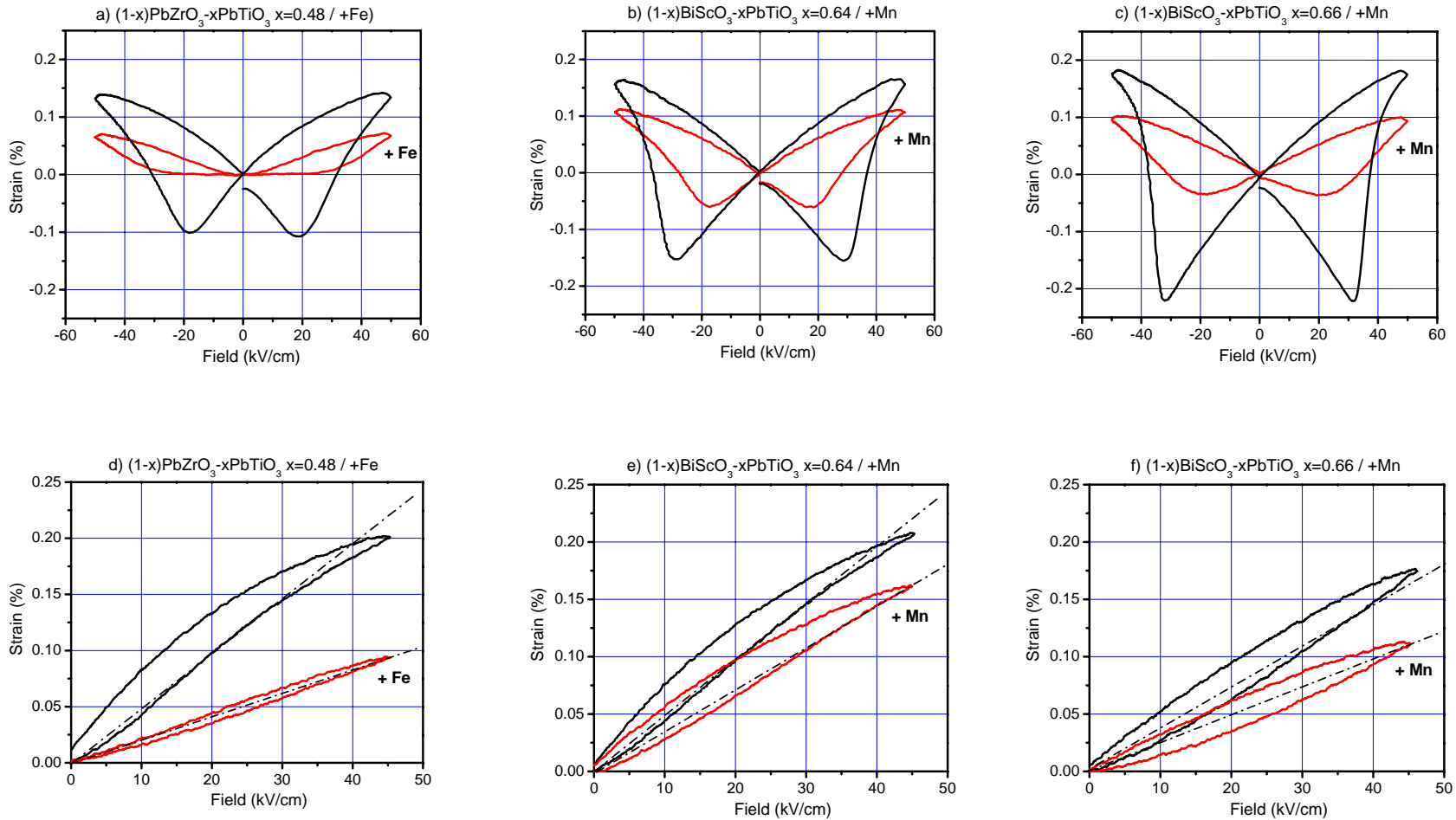


Figure 4.7 Bipolar and unipolar strain loop for unmodified and Fe modified $(1-x)\text{PbZrO}_3\text{-}x\text{PbTiO}_3$ $x=0.48$, and unmodified and Mn-modified $(1-x)\text{BiScO}_3\text{-}x\text{PbTiO}_3$ $x=0.64$ and 0.66 (measured at 50kV/cm , 1 Hz)

4.4.2 Piezoelectric constant (d_{33})

Piezoelectric constant d_{33} was measured using Berlincourt type d_{33} meter for the sets of 15 poled pellets for each composition. Average d_{33} for $(1-x)\text{PbZrO}_3-x\text{PbTiO}_3$ $x=0.48$, $(1-x)\text{BiScO}_3-x\text{PbTiO}_3$ $x=0.64$ and 0.66 were 215 pC/N, 382 pC/N and 256 pC/N respectively. Addition of acceptor dopants made these materials hard for poling and reduced the piezoelectric constant d_{33} . Complete summary of measured piezoelectric constant d_{33} is given in Table 4.4. Refer APPENDIX-G for the details of piezoelectric constant d_{33} for individual pellets. The measured low field piezoelectric constants d_{33} are $\sim 45\%$ to 85% compared to high field d_{33} obtained from unipolar loops for these materials.

4.4.3 Planar coupling coefficient (k_p)

Planar coupling coefficient k_p was measured using Impedance/ Gain- phase analyzer for two pellets for each compositions. $(1-x)\text{PbZrO}_3-x\text{PbTiO}_3$ $x=0.48$ showed the average $k_p = 0.26$ and $(1-x)\text{BiScO}_3-x\text{PbTiO}_3$ $x=0.64$ and 0.66 showed the average $k_p = 0.51$ and 0.42 respectively. Complete summary of measured planar coupling coefficient k_p is given in Table 4.4. Fe- modification helped to improved k_p for $(1-x)\text{PbZrO}_3-x\text{PbTiO}_3$ $x=0.48$.

Table 4.4, Measured electromechanical properties for (1-x)PbZrO₃-xPbTiO₃ and (1-x)BiScO₃-xPbTiO₃ pellets.

Material		Curie temperature (°C) T _c	Dielectric constant (1Khz) K		Dielectric loss (1Khz) D		Piezoelectric constant (pC/N) d ₃₃		Planar coupling coefficient k _p
			Average*	Range (Min-Max)	Average*	Range (Min-Max)	Average*	Range (Min-Max)	Average#
(1-x)PbZrO ₃ -xPbTiO ₃ x=0.48	Unmodified	386	766 (+/- 48)	696 - 841	0.011	0.010 - 0.014	215 (+/- 16)	193 - 236	0.26 (+/- 0.012)
	Fe-modified	388	885 (+/- 41)	823 - 970	0.006	0.004 - 0.008	177 (+/- 15)	162 - 207	0.37 (+/- 0.007)
(1-x)BiScO ₃ -xPbTiO ₃ x=0.64	Unmodified	436	1678 (+/- 99)	1547 - 1826	0.025	0.020 - 0.028	382 (+/- 27)	354 - 427	0.51 (+/- 0.005)
	Mn-modified	438	1103 (+/- 28)	1082 - 1127	0.009	0.008 - 0.010	234 (+/- 19)	207 - 256	0.35 (+/- 0.008)
(1-x)BiScO ₃ -xPbTiO ₃ x=0.66	Unmodified	446	1276 (+/- 71)	1151 - 1365	0.016	0.015 - 0.018	256 (+/- 20)	235 - 283	0.42 (+/- 0.006)
	Mn- modified	448	985 (+/- 28)	963 - 1015	0.005	0.005 - 0.006	109 (+/- 8)	103 - 118	0.18 (+/- 0.018)

* Average of 15 pellets, # Average of 2 pellets

4.5 Rayleigh analysis for dielectric and piezoelectric response

Rayleigh measurement for dielectric and piezoelectric responses were done on two polled pellets for each composition. K and d_{33} showed linear relation with the applied field. Plots for Rayleigh analysis for piezoelectric and dielectric responses as a function of applied electric field are shown in Figure 4.8 and Figure 4.9 respectively. The d_{33init} (Y-intercept) obtained from Rayleigh analysis were 357 pC/N, and 272 pC/N for $(1-x)\text{BiScO}_3-x\text{PbTiO}_3$ $x=0.64$ and 0.66 respectively, which are within $\pm 10\%$ compared to low field d_{33} measured for the same samples. Similarly K_{init} obtained from Rayleigh analysis were 750, 1639, and 1324 for $(1-x)\text{PbZrO}_3-x\text{PbTiO}_3$ $x=0.48$, $(1-x)\text{BiScO}_3-x\text{PbTiO}_3$ $x=0.64$ and $x=0.66$ respectively, which are within $\pm 1\%$ compared to low field K measured for the same samples. High values of α_d (10^{-14} Cm/NV) for the MPB compositions $(1-x)\text{PbZrO}_3-x\text{PbTiO}_3$ $x=0.48$ and $(1-x)\text{BiScO}_3-x\text{PbTiO}_3$ $x=0.64$ indicate significant role of the extrinsic contribution due to motion of non- 180° domain walls. The tetragonal composition $(1-x)\text{BiScO}_3-x\text{PbTiO}_3$ $x=0.66$ showed lower α_d (10^{-14} Cm/NV) and α_e (10^{-3} m/V). Rayleigh analysis for acceptor doped compositions showed more deviation from the low field measurements, which is most likely due to addition of dopant to these materials with out charge and site compensations. The summary of the results for the Rayleigh analysis for piezoelectric and dielectric responses is given in Table 4.5 along with low field d_{33} and K .

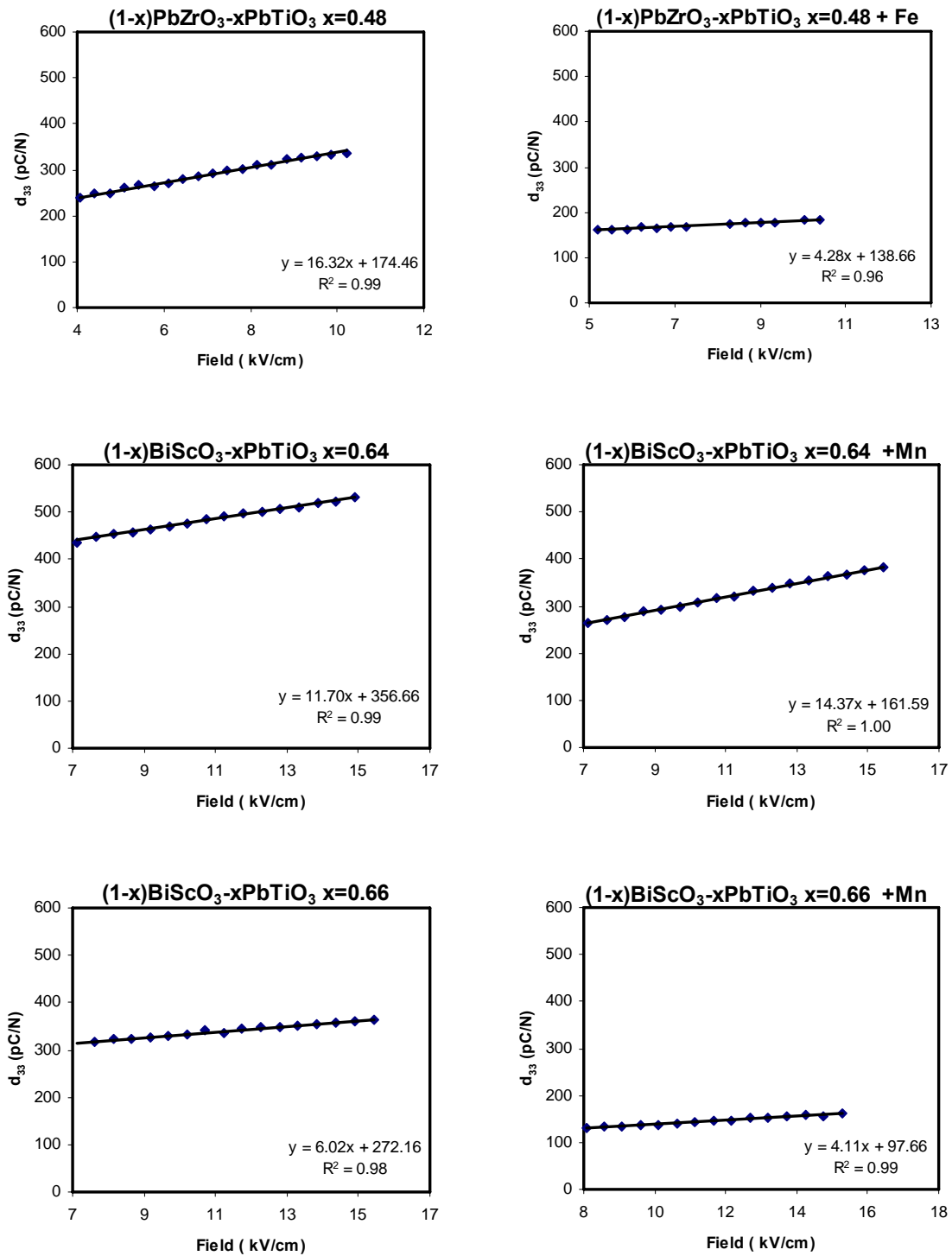


Figure 4.8 Rayleigh analysis, piezoelectric response as a function of applied electric field for unmodified and modified $(1-x)\text{PbZrO}_3-x\text{PbTiO}_3$ and $(1-x)\text{BiScO}_3-x\text{PbTiO}_3$.

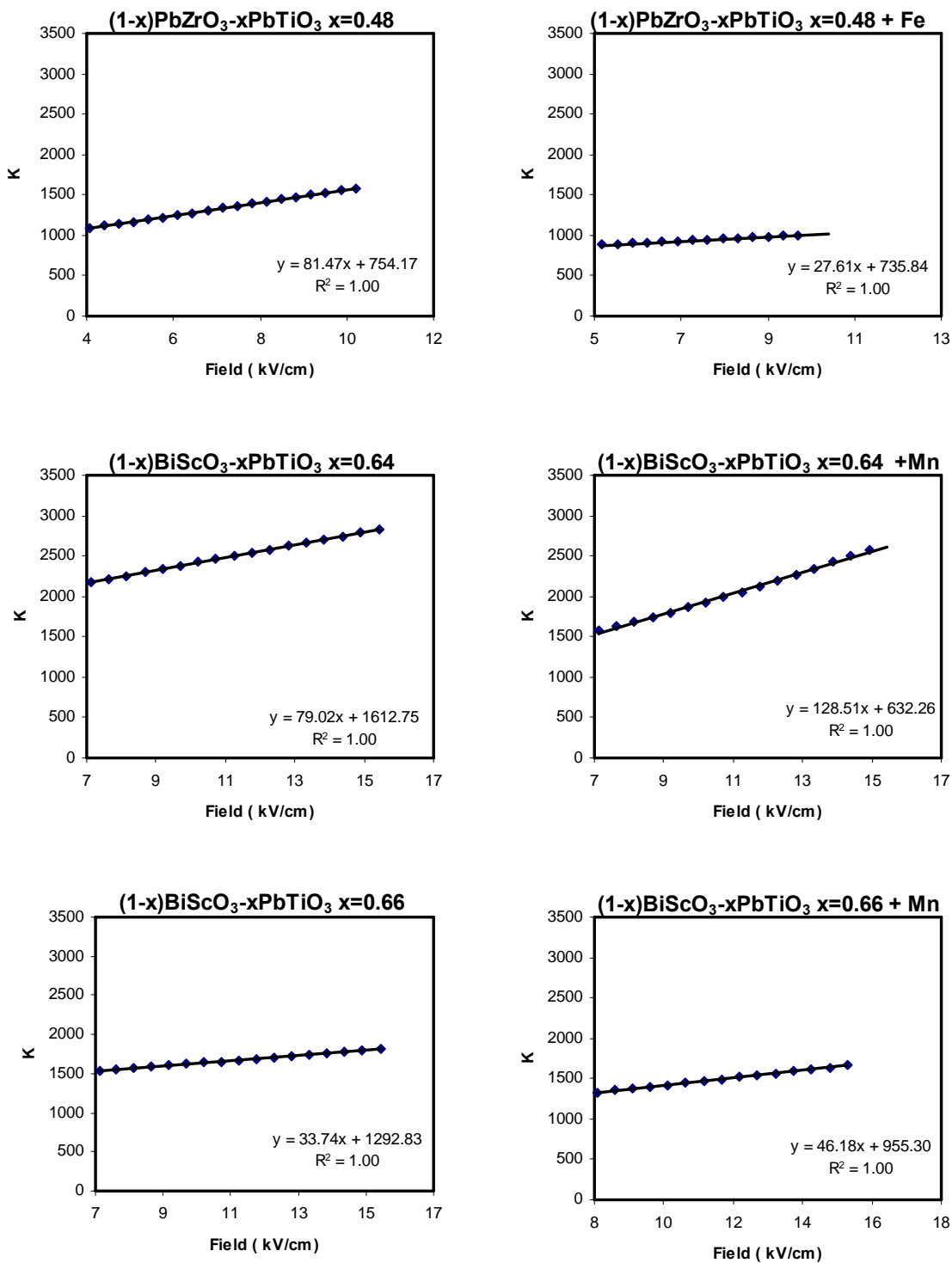


Figure 4.9 Rayleigh analysis, dielectric responses as a function of applied electric field for unmodified and modified $(1-x)\text{PbZrO}_3-x\text{PbTiO}_3$ and $(1-x)\text{BiScO}_3-x\text{PbTiO}_3$.

Table 4.5, Rayleigh parameters of piezoelectric and dielectric responses for (1-x)PbZrO₃-xPbTiO₃ and (1-x)BiScO₃-xPbTiO₃.

Material		Piezoelectric response		Dielectric response		Measured properties	
		$d_{33 \text{ init}}$ (pC/N)	α_d (10^{-14} Cm/NV)	$K \text{ init}$	α_ϵ (10^{-3} m/V)	d_{33} (pC/N)	K
(1-x)PbZrO ₃ -xPbTiO ₃ x=0.48	Unmodified	174	1.63	754	0.81	223	750
	Fe-modified	139	0.43	736	0.28	188	886
(1-x)BiScO ₃ -xPbTiO ₃ x=0.64	Unmodified	357	1.17	1613	0.79	390	1639
	Mn-modified	162	1.44	632	1.29	237	1111
(1-x)BiScO ₃ -xPbTiO ₃ x=0.66	Unmodified	272	0.60	1293	0.38	282	1324
	Mn- modified	98	0.41	955	0.46	117	1002

4.6 Summary and conclusion

The purpose of this study was to do the characterization of virgin pellets and obtain a set of electromechanical properties which would provide basis for further thermal degradation and aging study. Unpoled pellets were characterized to evaluate ferroelectric Curie temperature T_C , P-E hysteresis and strain- field loops. Dielectric constant K , dielectric loss D and piezoelectric constant d_{33} were measured on optimally poled pellets. Two pellets from each set were characterized for planar coupling coefficient k_p and Rayleigh analysis. Set of 15 pellets from each compositions within +/- 10% of the mean properties were selected for thermal degradation and aging study.

Ferroelectric Curie temperature T_C , dielectric constant K , and piezoelectric constant d_{33} measured for $(1-x)\text{PbZrO}_3\text{-}x\text{PbTiO}_3$ $x=0.48$ were 386°C , 766, 215 pC/N respectively which are similar to the properties reported by Jaffe et al.1971.³ $(1-x)\text{BiScO}_3\text{-}x\text{PbTiO}_3$ $x=0.64$ and 0.66 showed $T_C= 436^\circ\text{C}$ and 446°C , whereas Mn-modification to these compositions increased their T_C to 438°C and 448°C respectively. The T_C measured for $(1-x)\text{BiScO}_3\text{-}x\text{PbTiO}_3$ compositions were $\sim 15^\circ\text{C} - 20^\circ\text{C}$ less compared to valued reported by Eitel et al. 2002 and 2005.^{41,48} The average d_{33} , K and k_p for $(1-x)\text{BiScO}_3\text{-}x\text{PbTiO}_3$ $x=0.66$ were 256 pC/N, 1365, and 0.42 which are similar to value reported for prior studies.⁴¹ The MPB composition $(1-x)\text{BiScO}_3\text{-}x\text{PbTiO}_3$ $x=0.64$ showed average $d_{33} = 382$ pC/N, actual measurement for various sample in the set of 15 pellets showed d_{33} as high as 427 pC/N which is very close to the value reported by Eitel et al. 2002.⁴¹ The dielectric and piezoelectric properties for Mn-modified $(1-x)\text{BiScO}_3\text{-}x\text{PbTiO}_3$ are much less than reported by peer studies which is most likely due to addition

of dopant without charge and site compensation. For compositions near the MPB $(1-x)\text{BiScO}_3-x\text{PbTiO}_3$ system shows $\Delta T_C \sim 4^\circ\text{C}/\text{mol}\% \text{PbTiO}_3$.⁴² Low T_C obtained for the processed materials are possibly due to different raw materials, minor variation in compositions, and sintering conditions.

It can be concluded from this study that the set of piezoelectric and dielectric properties obtained from above characterization are comparable with the novel studies done in the past and would provide good basis for thermal degradation and aging study.

Chapter 5: Thermal degradation and aging

5.1 Introduction

Long term reliability of technological piezoelectric devices is a major concern for their applications. Many piezoelectric materials undergo processes of degradation and aging, associated with the change in their electromechanical properties, such as piezoelectric coefficient, dielectric constant, and electromechanical coupling factor etc.^{39,56} The most important parameters which cause degradation of piezoelectric properties are high temperature, stress and strong electrical field.¹⁹ Piezoelectric ceramics suffer from loss of polarization as dipoles have a tendency to revert back to random orientation at high temperature; this loss of polarization is called thermal degradation. Aging should be considered separately to thermal degradation which usually implies a large detrimental change to a property of a material. Aging is the spontaneous change of a material property with time, under zero external stress and constant temperature.⁵⁶ This study mainly focused to evaluate the isothermal aging effect on piezoelectric and dielectric properties of the high temperature piezoelectric ceramic $(1-x)\text{BiScO}_3-x\text{PbTiO}_3$ and compared to the commercially dominant piezoelectric ceramic $(1-x)\text{PbZrO}_3-x\text{PbTiO}_3$.

Unmodified and modified $(1-x)\text{PbZrO}_3-x\text{PbTiO}_3$ ($x=0.48$) and $(1-x)\text{BiScO}_3-x\text{PbTiO}_3$ ($x=0.64$ and 0.66) ceramics were prepared using conventional mixed oxides solid state method as discussed in Chapter 3. Characterization of the virgin poled pellets was done to evaluate initial piezoelectric and dielectric properties as discussed in Chapter 4. These pellets were kept at the controlled temperature of 250°C for

1000 hours. Change in the piezoelectric constant d_{33} , planar coupling coefficient k_p , dielectric constant K , and dielectric loss D was analyzed at predetermined intervals to evaluate aging rates.

5.2 Aging study

5.2.1 Thermal conditioning

Characterization of poled virgin pellets was done after 24 hours for piezoelectric constant d_{33} , planar coupling coefficient k_p , dielectric constant K , dielectric loss D , and Rayleigh measurement for dielectric and piezoelectric responses. Based on preliminary high temperature aging study carried out on limited samples for these material 250°C was selected as an optimum temperature for the thermal degradation and aging study. Temperatures more than 250°C were resulted in excessive increase of dielectric loss D and accelerated degradation of $(1-x)\text{PbZrO}_3-x\text{PbTiO}_3$. For the current aging study sets of pellets were heated to the temperature 250°C and removed from the oven after 1 min and allowed to cool down to ambient temperature. This was done to analyze the instantaneous thermal depoling effect. The characterization of the pellets was done and properties after 1min heating was considered as conditioned properties for further aging study.

5.2.2 Isothermal aging

Sets of 15 pellets from each compositions of unmodified and modified $(1-x)\text{PbZrO}_3-x\text{PbTiO}_3$ ($x=0.48$) and $(1-x)\text{BiScO}_3-x\text{PbTiO}_3$ ($x=0.64$ and 0.66) were reloaded in the oven maintained at the constant temperature of 250°C ($\pm 5^{\circ}\text{C}$) for total time of 1000h after instantaneous thermal degradation analysis as above. Characterization

of these pellets was done for piezoelectric and dielectric properties at predetermined intervals of 1h, 10h, 100h, 200h, 400h, 700h, and 1000h. Results were analyzed to establish the aging rates for piezoelectric constant d_{33} , and planar coupling coefficient k_p . Rayleigh analysis was done on two pellets from each composition to evaluate the change in piezoelectric and dielectric responses with the aging time. Aging of the piezoelectric and dielectric properties show linear change with time on logarithmic scale.⁵⁶ Aging rates were calculated (%/decade) from the slope of the graphs. Variation in aging rate for the individual samples were taken into consideration and reported as uncertainty along with the average values.

5.3 Results and discussion

5.3.1 Thermal conditioning

Unmodified and modified $(1-x)\text{PbZrO}_3-x\text{PbTiO}_3$ ($x=0.48$) and $(1-x)\text{BiScO}_3-x\text{PbTiO}_3$ ($x=0.64$ and 0.66) pellets were heated to the temperature 250°C for 1min and cooled down to ambient temperature. Piezoelectric and dielectric characterization was done to evaluate instantaneous thermal degradation for piezoelectric constant d_{33} , planar coupling coefficient k_p , dielectric constant K , and dielectric loss D . Piezoelectric and dielectric properties before and after thermal conditioning for $(1-x)\text{PbZrO}_3-x\text{PbTiO}_3$ and $(1-x)\text{BiScO}_3-x\text{PbTiO}_3$ are summarized in Table 5.1. As expected piezoelectric constant d_{33} , and planar coupling coefficient k_p showed reduction in comparison with virgin properties. Unmodified $(1-x)\text{BiScO}_3-x\text{PbTiO}_3$ ($x=0.64$ and 0.66) showed reduction in dielectric constant K whereas

Table 5.1, Electromechanical properties for (1-x)PbZrO₃-xPbTiO₃ and (1-x)BiScO₃-xPbTiO₃ pellets after thermal conditioning at 250⁰C for 1 min, compared to poled properties.

Material		Curie temperature (⁰ C) T _c	Piezoelectric constant *		Planar coupling coefficient #		Dielectric constant *		Dielectric loss *	
			(10 ⁻¹² C/N)		k _p		(1Khz) K		(1Khz) D	
			Polled	Conditioned	Polled	Conditioned	Polled	Conditioned	Polled	Conditioned
(1-x)PbZrO ₃ -xPbTiO ₃ x=0.48	Unmodified	386	215	200	0.26	0.22	0.011	0.013	766	786
	Fe modified	388	177	145	0.37	0.32	0.006	0.004	885	941
(1-x)BiScO ₃ -xPbTiO ₃ x=0.64	Unmodified	436	382	356	0.51	0.48	0.025	0.034	1678	1655
	Mn modified	438	234	228	0.35	0.35	0.009	0.019	1103	1187
(1-x)BiScO ₃ -xPbTiO ₃ x=0.66	Unmodified	446	256	245	0.42	0.40	0.016	0.018	1276	1264
	Mn modified	448	109	84	0.18	0.15	0.005	0.010	985	1021

Polled properties – after 24 hrs, * Average of 15 pellets, # Average of 2 pellets,

Mn-modified $(1-x)\text{BiScO}_3\text{-xPbTiO}_3$ ($x=0.64$ and 0.66) as well as unmodified and Fe-modified $(1-x)\text{PbZrO}_3\text{-xPbTiO}_3$ ($x=0.48$) showed the improvement in K after 1 min heating at 250°C . Dielectric loss D was reduced from 0.006 to 0.004 for Fe-modified $(1-x)\text{PbZrO}_3\text{-xPbTiO}_3$ ($x=0.48$) whereas all other material showed little increase in dielectric loss D after the thermal treatment.

5.3.2 Piezoelectric constant (d_{33})

Piezoelectric constant d_{33} was measured using Berlincourt type d_{33} meter for the set of 15 pellets for unmodified and Fe-modified $(1-x)\text{PbZrO}_3\text{-xPbTiO}_3$ ($x=0.48$), and unmodified and Mn-modified $(1-x)\text{BiScO}_3\text{-xPbTiO}_3$ ($x=0.64$ and 0.66) at the predetermined intervals as stated above. The degradation of piezoelectric constant d_{33} as a function of aging time is shown in the Figure 5.1. At the high temperature the dipole have tendency to revert back to random orientation resulted in decrease of piezoelectric constant d_{33} with the increase in temperature similarly with time dipoles get more time to revert back to random orientation. As expected all material showed reduction in piezoelectric constant d_{33} with the increase in aging time. Analysis of the measured data was done to calculate aging rate for the piezoelectric constant d_{33} . Aging rate for piezoelectric constant d_{33} for unmodified, and Fe-modified $(1-x)\text{PbZrO}_3\text{-xPbTiO}_3$ and $(1-x)\text{BiScO}_3\text{-xPbTiO}_3$ are summarized in Table 5.2. Unmodified $(1-x)\text{PbZrO}_3\text{-xPbTiO}_3$ ($x=0.48$) showed high aging rate of 4.8%/decade. Fe- modification to $(1-x)\text{PbZrO}_3\text{-xPbTiO}_3$ ($x=0.48$) reduced the piezoelectric constant d_{33} to $145 (10^{-12} \text{ C/N})$ from $200 (10^{-12} \text{ C/N})$ but assisted to reduce aging rate to 0.9%/decade. Tetragonal $(1-x)\text{BiScO}_3\text{-xPbTiO}_3$ ($x=0.66$) showed very low aging rate of 0.8% /decade and MPB composition

(1-x)BiScO₃-xPbTiO₃ x=0.64 showed moderate aging rate of 2.1%/decade. Mn-modification to (1-x)BiScO₃-xPbTiO₃ did not help to lower the aging rates.

5.3.3 Planar coupling coefficient (k_p)

Planar coupling coefficient k_p was measured using gain-impedance analyses for two pellets for each compositions of unmodified and Fe-modified (1-x)PbZrO₃-xPbTiO₃ (x=0.48), unmodified and Mn-modified (1-x)BiScO₃-xPbTiO₃ (x=0.64 and 0.66) at the predetermined intervals as stated above. The degradation of planar coupling coefficient k_p as a function of aging time is shown in the Figure 5.2. k_p showed decreasing trends with increase in aging time for all above materials. Aging rates for planar coupling coefficient k_p calculated based on the slope of the plots are summarized in Table 5.2. Unmodified (1-x)PbZrO₃-xPbTiO₃ (x=0.48) showed high aging rate of 3.9%/decade for planar coupling coefficient k_p . Fe- modification to (1-x)PbZrO₃-xPbTiO₃ (x=0.48) improved planar coupling coefficient k_p from 0.22 to 0.32 and also reduced the aging rate to 0.6%/decade from 3.9%/decade. (1-x)BiScO₃-xPbTiO₃ x=0.66 shows very low aging rate of 0.6% /decade, followed by x=0.64, 0.8%/decade. Mn-modification to (1-x)BiScO₃-xPbTiO₃ (x=0.64 and 0.66) did not help to improve the aging behavior.

5.3.4 Dielectric constant K and dielectric loss D

Dielectric characterization of unmodified and modified (1-x)PbZrO₃-xPbTiO₃ and (1-x)BiScO₃-xPbTiO₃ pellets was done at using multi frequency LCR meter (Model-4274A, Hewlett Packard) at predetermined time interval as stated above. Figure 5.3 and 5.4 shows the plots for measured dielectric constant K and dielectric loss D as a function

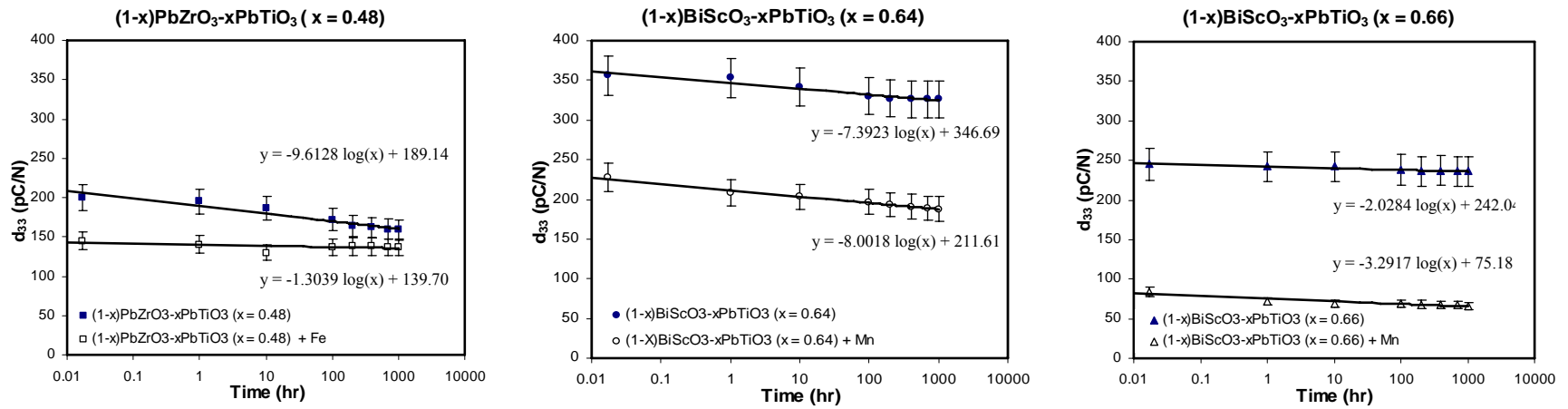


Figure 5.1 Aging study at 250°C, piezoelectric constant d_{33} as a function of aging time for unmodified and modified (1-x)PbZrO₃- xPbTiO₃ x=0.48, and (1-x)BiScO₃-xPbTiO₃ x=0.64 and 0.66.

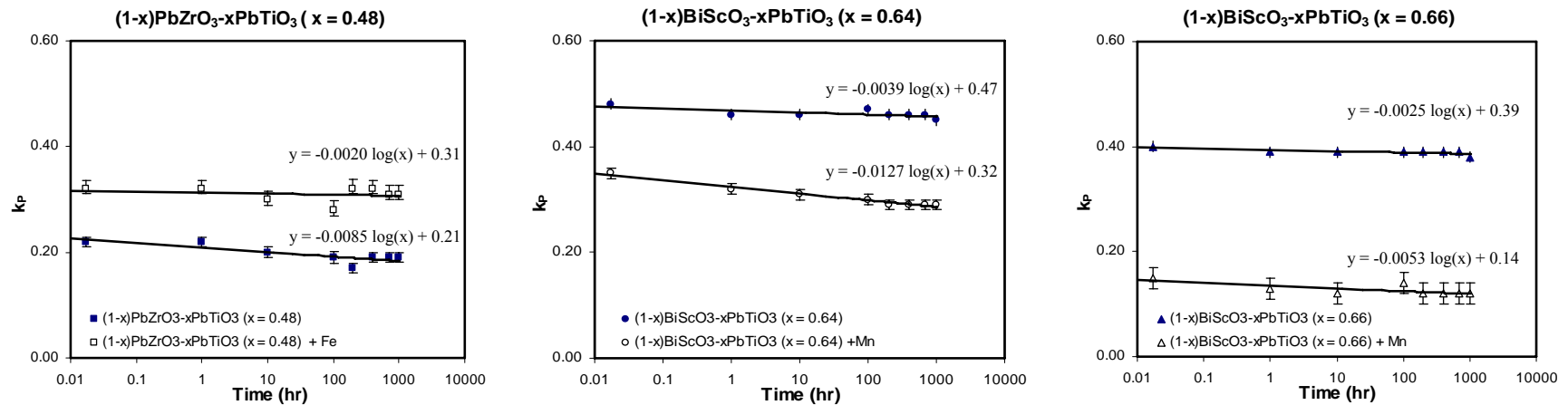


Figure 5.2 Aging study at 250°C, planar coupling coefficient k_p as a function of aging time for unmodified and modified (1-x)PbZrO₃-xPbTiO₃ x=0.48, and (1-x)BiScO₃-xPbTiO₃ x=0.64 and 0.66.

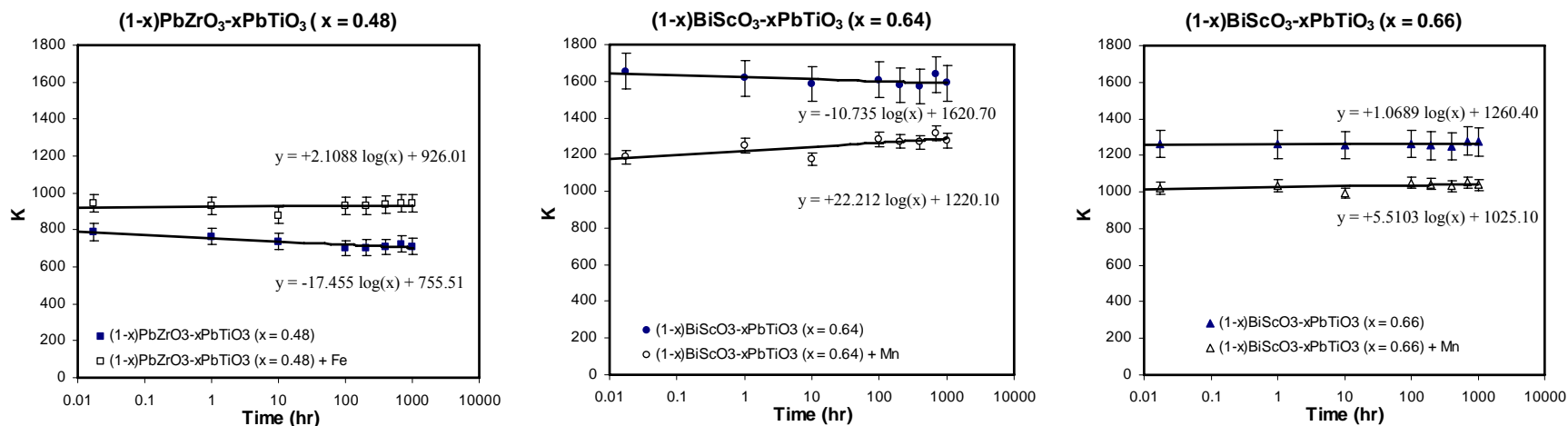
of aging time. Aging rates for dielectric constant K calculated based on the slope of the plots are summarized in Table 5.2. Unmodified $(1-x)\text{PbZrO}_3\text{-}x\text{PbTiO}_3$ ($x=0.48$) shows high aging rate of 2.2%/decade for dielectric constant K. Fe-modification to $(1-x)\text{PbZrO}_3\text{-}x\text{PbTiO}_3$ ($x=0.48$) changed the behavior of material and K showed improvement with aging. Aging rate for Fe-modified $(1-x)\text{PbZrO}_3\text{-}x\text{PbTiO}_3$ ($x=0.48$) was -0.2%/decade. $(1-x)\text{BiScO}_3\text{-}x\text{PbTiO}_3$ $x=0.64$ shows moderate aging rate of 0.6% /decade, whereas $(1-x)\text{BiScO}_3\text{-}x\text{PbTiO}_3$ $x=0.66$ showed very high resistance against dielectric aging, calculated aging rate was -0.08% /decade. Mn-modification to $(1-x)\text{BiScO}_3\text{-}x\text{PbTiO}_3$ ($x=0.64$ and 0.66) did not help to improve the aging behavior.

Dielectric loss D did not show any abnormal increase during 1000 hr aging period for any of the above compositions. Unmodified and Fe-modified $(1-x)\text{PbZrO}_3\text{-}x\text{PbTiO}_3$ ($x=0.48$) and unmodified and Mn-modified $(1-x)\text{BiScO}_3\text{-}x\text{PbTiO}_3$ ($x=0.66$) showed dielectric loss D less than 0.02 whereas unmodified and Mn-modified $(1-x)\text{BiScO}_3\text{-}x\text{PbTiO}_3$ ($x=0.64$) showed dielectric loss D less than 0.04.

Table 5.2, Aging rate for piezoelectric constant d_{33} , planar coupling coefficient k_p , and dielectric constant K for $(1-x)\text{PbZrO}_3-x\text{PbTiO}_3$ and $(1-x)\text{BiScO}_3-x\text{PbTiO}_3$ (at 250°C).

Material	Curie temperature ($^\circ\text{C}$) T_c	Piezoelectric constant * (10^{-12} C/N) d_{33}			Planar coupling coefficient # k_p			Dielectric constant * (1Khz) K			
		Poled	Conditioned	Aging rate (%/ decade)	Poled	Conditioned	Aging rate (%/ decade)	Poled	Conditioned	Aging rate (%/ decade)	
$(1-x)\text{PbZrO}_3-x\text{PbTiO}_3$ $x=0.48$	Unmodified	386	215	200	4.8	0.26	0.22	3.9	766	786	2.2
	Fe modified	388	177	145	0.9	0.37	0.32	0.6	885	941	-0.2
$(1-x)\text{BiScO}_3-x\text{PbTiO}_3$ $x=0.64$	Unmodified	436	382	356	2.1	0.51	0.48	0.8	1678	1655	0.6
$(1-x)\text{BiScO}_3-x\text{PbTiO}_3$ $x=0.66$	Unmodified	446	256	245	0.8	0.42	0.40	0.6	1276	1264	-0.08

* Average of 15 pellets, # Average of 2 pellets, poled properties (after 24 hrs)



99 **Figure 5.3.** Aging study at 250⁰C, dielectric constant K as a function of aging time for unmodified and modified (1-x)PbZrO₃-xPbTiO₃ x=0.48, and (1-x)BiScO₃-xPbTiO₃ x=0.64 and 0.66.

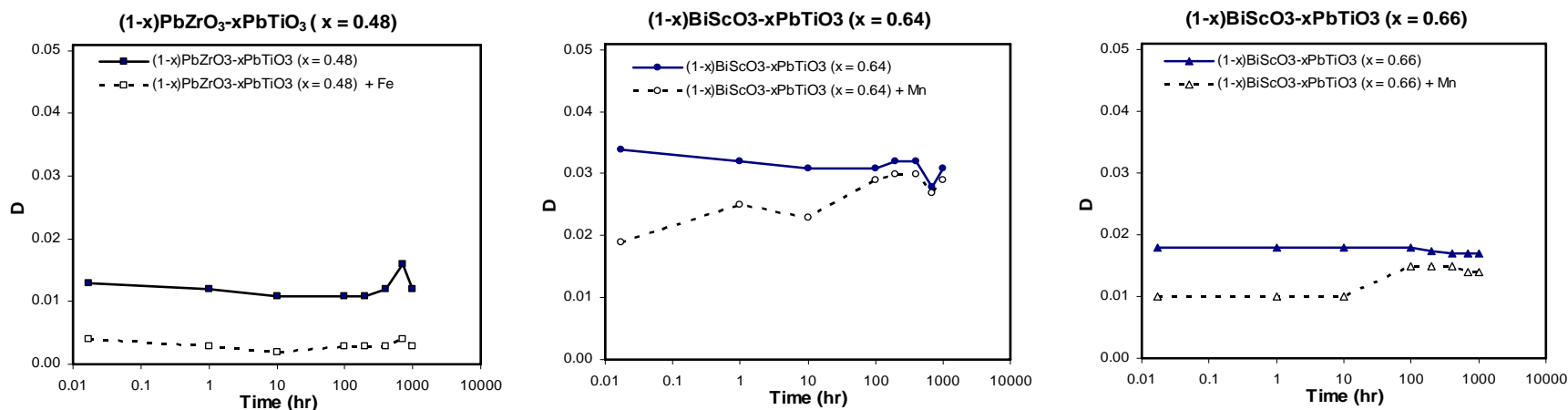


Figure 5.4. Aging study at 250⁰C, dielectric loss D as a function of aging time for unmodified and modified (1-x)PbZrO₃-xPbTiO₃ x=0.48, and (1-x)BiScO₃-xPbTiO₃ x=0.64 and 0.66.

5.4 Rayleigh analysis during aging study

Rayleigh analysis was done to evaluate change in non-linear dielectric and piezoelectric responses as a function of aging time for unmodified and modified $(1-x)\text{PbZrO}_3\text{-}x\text{PbTiO}_3$ and $(1-x)\text{BiScO}_3\text{-}x\text{PbTiO}_3$. Plots for dielectric constant K_{init} and α_ϵ (10^{-3} m/V) as a function of aging time for unmodified and modified $(1-x)\text{PbZrO}_3\text{-}x\text{PbTiO}_3$ and $(1-x)\text{BiScO}_3\text{-}x\text{PbTiO}_3$ are shown in Figure 5.5 and 5.6 respectively. K_{init} for unmodified and modified $(1-x)\text{PbZrO}_3\text{-}x\text{PbTiO}_3$ and $(1-x)\text{BiScO}_3\text{-}x\text{PbTiO}_3$ shows almost constant response for the aging period of 1000 hrs. Slope for the dielectric response α_ϵ (10^{-3} m/V) decreases linearly with increase in aging time except for Fe-modified $(1-x)\text{PbZrO}_3\text{-}x\text{PbTiO}_3$ ($x=0.48$).

Piezoelectric response for $d_{33\text{init}}$ (pC/N) and α_d (10^{-14} Cm/NV) as a function of aging time are shown in Figure 5.7 and 5.8 respectively. $(1-x)\text{BiScO}_3\text{-}x\text{PbTiO}_3$ ($x=0.66$ and 0.64), unmodified and Fe-modified $(1-x)\text{PbZrO}_3\text{-}x\text{PbTiO}_3$ ($x=0.48$) shows almost steady response for $d_{33\text{init}}$ throughout the aging period of 1000h. Mn-modified $(1-x)\text{BiScO}_3\text{-}x\text{PbTiO}_3$ ($x=0.64$ and 0.66) shows little degradation for $d_{33\text{init}}$ with the increase in aging time. Slope for the piezoelectric response α_d (10^{-14} Cm/NV) shows decreasing trends with increase in time for $(1-x)\text{PbZrO}_3\text{-}x\text{PbTiO}_3$ ($x=0.48$), unmodified and Mn-modified $(1-x)\text{BiScO}_3\text{-}x\text{PbTiO}_3$ ($x=0.64$).

The overall piezoelectric response can be expressed as $d_{\text{initial}} = d_{\text{intrinsic}} + d_{\text{extrinsic, reversible}}$ and α is proportional to $d_{\text{extrinsic, irreversible}}$. The above plots show that in general d_{33} and α have the similar trends during aging. There is no apparent change in relation of intrinsic and extrinsic contributions to piezoelectric coefficient, which suggest significant contribution of depoling in the aging of these materials.

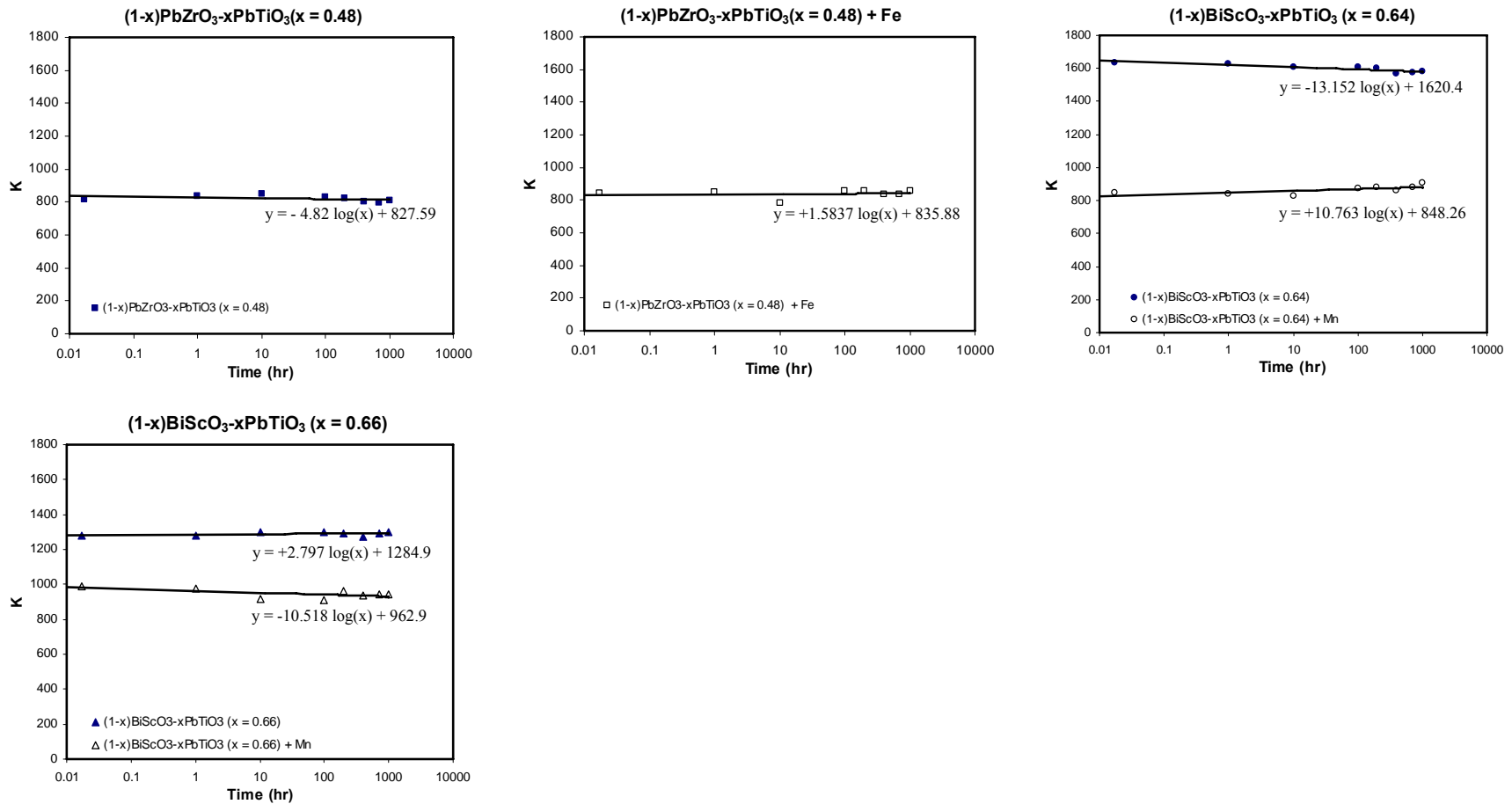


Figure 5.5 Aging study at 250°C , Rayleigh analysis for K as a function of aging time for unmodified and modified $(1-x)\text{PbZrO}_3\text{-}x\text{PbTiO}_3$ $x=0.48$, and $(1-x)\text{BiScO}_3\text{-}x\text{PbTiO}_3$ $x=0.64$ and 0.66 .

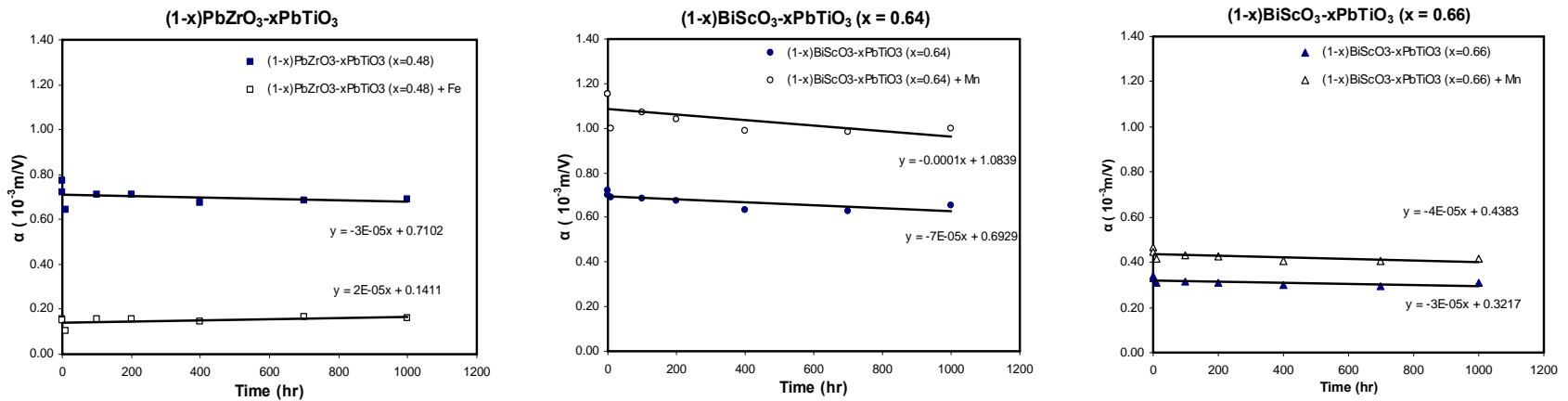


Figure 5.6 Aging study at 250⁰C, Rayleigh analysis of slope α_c (10^{-3} m/V) for dielectric response as a function of aging time for unmodified and modified (1-x)PbZrO₃-xPbTiO₃ x=0.48, and (1-x)BiScO₃-xPbTiO₃ x=0.64 and 0.66.

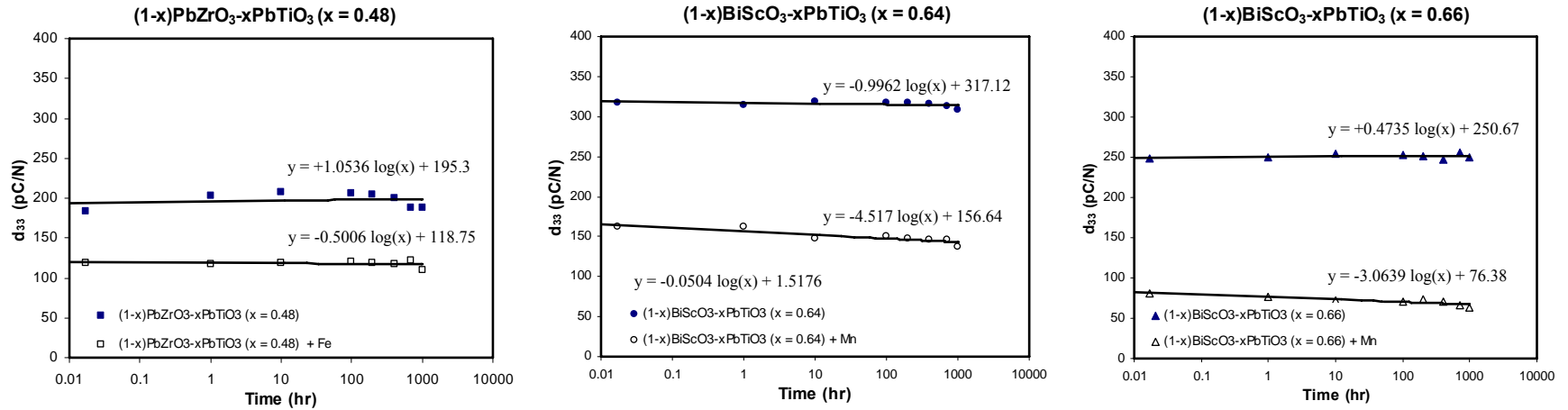


Figure 5.7 Aging study at 250⁰C, Rayleigh analysis for d_{33} as a function of aging time for unmodified and modified (1-x)PbZrO₃-xPbTiO₃ x=0.48, and (1-x)BiScO₃-xPbTiO₃ x=0.64 and 0.66.

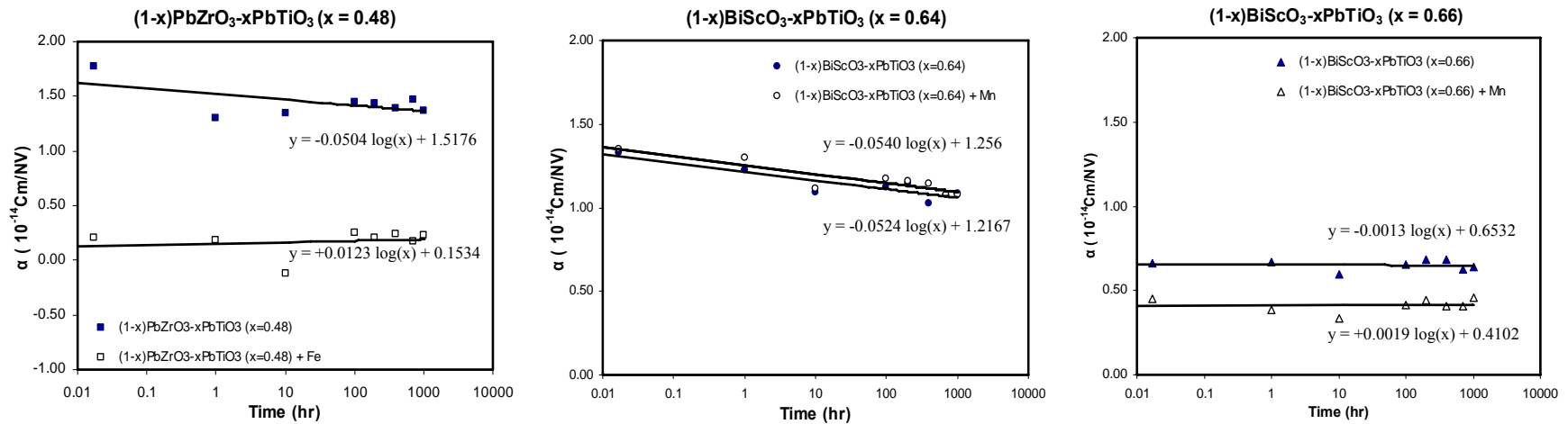


Figure 5.8 Aging study at 250⁰C, Rayleigh analysis of slope α_d (10^{-14} Cm/NV) for piezoelectric response as a function of aging time for unmodified and modified (1-x)PbZrO₃-xPbTiO₃ x=0.48, and (1-x)BiScO₃-xPbTiO₃ x=0.64 and 0.66.

5.5 Summary and conclusion

Purpose of this study was to evaluate thermal degradation and aging behavior for $(1-x)\text{BiScO}_3-x\text{PbTiO}_3$ ceramics and compare it with $(1-x)\text{PbZrO}_3-x\text{PbTiO}_3$. $(1-x)\text{PbZrO}_3-x\text{PbTiO}_3$ $x=0.48$ showed high aging rates of 4.8%/decade for piezoelectric constant d_{33} , 3.9%/decade for planar coupling coefficient k_p , and 2.2%/decade for dielectric constant K , which were reduced to 0.9%/decade, 0.6%/decade, and -0.2%/decade respectively by Fe modification. The MPB composition of $(1-x)\text{BiScO}_3-x\text{PbTiO}_3$ $x=0.64$ showed moderate aging rates of 2.1%/decade for piezoelectric constant d_{33} , 0.8%/decade for planar coupling coefficient k_p , and 0.6%/decade for dielectric constant K . Tetragonal $(1-x)\text{BiScO}_3-x\text{PbTiO}_3$ $x=0.66$ found to have the highest resistance against thermal aging. It showed aging rate of 0.8%/decade for piezoelectric constant d_{33} , 0.6%/decade for planar coupling coefficient k_p , and -0.08%/decade for dielectric constant K . Rayleigh analysis for piezoelectric response indicates significant contribution of depoling mechanism in the aging of these materials.

Chapter 6: Summary and future work

6.1 Summary

6.1.1 Thermal degradation and aging study for $(1-x)\text{PbZrO}_3\text{-}x\text{PbTiO}_3$ and $(1-x)\text{BiScO}_3\text{-}x\text{PbTiO}_3$ ceramics

Lots of work has been done on the development of new piezoelectric materials to meet the requirements of various applications in extreme operating conditions. Recently materials based on $(1-x)\text{BiScO}_3\text{-}x\text{PbTiO}_3$ were developed with $T_C \sim 450^\circ\text{C}$, and $d_{33} \sim 500$ pC/N.⁴¹ Enhanced room temperature properties and higher transition temperature makes this material promising for high temperature applications above 200°C .

For technologically important piezoelectric devices one of the most important requirements is long term reliability. Until now there has been less work done on long term degradation and life time analysis of these materials and no widely accepted technique exists for reliability and lifetime testing. Recently Chen et al. 2006 reported that tetragonal compositions of $(1-x)\text{BiScO}_3\text{-}x\text{PbTiO}_3$ showed resistance to thermal depoling up to the temperature close to their ferroelectric Curie temperature $T_C \sim 445^\circ\text{C}$.⁴⁶ This project was focused to study the thermal degradation and aging study for $(1-x)\text{BiScO}_3\text{-}x\text{PbTiO}_3$, demonstrate improved aging of $(1-x)\text{BiScO}_3\text{-}x\text{PbTiO}_3$ compared with $(1-x)\text{PbZrO}_3\text{-}x\text{PbTiO}_3$, and establish a methodology for lifetime testing of piezoelectric materials.

For the current work commonly used $(1-x)\text{PbZrO}_3\text{-}x\text{PbTiO}_3$ and recently developed high temperature piezoelectric ceramic $(1-x)\text{BiScO}_3\text{-}x\text{PbTiO}_3$ were prepared using solid state route. The MPB and tetragonal compositions with and without

modification of acceptor dopants were used for the thermal degradation and aging study. Sets of 15 pellets for each compositions were characterized after 24 hours from poling for piezoelectric constant d_{33} , planar coupling coefficient k_p , dielectric constant K , dielectric loss D , and Rayleigh analysis for dielectric and piezoelectric responses. The conditioning treatment was done at 250°C for 1 min to evaluate instantaneous thermal degradation. All compositions showed 5 to 20% reduction in piezoelectric constant d_{33} , and planar coupling coefficient k_p due to the thermal depoling effect, which is consistent with previous researches.^{39,56} After the conditioning treatment, pellets were reheated to the temperature of 250°C for 1000 hrs. Changes in the above properties were evaluated at predetermined intervals of 1 h, 10 h, 100 h, 200h, 400h, 700h and 1000h. The results were analyzed to find out aging of piezoelectric and dielectric properties. Aging rates were calculated for piezoelectric constant d_{33} and planar coupling coefficient k_p .

The MPB composition of $(1-x)\text{PbZrO}_3-x\text{PbTiO}_3$ ($x=0.48$) has Curie temperature $T_C=386^{\circ}\text{C}$ and showed very high aging rate of 4.8%/decade for piezoelectric constant d_{33} , 3.9%/decade for planar coupling coefficient k_p , and 2.2%/decade for dielectric constant K . High aging rates for $(1-x)\text{PbZrO}_3-x\text{PbTiO}_3$ ($x=0.48$) is most likely due to the high temperature ($\sim 2/3 T_C$) used of the aging study. As a rule of thumb, in order to minimize the aging effect maximum application of piezoelectric materials is generally restricted to $\sim 1/2 T_C$.⁵² Purpose of this study was to evaluate the promise of $(1-x)\text{BiScO}_3-x\text{PbTiO}_3$ system as a high temperature piezoelectric material, hence high temperature 250°C was selected for the study.

Fe-modification to $(1-x)\text{PbZrO}_3-x\text{PbTiO}_3$ ($x=0.48$) changed the behavior of this material and it showed very high degradation for d_{33} ($\sim 20\%$) and k_p ($\sim 15\%$) in

conditioning treatment at 250⁰C. After initial degradation in the conditioning treatment this material showed low aging rates 0.9%/decade for d_{33} , and 0.6%/decade for k_p , and -0.2 %/decade for K.

Acceptor doping to (1-x)PbZrO₃-xPbTiO₃ (x=0.48) create anion vacancies. The mobility of defect dipoles is relatively high in acceptor doped materials due to easy movement of vacancies in oxygen octahedra network.¹⁵ Fe-modified (1-x)PbZrO₃-xPbTiO₃ (x=0.48) showed high degradation of d_{33} and k_p in the conditioning treatment which is most likely due to relatively high mobility of defect dipoles during initial period. The instantaneous aging effect in Fe-modified (1-x)PbZrO₃-xPbTiO₃ (x=0.48) was also evident from pinched ferroelectric P-E hysteresis loop (Figure 4.1) for this material. Alignment of defect dipoles in the direction of polarization vector within the domain stabilizes the domain structure which possibly helped to reduce aging rate after initial degradation.

BiScO₃ has lower tolerance factor (t=0.907) compared to PbZrO₃ (t=0.96) which results higher T_C for (1-x)BiScO₃-xPbTiO₃ compared to (1-x)PbZrO₃-xPbTiO₃.⁴⁰ Recently Chen et al. 2006 studied thermal stability for (1-x)BiScO₃-xPbTiO₃ and observed that the tetragonal phase shows excellent thermal stability up to ~440⁰C whereas the MPB and rhombohedral compositions began to depole when the temperature were >300⁰C.⁴⁶

The MPB composition (1-x)BiScO₃-xPbTiO₃ (x=0.64) has Curie temperature $T_C=436^0$ C and showed less than 10% reduction for d_{33} and k_p after conditioning treatment at 250⁰C. This indicates higher depoling resistance of (1-x)BiScO₃-xPbTiO₃ system

compare to $(1-x)\text{PbZrO}_3-x\text{PbTiO}_3$. Calculated aging rate for $(1-x)\text{BiScO}_3-x\text{PbTiO}_3$ ($x=0.64$) were 2.1%/decade for d_{33} , and 0.8%/decade for k_p , and 0.6%/decade for K .

The tetragonal composition $(1-x)\text{BiScO}_3-x\text{PbTiO}_3$ ($x=0.66$) has Curie temperature $T_C=446^\circ\text{C}$ and showed least degradation due to thermal depoling, less than 5% for d_{33} and k_p after conditioning at 250°C . Tetragonal phase also showed very high resistance against the aging of electromechanical properties. Calculated aging rates for $(1-x)\text{BiScO}_3-x\text{PbTiO}_3$ ($x=0.66$) were 0.8%/decade, 0.6%/decade, and -0.08%/decade for piezoelectric constant d_{33} , planar coupling coefficient k_p , and dielectric constant K respectively.

It was concluded through the dielectric aging study of BaTiO_3 in 1950's that aging rate reduces as the tetragonal distortion of the perovskite unit cell is increases⁶. The same behavior is evident for $(1-x)\text{BiScO}_3-x\text{PbTiO}_3$ system. The MPB composition $(1-x)\text{BiScO}_3-x\text{PbTiO}_3$ ($x=0.64$) has the coexistence of rhombohedral and tetragonal phases to give 14 possible polarization directions to optimize crystallographic orientation and resulting high dielectric and piezoelectric properties. The tetragonal $(1-x)\text{BiScO}_3-x\text{PbTiO}_3$ ($x=0.66$) has high distorted perovskite unit cells ($c/a = 1.028$) compared to the MPB composition ($c/a=1.023$) and showed high resistance against aging.

The Rayleigh analysis for piezoelectric response showed that there is no apparent change in the relation of intrinsic and extrinsic contributions to piezoelectric coefficient, which suggest significant contribution of depoling mechanism in the aging of these materials.

Thermal degradation and aging study conducted can be concluded that $(1-x)\text{BiScO}_3-x\text{PbTiO}_3$ has more stability compared to $(1-x)\text{PbZrO}_3-x\text{PbTiO}_3$ at high temperature $>200^\circ\text{C}$. The tetragonal $(1-x)\text{BiScO}_3-x\text{PbTiO}_3$ ($x=0.66$) in particular has

very low aging rates of 0.8%/decade, 0.6%/decade and -0.08%/decade for piezoelectric constant d_{33} and planar coupling coefficient k_p , and dielectric constant K respectively. This makes claim of $(1-x)\text{BiScO}_3\text{-}x\text{PbTiO}_3$ ($x=0.66$) stronger for the high temperature piezoelectric sensor applications.

6.1.2 Development of methodology for lifetime testing for piezoelectric ceramics

The second goal of this study was to establish a methodology for lifetime testing of piezoelectric materials. For the current study, temperature of 250°C was selected based on preliminary study. During thermal degradation and aging study it was observed that heating of pellets to the temperature 250°C for 1 min caused 5 to 20% reduction in piezoelectric constant d_{33} and planar coupling coefficient k_p , and dielectric constant K . Outcome of this study indicate that instantaneous thermal degradation and aging should be evaluated separately. The aging study showed that most of the reduction in electromechanical properties occurred up to 500hrs, this should be considered to decide the length of aging study. In the past aging studies were done generally up to 10^4 min.^{39,56}

6.2 Future work

6.2.1 Aging study for acceptor doped $(1-x)\text{BiScO}_3\text{-}x\text{PbTiO}_3$

Fe-modification to $(1-x)\text{PbZrO}_3\text{-}x\text{PbTiO}_3$ ($x=0.48$) helped to reduce the aging rates for d_{33} , and k_p after initial conditioning treatment. Mn-modification to $(1-x)\text{BiScO}_3\text{-}x\text{PbTiO}_3$ did not help to improve the aging behavior of the system. Winotai et al. 2005 studied the effect of Fe_2O_3 doping on $(1-x)\text{BiScO}_3\text{-}x\text{PbTiO}_3$ ($x=0.64$) and reported

improvement in overall piezoelectric properties with addition of 1 mol% Fe_2O_3 .³⁶ Thermal degradation and aging study of $(1-x)\text{BiScO}_3-x\text{PbTiO}_3$ with Fe^{3+} , and other acceptor dopant like Nb^{5+} can be conducted to develop and evaluate better material with higher thermal stability and higher resistance against the piezoelectric and dielectric aging.

For the current study Mn-doping to $(1-x)\text{BiScO}_3-x\text{PbTiO}_3$ was done without charge compensation and site balance and did not help to improve aging behavior. In future thermal degradation and aging study can be tried for the compositions with charge compensation and site balance.

6.2.2 Methodology for lifetime testing for piezoelectric ceramics

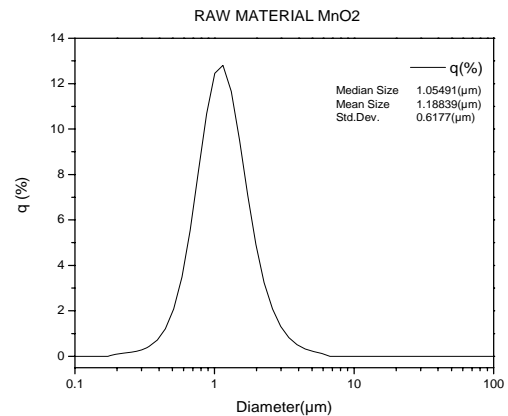
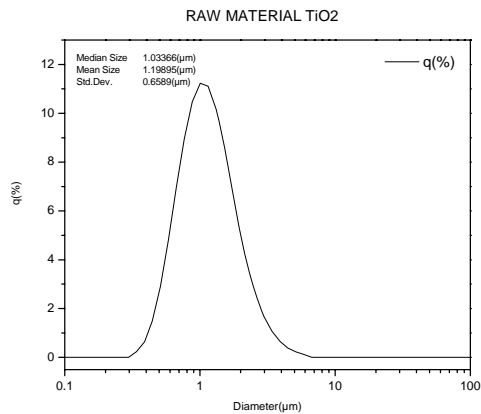
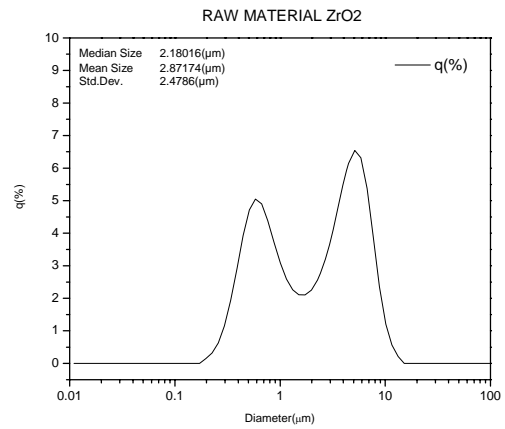
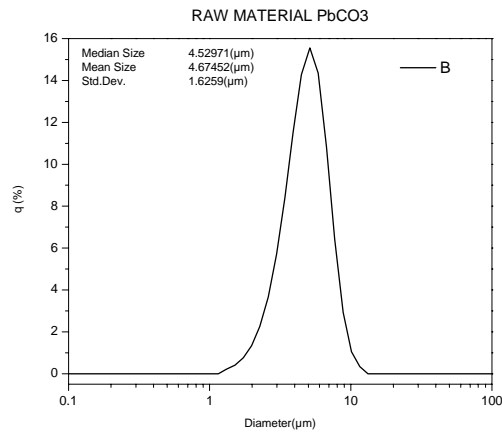
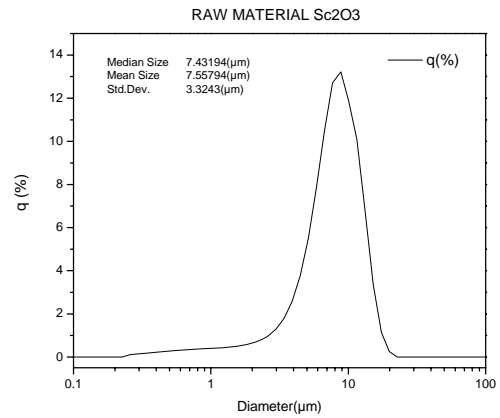
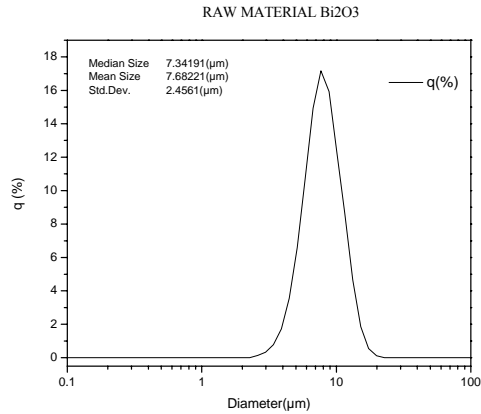
Rayleigh law is being used in piezoelectric materials to quantify the irreversible and reversible piezoelectric response. Rayleigh law indicates a linear dependence of the piezoelectric constant and dielectric constant with the increasing field, particularly in low field region where density and domain wall structure remain unchanged. The piezoelectric response in ferroelectric materials contains both intrinsic and extrinsic contribution.^{12,16-18} Intrinsic contributions are mainly due to the strain in crystal lattice, in general those are reversible with no loss. Extrinsic contributions are mainly due to the motion of non 180° domain walls, generally those are non linear and lossy and varies as a function of time, frequency, and field.

For the current work Rayleigh analysis was done to evaluate aging effect on overall dielectric and piezoelectric response and observed that there is no apparent change in the relation of intrinsic and extrinsic contributions to piezoelectric coefficient.

Future work can be focused to study the change in intrinsic, extrinsic reversible and nonreversible components separately during aging study by using Rayleigh analysis.

Appendix – A

Particle size and distribution for metal oxides / carbonate powders.



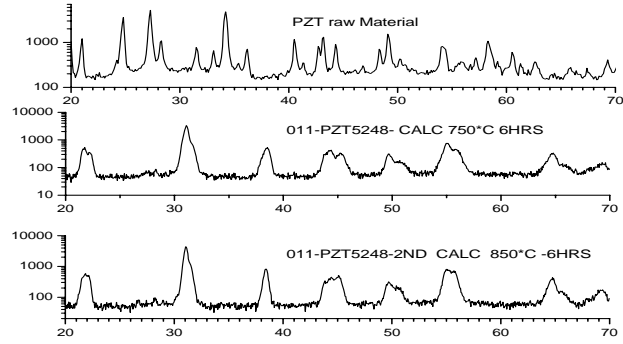
Appendix – B

LOI results for metal oxides / carbonate powders.

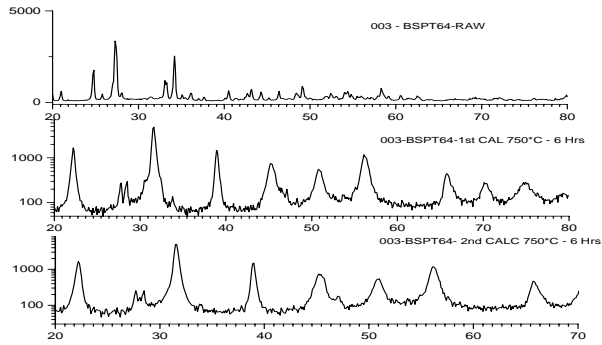
Material	LOI parameter	Multiplying factors		Average
		LOI-I	LOI-II	
PbCO ₃	650 ⁰ C - 2 Hrs	1.1656	1.1657	1.1657
ZrO ₂	650 ⁰ C - 2 Hrs	1.0027	1.0027	1.0027
TiO ₂	650 ⁰ C - 2 Hrs	1.0034	1.0033	1.0034
Bi ₂ O ₃	600 ⁰ C – 2 Hrs	1.0025	1.0024	1.0025
SC ₂ O ₃	650 ⁰ C – 2 Hrs	1.0263	1.0262	1.0262

Appendix – C

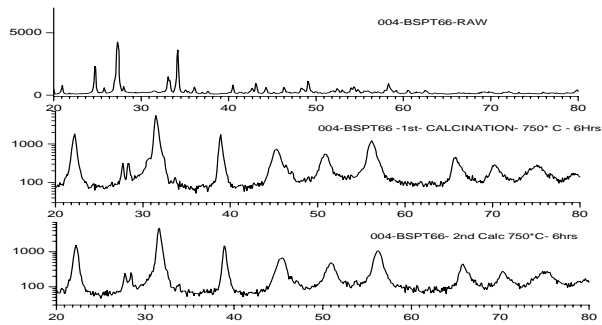
XRD scans for PZT and BSPT powders before and after calcinations



PZT (X = 0.48)



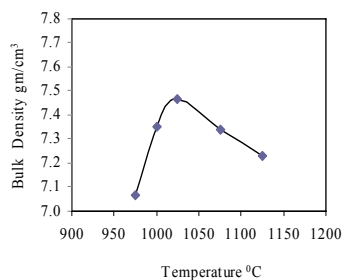
BSPT (X = 0.64)



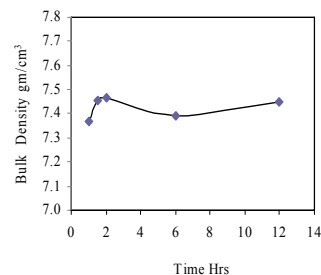
BSPT (X = 0.66)

Appendix – D

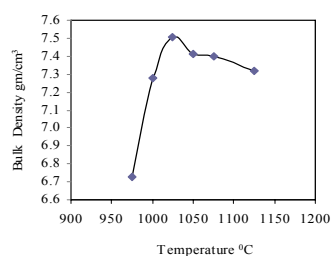
Sintering study for PZT and BSPT (bulk density- for variable time & temperature)



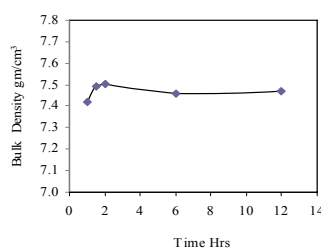
BSPT 64, Time 2 Hr



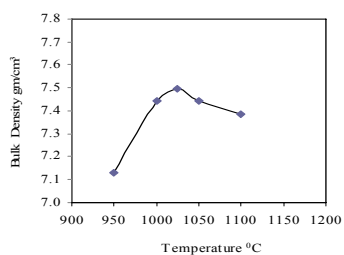
BSPT 64, Temperature 1025°C



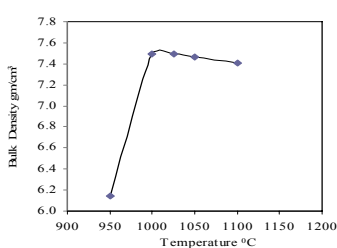
BSPT 66, Time 2 Hr



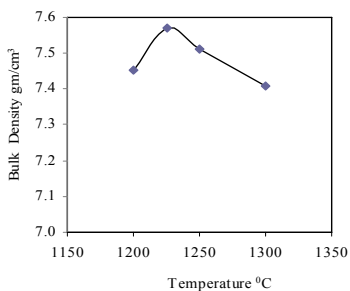
BSPT 66, Temperature 1025°C



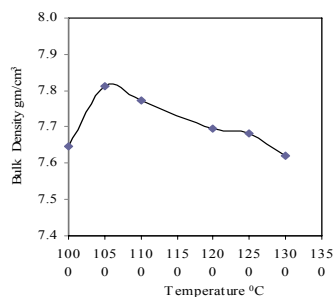
BSPT 64 + 0.2% MnO₂, Time 1 Hr



BSPT 66 + 0.2% MnO₂, Time 1 Hr



PZT 5248, Time 1.5 Hrs



PZT5248 + 0.2% Fe₂O₃, Time 1.5 Hrs

Appendix - E

Dielectric properties of poled pellets at various frequencies

Material : PZT (x= 0.48)

Sample No	100Hz		1 KHz		10 KHz		100 KHz	
	K	D	K	D	K	D	K	D
1	768	0.014	754	0.012	741	0.013	743	0.013
2	724	0.013	712	0.011	700	0.012	705	0.013
3	785	0.012	772	0.012	758	0.013	757	0.014
4	841	0.011	828	0.011	815	0.012	816	0.013
5	756	0.011	744	0.011	731	0.012	742	0.013
6	714	0.011	703	0.010	692	0.011	696	0.012
7	696	0.011	686	0.009	677	0.010	686	0.010
8	722	0.010	713	0.009	702	0.011	706	0.012
9	737	0.012	725	0.011	713	0.013	715	0.013
10	754	0.010	743	0.010	733	0.011	735	0.012
11	762	0.011	750	0.010	739	0.012	736	0.013
12	791	0.010	779	0.010	767	0.011	768	0.012
13	834	0.010	822	0.011	808	0.012	809	0.013
14	838	0.010	826	0.010	813	0.011	813	0.013

Material : PZT (x=0.48) + Fe

Sample No	100Hz		1 KHz		10 KHz		100 KHz	
	K	D	K	D	K	D	K	D
1	871	0.008	863	0.005	858	0.004	873	0.004
2	871	0.007	865	0.004	860	0.004	876	0.004
3	837	0.004	832	0.003	828	0.003	843	0.004
4	860	0.004	855	0.003	851	0.004	865	0.005
5	893	0.004	889	0.003	885	0.003	906	0.004
6	906	0.007	899	0.004	894	0.004	913	0.004
7	924	0.007	917	0.004	912	0.004	931	0.004
8	866	0.005	861	0.004	857	0.004	873	0.004
9	856	0.005	851	0.004	846	0.004	864	0.004
10	823	0.007	817	0.004	812	0.004	830	0.004
11	931	0.007	924	0.004	919	0.004	946	0.004
12	891	0.005	886	0.004	881	0.004	903	0.004
13	880	0.005	874	0.004	870	0.004	891	0.004
14	892	0.007	885	0.004	880	0.004	898	0.004
15	970	0.005	964	0.004	958	0.004	988	0.005

Continued...

Material : BSPT64

Sample No	100Hz		1 KHz		10 KHz		100 KHz	
	K	D	K	D	K	D	K	D
1	1822.6603	0.024	1755	0.029	1671.1754	0.042	1644.1986	0.075
2	1826.1762	0.028	1748	0.034	1653.0969	0.048	1644.2535	0.085
3	1709.8559	0.025	1643	0.031	1559.5055	0.045	1535.7659	0.080
4	1803.2321	0.027	1732	0.031	1646.1392	0.044	1626.1235	0.079
5	1564.1081	0.026	1500	0.033	1420.1187	0.046	1409.613	0.076
6	1547.2738	0.026	1484	0.033	1403.5248	0.046	1391.394	0.076
7	1746.3015	0.021	1692	0.024	1627.1233	0.034	1622.8007	0.063
8	1588.5052	0.026	1523	0.033	1441.2308	0.046	1427.0822	0.077
9	1709.4055	0.020	1657	0.024	1593.0375	0.035	1581.802	0.065
10	1718.5303	0.026	1648	0.033	1559.3239	0.046	1544.5588	0.076
11	1645.602	0.025	1579	0.033	1494.5201	0.046	1482.6091	0.077
12	1590.7849	0.025	1526	0.032	1445.0833	0.046	1430.6388	0.075
13	1604.8709	0.026	1539	0.033	1457.0036	0.046	1444.2564	0.077
14	1593.9948	0.026	1529	0.033	1446.6766	0.046	1432.4996	0.076
15	1700.7201	0.022	1639	0.029	1558.028	0.044	1553.1496	0.080

Material : BSPT64 + Mn

Sample No	100Hz		1 KHz		10 KHz		100 KHz	
	K	D	K	D	K	D	K	D
1	1095.3026	0.009	1080	0.012	1057.8004	0.021	1050.0618	0.042
2	1098.5398	0.008	1084	0.011	1061.4895	0.021	1052.227	0.042
3	1124.0723	0.008	1108	0.012	1085.4401	0.021	1082.3246	0.043
4	1102.594	0.008	1088	0.011	1065.6768	0.021	1060.7545	0.043
5	1120.4373	0.008	1105	0.011	1082.9048	0.021	1078.5978	0.042
6	1102.5056	0.009	1087	0.011	1065.3216	0.021	1059.1243	0.042
7	1104.7964	0.009	1089	0.012	1065.7887	0.021	1057.6097	0.043
8	1094.8347	0.010	1078	0.013	1053.462	0.022	1041.7294	0.043
9	1085.157	0.008	1071	0.011	1049.4239	0.021	1031.8708	0.043
10	1097.158	0.009	1081	0.013	1056.9645	0.022	1046.288	0.044
11	1127.3846	0.009	1111	0.012	1087.3189	0.022	1076.2239	0.044
12	1081.6743	0.008	1068	0.011	1045.3723	0.021	1031.2207	0.042
13	1115.1846	0.009	1099	0.012	1074.6654	0.022	1062.5701	0.043
14	1106.7572	0.009	1091	0.012	1067.4495	0.021	1055.1659	0.043
15	1084.1354	0.008	1071	0.011	1049.6793	0.020	1032.4513	0.042

Continued...

Material : BSPT66

Sample No	100Hz		1 KHz		10 KHz		100 KHz	
	K	D	K	D	K	D	K	D
1	1242	0.016	1212	0.017	1181	0.020	1188	0.029
2	1169	0.015	1142	0.017	1113	0.020	1117	0.027
3	1151	0.015	1124	0.017	1096	0.020	1100	0.027
4	1302	0.015	1272	0.017	1238	0.021	1246	0.031
5	1288	0.015	1258	0.017	1225	0.021	1232	0.031
6	1365	0.015	1333	0.017	1298	0.021	1306	0.031
7	1280	0.015	1250	0.017	1217	0.021	1225	0.031
8	1306	0.018	1273	0.018	1238	0.022	1243	0.031
9	1195	0.016	1166	0.017	1136	0.020	1137	0.029
10	1231	0.016	1201	0.017	1170	0.021	1172	0.029
11	1286	0.016	1255	0.018	1221	0.022	1228	0.033
12	1261	0.016	1230	0.018	1196	0.022	1200	0.032
13	1358	0.016	1323	0.019	1282	0.025	1292	0.038
14	1365	0.016	1331	0.019	1292	0.024	1303	0.037
15	1357	0.016	1324	0.018	1285	0.023	1297	0.035
16	1262	0.015	1232	0.017	1199	0.021	1206	0.032

Material : BSPT66 + Mn

Sample No	100Hz		1 KHz		10 KHz		100 KHz	
	K	D	K	D	K	D	K	D
1	985	0.006	976	0.007	963	0.012	951	0.022
2	994	0.005	985	0.006	975	0.010	965	0.019
3	1007	0.006	998	0.007	985	0.011	975	0.020
4	1011	0.006	1002	0.006	992	0.009	986	0.017
5	963	0.005	956	0.006	946	0.009	938	0.017
6	1009	0.005	1001	0.006	991	0.009	982	0.018
7	970	0.006	962	0.006	951	0.010	941	0.019
8	981	0.006	972	0.007	961	0.010	953	0.017
9	974	0.005	966	0.006	956	0.009	951	0.017
10	988	0.006	978	0.008	965	0.012	952	0.022
11	964	0.005	957	0.006	947	0.009	943	0.017
12	967	0.005	960	0.006	950	0.009	945	0.017
13	984	0.006	975	0.006	965	0.010	956	0.018
14	986	0.005	978	0.006	968	0.009	960	0.018
15	1015	0.005	1007	0.006	996	0.009	988	0.017
16	963	0.005	956	0.006	946	0.009	941	0.016

Appendix - F

Details of dielectric properties (1 KHz) with the aging time at 250⁰C

Material :PZT (x=0.48)

Sample No	Poled		1Min		1Hr		10Hr		100Hr		200Hr		400Hr		700Hr		1000Hr	
	K	D	K	D	K	D	K	D	K	D	K	D	K	D	K	D	K	D
1	768	0.014	778	0.013	759	0.012	721	0.010	674	0.010	679	0.011	674	0.01	686	0.011	678	0.01
2	724	0.013	739	0.014	719	0.013	678	0.011	635	0.010	630	0.011	645	0.013	659	0.018	648	0.013
3	785	0.012	800	0.014	781	0.013	752	0.013	704	0.011	712	0.012	717	0.013	731	0.017	717	0.013
4	841	0.011	876	0.014	858	0.013	840	0.012	792	0.011	799	0.012	809	0.012	826	0.017	811	0.012
5	756	0.011	757	0.012	743	0.013	694	0.011	682	0.010	684	0.011	667	0.012	676	0.015	664	0.012
6	714	0.011	733	0.013	712	0.012	668	0.011	597	0.010	601	0.011	611	0.012	622	0.017	609	0.012
7	696	0.011	701	0.010	686	0.009	623	0.006	624	0.009	632	0.01	641	0.011	657	0.015	645	0.010
8	722	0.010	757	0.013	731	0.011	688	0.011	641	0.010	637	0.01	654	0.012	666	0.016	653	0.012
9	737	0.012	767	0.014	746	0.012	703	0.011	664	0.011	662	0.011	671	0.012	683	0.017	670	0.012
10	754	0.010	778	0.014	761	0.012	752	0.012	715	0.011	717	0.012	724	0.013	736	0.015	726	0.012
11	762	0.011	775	0.013	733	0.011	731	0.011	714	0.010	715	0.01	700	0.012	712	0.015	700	0.012
12	791	0.010	818	0.014	794	0.011	797	0.012	754	0.012	755	0.012	764	0.013	779	0.016	766	0.013
13	834	0.010	862	0.014	839	0.012	827	0.010	811	0.012	811	0.011	823	0.013	839	0.016	825	0.013
14	838	0.010	866	0.013	843	0.011	843	0.011	815	0.011	815	0.011	826	0.013	841	0.016	827	0.012
Avg	766	0.011	786	0.013	764.8	0.0118	736.8	0.0109	702	0.011	704	0.011	709	0.012	722	0.016	710	0.012
Ratio	1.00	1.00	1.03	1.19	1.00	1.06	0.962	0.98	0.92	0.95	0.92	1.00	0.93	1.10	0.94	1.42	0.93	1.08

Continued...

Material :PZT (x=0.48) +Fe

Sample No	Poled		1Min		1Hr		10Hr		100Hr		200Hr		400Hr		700Hr		1000Hr	
	K	D	K	D	K	D	K	D	K	D	K	D	K	D	K	D	K	D
1	871	0.008	913	0.004	903	0.003	851	0.002	901	0.003	899	0.003	904	0.003	912	0.004	918	0.003
2	871	0.007	926	0.004	911	0.003	861	0.002	916	0.003	916	0.003	920	0.003	929	0.004	932	0.003
3	837	0.004	905	0.004	890	0.003	841	0.002	898	0.003	898	0.003	903	0.003	912	0.004	913	0.003
4	860	0.004	928	0.004	915	0.003	863	0.002	919	0.003	919	0.003	924	0.003	932	0.004	935	0.003
5	893	0.004	959	0.003	947	0.003	898	0.002	954	0.003	955	0.003	957	0.003	964	0.004	967	0.003
6	906	0.007	952	0.004	943	0.003	891	0.002	947	0.003	946	0.003	947	0.003	954	0.004	957	0.003
7	924	0.007	962	0.004	951	0.003	897	0.002	958	0.003	958	0.003	960	0.003	968	0.004	970	0.003
8	866	0.005	945	0.004	928	0.003	873	0.002	932	0.003	933	0.003	937	0.003	946	0.004	949	0.003
9	856	0.005	929	0.004	918	0.003	864	0.002	921	0.003	919	0.003	926	0.003	933	0.004	939	0.003
10	823	0.007	861	0.003	852	0.003	803	0.002	849	0.003	847	0.003	849	0.003	856	0.004	862	0.003
11	931	0.007	990	0.003	982	0.003	927	0.002	977	0.003	975	0.003	977	0.003	984	0.004	992	0.003
12	891	0.005	944	0.003	937	0.003	888	0.002	937	0.003	935	0.003	936	0.003	943	0.004	948	0.003
13	880	0.005	939	0.003	929	0.003	880	0.002	933	0.003	932	0.003	936	0.003	943	0.004	948	0.003
14	892	0.007	939	0.003	930	0.003	878	0.002	935	0.003	934	0.003	939	0.003	947	0.003	950	0.003
15	970	0.005	1020	0.005	994	0.003	934	0.002	997	0.004	998	0.003	1010	0.005	1018	0.005	1014	0.004
Avg	885	0.006	941	0.004	929	0.003	877	0.002	932	0.003	931	0.003	935	0.003	943	0.004	946	0.003
Ratio	1.00	1.00	1.06	0.63	1.05	0.52	0.99	0.34	1.05	0.53	1.05	0.52	1.06	0.54	1.07	0.69	1.07	0.53

Continued...

Material :BSPT64

Sample No	Poled		1Min		1Hr		10Hr		100Hr		200Hr		400Hr		700Hr		1000Hr	
	K	D	K	D	K	D	K	D	K	D	K	D	K	D	K	D	K	D
1	1823	0.024	1742	0.030	1692	0.028	1646	0.026	1684	0.027	1655	0.027	1648	0.027	1703	0.024	1668	0.026
2	1826	0.028	1791	0.034	1747	0.032	1709	0.031	1712	0.030	1678	0.029	1660	0.029	1713	0.025	1670	0.028
3	1710	0.025	1656	0.033	1608	0.031	1561	0.029	1577	0.029	1555	0.028	1544	0.029	1598	0.025	1561	0.028
4	1803	0.027	1726	0.032	1670	0.030	1622	0.028	1634	0.027	1613	0.027	1601	0.027	1655	0.024	1617	0.026
5	1564	0.026	1567	0.038	1544	0.036	1498	0.034	1537	0.037	1518	0.037	1507	0.037	1580	0.032	1526	0.036
6	1547	0.026	1538	0.038	1513	0.037	1488	0.036	1511	0.037	1490	0.037	1483	0.037	1557	0.032	1504	0.036
7	1746	0.021	1674	0.025	1636	0.022	1607	0.021	1629	0.021	1609	0.021	1606	0.021	1651	0.019	1625	0.020
8	1589	0.026	1590	0.038	1567	0.035	1546	0.035	1554	0.037	1537	0.037	1528	0.037	1604	0.032	1550	0.036
9	1709	0.020	1648	0.024	1612	0.023	1584	0.022	1607	0.022	1589	0.022	1579	0.022	1625	0.02	1597	0.021
10	1719	0.026	1732	0.038	1678	0.037	1646	0.036	1680	0.037	1657	0.037	1647	0.037	1731	0.033	1670	0.036
11	1646	0.025	1657	0.038	1616	0.037	1584	0.036	1617	0.037	1594	0.037	1585	0.037	1665	0.032	1607	0.036
12	1591	0.025	1598	0.038	1556	0.037	1529	0.036	1559	0.037	1536	0.037	1527	0.038	1603	0.033	1547	0.036
13	1605	0.026	1613	0.038	1576	0.037	1546	0.036	1576	0.037	1556	0.037	1546	0.037	1620	0.032	1565	0.036
14	1594	0.026	1598	0.038	1545	0.035	1519	0.034	1560	0.037	1538	0.037	1527	0.037	1601	0.032	1546	0.036
15	1701	0.022	1693	0.033	1685	0.030	1661	0.030	1665	0.030	1646	0.031	1632	0.031	1692	0.026	1645	0.029
Avg	1678	0.025	1655	0.034	1616	0.032	1583	0.031	1607	0.032	1580	0.032	1571	0.0323	1636	0.028	1589.4	0.031
Ratio	1.00	1.00	0.99	1.38	0.96	1.30	0.94	1.26	0.96	1.29	0.94	1.29	0.94	1.30	0.97	1.13	0.95	1.25

Continued...

Material :BSPT64+Mn

Sample No	Poled		1Min		1Hr		10Hr		100Hr		200Hr		400Hr		700Hr		1000Hr	
	K	D	K	D	K	D	K	D	K	D	K	D	K	D	K	D	K	D
1	1095	0.009	1187	0.021	1230	0.024	1160	0.022	1265	0.027	1261	0.029	1248	0.029	1298	0.026	1260	0.027
2	1099	0.008	1189	0.021	1275	0.029	1169	0.023	1277	0.029	1262	0.03	1256	0.03	1307	0.027	1268	0.029
3	1124	0.008	1210	0.014	1228	0.015	1236	0.024	1343	0.029	1329	0.03	1330	0.03	1385	0.027	1345	0.028
4	1103	0.008	1152	0.015	1162	0.016	1188	0.024	1297	0.029	1284	0.03	1279	0.03	1367	0.027	1291	0.029
5	1120	0.008	1231	0.020	1314	0.030	1199	0.024	1315	0.030	1298	0.03	1295	0.03	1346	0.027	1304	0.029
6	1103	0.009	1202	0.021	1299	0.030	1182	0.024	1290	0.029	1250	0.025	1276	0.03	1326	0.027	1287	0.029
7	1105	0.009	1202	0.022	1290	0.030	1176	0.023	1278	0.028	1273	0.03	1267	0.03	1321	0.027	1268	0.027
8	1095	0.010	1180	0.021	1271	0.029	1163	0.023	1270	0.030	1256	0.03	1249	0.03	1302	0.027	1258	0.029
9	1085	0.008	1169	0.021	1252	0.031	1152	0.023	1256	0.030	1244	0.03	1236	0.03	1287	0.027	1244	0.029
10	1097	0.009	1197	0.023	1238	0.024	1176	0.025	1287	0.031	1272	0.031	1267	0.031	1319	0.028	1278	0.03
11	1127	0.009	1193	0.014	1213	0.016	1196	0.023	1300	0.030	1289	0.03	1283	0.03	1334	0.026	1295	0.029
12	1082	0.008	1124	0.015	1165	0.017	1135	0.023	1237	0.029	1226	0.03	1217	0.03	1268	0.027	1227	0.028
13	1115	0.009	1207	0.021	1291	0.029	1181	0.023	1292	0.030	1278	0.03	1272	0.03	1304	0.024	1283	0.029
14	1107	0.009	1198	0.022	1275	0.030	1169	0.023	1277	0.030	1263	0.03	1259	0.031	1311	0.027	1266	0.029
15	1084	0.008	1172	0.020	1232	0.027	1146	0.023	1246	0.029	1231	0.028	1227	0.03	1276	0.026	1233	0.028
Avg	1103	0.009	1187	0.019	1249	0.025	1175	0.023	1282	0.029	1270	0.030	1267	0.030	1319	0.027	1276.9	0.029
Ratio	1.00	1.00	1.08	2.26	1.13	2.92	1.07	2.71	1.16	3.41	1.15	3.45	1.15	3.50	1.20	3.11	0.76	1.15

Continued...

Material :BSPT66

Sample No	Poled		1Min		1Hr		10Hr		100Hr		200Hr		400Hr		700Hr		1000Hr	
	K	D	K	D	K	D	K	D	K	D	K	D	K	D	K	D	K	D
1	1151	0.015	1299	0.017	1294	0.017	1292	0.017	1298	0.017	1150	0.016	1147	0.016	1174	0.016	1160	0.016
2	1169	0.015	1155	0.017	1154	0.017	1141	0.016	1147	0.016	1143	0.016	1139	0.016	1166	0.016	1152	0.016
3	1262	0.015	1256	0.019	1259	0.019	1251	0.018	1259	0.018	1330	0.017	1323	0.017	1353	0.016	1335	0.016
4	1280	0.015	1273	0.018	1270	0.018	1267	0.017	1274	0.017	1245	0.017	1239	0.017	1269	0.016	1252	0.016
5	1288	0.015	1295	0.017	1294	0.017	1295	0.018	1305	0.018	1303	0.017	1298	0.017	1330	0.016	1313	0.017
6	1302	0.015	1284	0.018	1283	0.018	1271	0.017	1278	0.017	1205	0.017	1199	0.017	1228	0.016	1212	0.017
7	1365	0.015	1265	0.018	1263	0.018	1260	0.018	1267	0.017	1359	0.017	1353	0.017	1385	0.016	1367	0.016
8	1195	0.016	1168	0.018	1162	0.017	1153	0.017	1160	0.017	1271	0.017	1266	0.017	1297	0.017	1278	0.017
9	1231	0.016	1205	0.018	1196	0.017	1188	0.017	1196	0.017	1083	0.016	1081	0.016	1106	0.016	1093	0.016
10	1242	0.016	1223	0.018	1215	0.017	1205	0.016	1212	0.016	1262	0.017	1258	0.016	1289	0.016	1272	0.016
11	1261	0.016	1234	0.019	1230	0.019	1222	0.018	1228	0.018	1185	0.018	1181	0.018	1212	0.017	1194	0.018
12	1286	0.016	1266	0.019	1262	0.019	1257	0.018	1265	0.018	1300	0.018	1295	0.018	1328	0.017	1310	0.018
13	1357	0.016	1322	0.019	1320	0.02	1323	0.020	1335	0.020	1374	0.021	1369	0.021	1410	0.019	1386	0.021
14	1358	0.016	1338	0.020	1338	0.021	1333	0.020	1354	0.021	1330	0.02	1326	0.02	1364	0.019	1342	0.02
15	1365	0.016	1355	0.021	1354	0.021	1348	0.020	1361	0.020	1328	0.02	1324	0.02	1362	0.018	1342	0.019
16	1306	0.018	1280	0.019	1269	0.019	1265	0.018	1270	0.018	1280	0.018	1275	0.018	1307	0.017	1289	0.017
Avg	1276	0.016	1264	0.018	1260	0.018	1254	0.018	1263	0.018	1253	0.017	1248	0.0174	1279	0.0166	1274.8	0.017
Ratio	1.00	1.00	0.99	1.17	0.99	1.17	0.98	1.13	0.99	1.13	0.98	1.11	0.98	1.11	1.00	1.06	0.76	0.70

Continued...

Material : BSPT66+Mn

Sample No	Poled		1Min		1Hr		10Hr		100Hr		200Hr		400Hr		700Hr		1000Hr	
	K	D	K	D	K	D	K	D	K	D	K	D	K	D	K	D	K	D
1	985	0.006	1032	0.012	1069	0.019	1022	0.015	1072	0.018	1065	0.018	1057	0.018	1078	0.016	1061	0.017
2	994	0.005	1041	0.010	1069	0.016	1019	0.012	1075	0.016	1067	0.016	1057	0.016	1078	0.015	1061	0.015
3	1007	0.006	1051	0.011	1073	0.016	1020	0.011	1078	0.015	1067	0.015	1059	0.015	1080	0.015	1063	0.015
4	1011	0.006	1018	0.008	1006	0.008	998	0.009	1059	0.014	1051	0.014	1039	0.014	1058	0.014	1044	0.014
5	963	0.005	1005	0.011	1022	0.014	970	0.009	1027	0.014	1020	0.014	1010	0.014	1029	0.014	1013	0.014
6	1009	0.005	1042	0.008	1042	0.009	1031	0.011	1088	0.015	1081	0.015	1071	0.015	1091	0.014	1075	0.015
7	970	0.006	1016	0.011	1038	0.015	987	0.011	1042	0.015	1034	0.015	1023	0.015	1042	0.014	1026	0.014
8	981	0.006	1014	0.011	1027	0.014	969	0.008	1031	0.014	1025	0.015	1014	0.014	1033	0.014	1019	0.014
9	974	0.005	1004	0.011	1016	0.014	958	0.008	1021	0.014	1015	0.014	1003	0.014	1023	0.014	1006	0.014
10	988	0.006	1007	0.010	1001	0.010	1015	0.015	1062	0.018	1055	0.018	1049	0.018	1074	0.017	1056	0.018
11	964	0.005	1001	0.011	1013	0.014	964	0.009	1019	0.014	1013	0.014	1005	0.014	1023	0.014	1008	0.013
12	967	0.005	984	0.008	980	0.008	958	0.008	1016	0.014	1010	0.014	1000	0.014	1018	0.013	1005	0.013
13	984	0.006	1028	0.011	1053	0.015	998	0.010	1052	0.015	1046	0.015	1035	0.014	1055	0.014	1040	0.014
14	986	0.005	1035	0.011	1059	0.015	1008	0.011	1061	0.015	1054	0.015	1044	0.015	1064	0.014	1048	0.014
15	1015	0.005	1064	0.011	1084	0.015	1030	0.010	1086	0.014	1080	0.014	1069	0.014	1088	0.014	1073	0.014
16	963	0.005	996	0.011	1009	0.014	955	0.008	1012	0.014	1007	0.014	997	0.014	1014	0.013	1000	0.013
Avg	985	0.005	1021	0.010	1035	0.014	994	0.010	1050	0.015	1043	0.015	1033	0.015	1053	0.0144	1038.4	0.014
Ratio	1.00	1.00	1.04	1.91	1.05	2.48	1.01	1.90	1.07	2.75	1.06	2.78	1.05	2.76	1.07	2.65	0.62	0.58

Appendix - G

Details of piezoelectric constant d_{33} with the aging time at 250⁰C

Material : PZT (x- 0.48)

S.No	Poled	1 Min	1 Hr	10Hr	100Hr	200Hr	400Hr	700Hr	1000Hr
1	208	195	189	186	176	156	155	154	154
2	226	202	198	192	183	159	159	159	158
3	218	191	188	177	158	152	154	154	153
4	216	190	187	184	168	161	161	155	156
5	236	232	232	209	196	191	187	180	178
6	221	212	209	205	190	185	182	172	169
7	220	213	211	195	186	181	176	169	167
8	228	222	216	201	177	173	171	168	166
9	220	210	207	197	172	164	162	162	162
10	193	183	183	177	166	158	157	158	158
11	223	192	168	166	158	154	147	149	149
12	193	187	182	175	159	155	153	154	155
13	199	185	178	174	159	156	155	158	156
14	210	183	179	170	157	152	150	147	146
Avg	215	200	195	186	172	164	162	160	159
Ratio	1.00	0.93	0.91	0.87	0.80	0.76	0.75	0.74	0.74

Material : PZT (x- 0.48) + Fe

S.No	Poled	1 Min	1 Hr	10Hr	100Hr	200Hr	400Hr	700Hr	1000Hr
1	179	144	143	128	133	133	134	134	134
2	172	135	131	122	134	134	131	129	127
3	162	132	126	115	125	126	124	122	123
4	172	129	126	118	124	125	125	125	126
5	180	145	141	131	136	136	137	135	135
6	175	146	140	135	140	140	141	137	135
7	172	144	138	132	137	138	136	137	138
8	164	135	128	119	127	128	127	128	125
9	171	139	135	126	131	134	134	132	133
10	176	147	145	131	138	137	139	139	136
11	198	168	165	152	158	158	158	157	158
12	188	158	153	144	144	147	144	144	145
13	180	142	138	133	138	141	141	137	137
14	166	137	132	123	135	135	136	137	138
15	207	170	163	148	156	157	158	160	159
Avg	177	145	140	130	137	138	138	137	137
Ratio	1.00	0.82	0.79	0.74	0.77	0.78	0.78	0.77	0.77

Continued...

Material : BSPT64

S.No	Poled	1 Min	1 Hr	10Hr	100Hr	200Hr	400Hr	700Hr	1000Hr
1	358	321	311	300	284	277	281	281	281
2	427	398	389	379	364	360	353	351	341
3	369	345	336	330	305	298	292	292	291
4	376	343	331	323	298	296	293	292	290
5	388	371	363	356	351	348	346	347	347
6	389	364	356	353	345	341	342	341	340
7	349	308	398	296	284	282	281	280	281
8	390	355	342	340	332	334	337	338	339
9	354	327	313	307	297	294	292	289	290
10	382	365	358	351	342	337	341	341	347
11	387	370	363	355	349	346	351	352	353
12	380	361	359	354	346	338	337	337	338
13	387	362	355	354	347	349	347	348	350
14	390	371	357	355	351	346	347	346	346
15	405	373	367	363	354	352	352	348	350
Avg	382	356	353	341	330	327	326	326	326
Ratio	1.00	0.93	0.92	0.89	0.86	0.85	0.85	0.85	0.85

Material : BSPT64+Mn

S.No	Poled	1 Min	1 Hr	10Hr	100Hr	200Hr	400Hr	700Hr	1000Hr
1	235	232	213	205	201	200	198	196	193
2	228	224	207	198	193	190	189	187	185
3	256	250	246	239	235	227	226	229	226
4	256	244	231	231	222	217	215	212	214
5	245	244	221	219	212	209	205	199	201
6	249	245	214	211	207	207	204	198	195
7	235	232	211	206	199	197	195	192	189
8	236	226	203	201	194	192	189	186	185
9	210	206	186	175	169	164	161	157	156
10	246	242	214	213	205	206	209	199	199
11	237	218	198	189	186	178	178	180	181
12	218	210	194	188	182	178	175	175	172
13	231	226	204	201	189	186	185	185	182
14	225	219	198	194	185	182	177	177	178
15	207	199	176	170	170	165	162	158	157
Avg	234	228	208	203	197	193	191	189	188
Ratio	1.00	0.97	0.89	0.87	0.84	0.83	0.82	0.81	0.80

Continued...

Material : BSPT66

S.No	Poled	1 Min	1 Hr	10Hr	100Hr	200Hr	400Hr	700Hr	1000Hr
1	242	233	229	228	219	215	217	217	215
2	237	228	218	217	210	207	211	209	208
3	258	253	248	248	245	242	240	241	241
4	254	243	240	240	235	233	233	231	229
5	263	248	246	245	242	243	244	243	245
6	265	248	247	246	242	238	241	244	243
7	252	243	239	242	237	237	238	234	235
8	243	228	227	226	224	217	219	215	217
9	236	219	215	215	212	211	211	209	210
10	235	226	219	217	215	216	215	216	215
11	264	257	249	249	245	245	245	244	244
12	243	229	227	225	224	221	220	219	217
13	283	279	278	278	273	277	278	273	272
14	283	274	274	274	270	269	270	270	271
15	282	276	274	274	270	269	271	271	272
16	256	241	237	244	239	237	238	237	235
Avg	256	245	242	242	238	236	237	236	236
Ratio	1.00	0.96	0.94	0.94	0.93	0.92	0.93	0.92	0.92

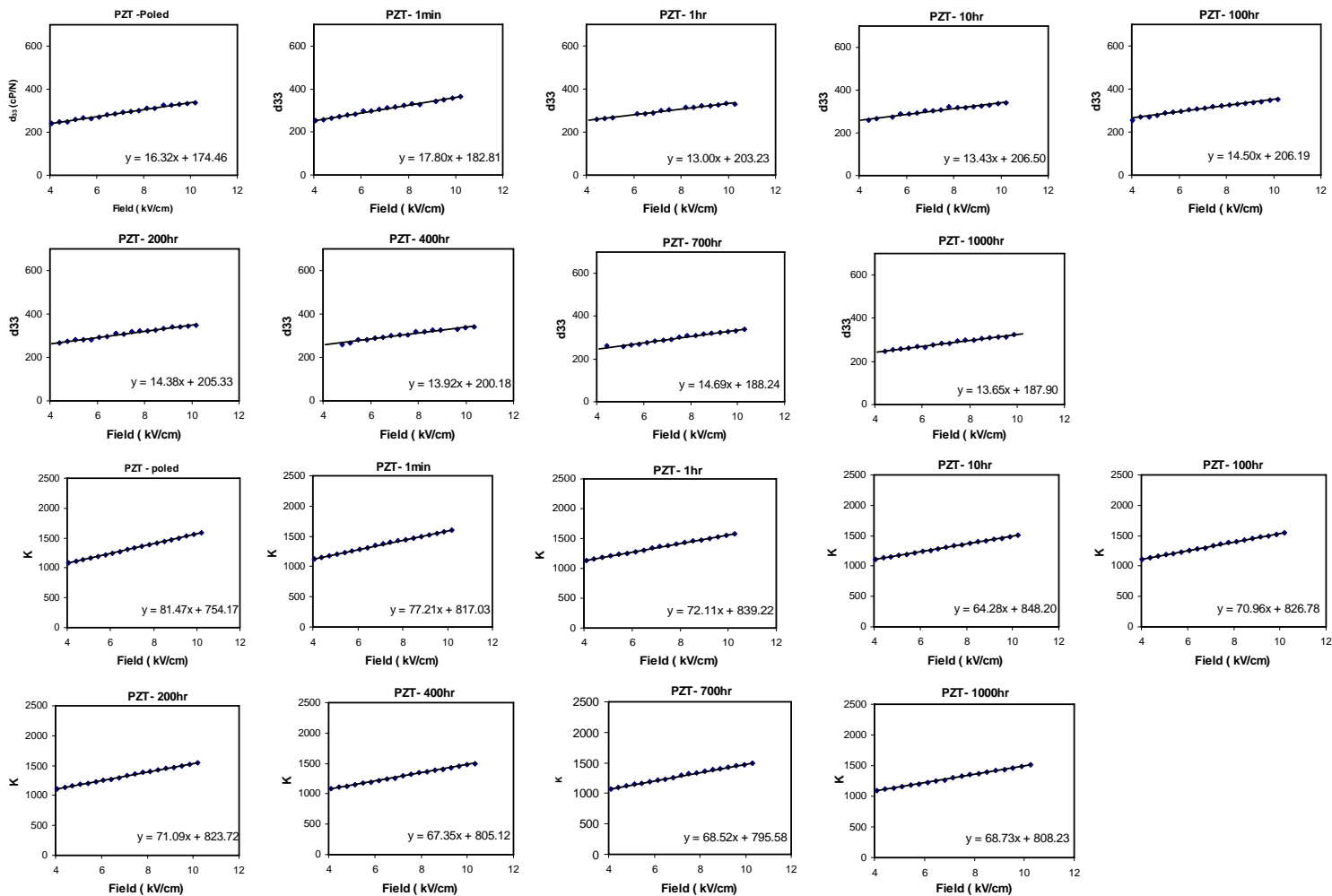
Material : BSPT66 + Mn

S.No	Poled	1 Min	1 Hr	10Hr	100Hr	200Hr	400Hr	700Hr	1000Hr
1	107	93	79	75	74	74	74	74	73
2	106	86	71	68	66	64	63	64	64
3	106	84	70	66	65	64	64	64	64
4	111	88	69	65	65	66	65	64	64
5	104	79	65	63	63	63	61	59	59
6	106	83	71	65	64	63	62	63	62
7	103	77	65	62	60	59	60	59	58
8	105	78	71	67	67	69	69	68	69
9	112	86	76	72	72	71	69	69	66
10	117	86	74	77	77	74	82	83	80
11	118	89	79	78	76	74	74	74	72
12	117	87	77	77	76	74	75	75	74
13	105	82	70	69	69	67	65	66	64
14	104	82	69	68	66	64	64	63	62
15	103	80	69	66	65	64	63	62	62
16	114	82	72	72	71	71	69	68	66
Avg	109	84	72	69	69	68	67	67	66
Ratio	1.00	0.77	0.66	0.64	0.63	0.62	0.62	0.62	0.61

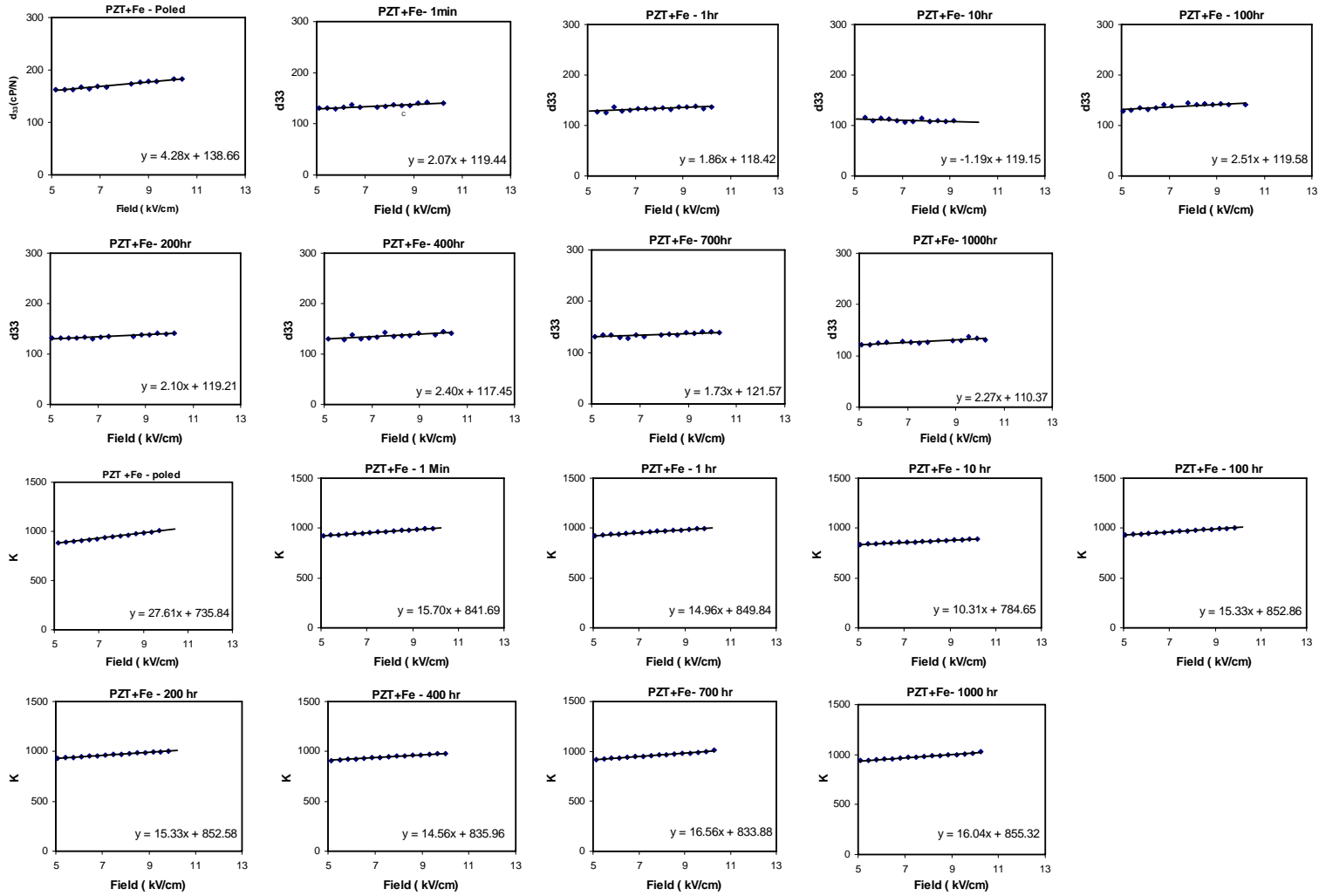
Appendix - H

Rayleigh analysis for piezoelectric and dielectric response during aging

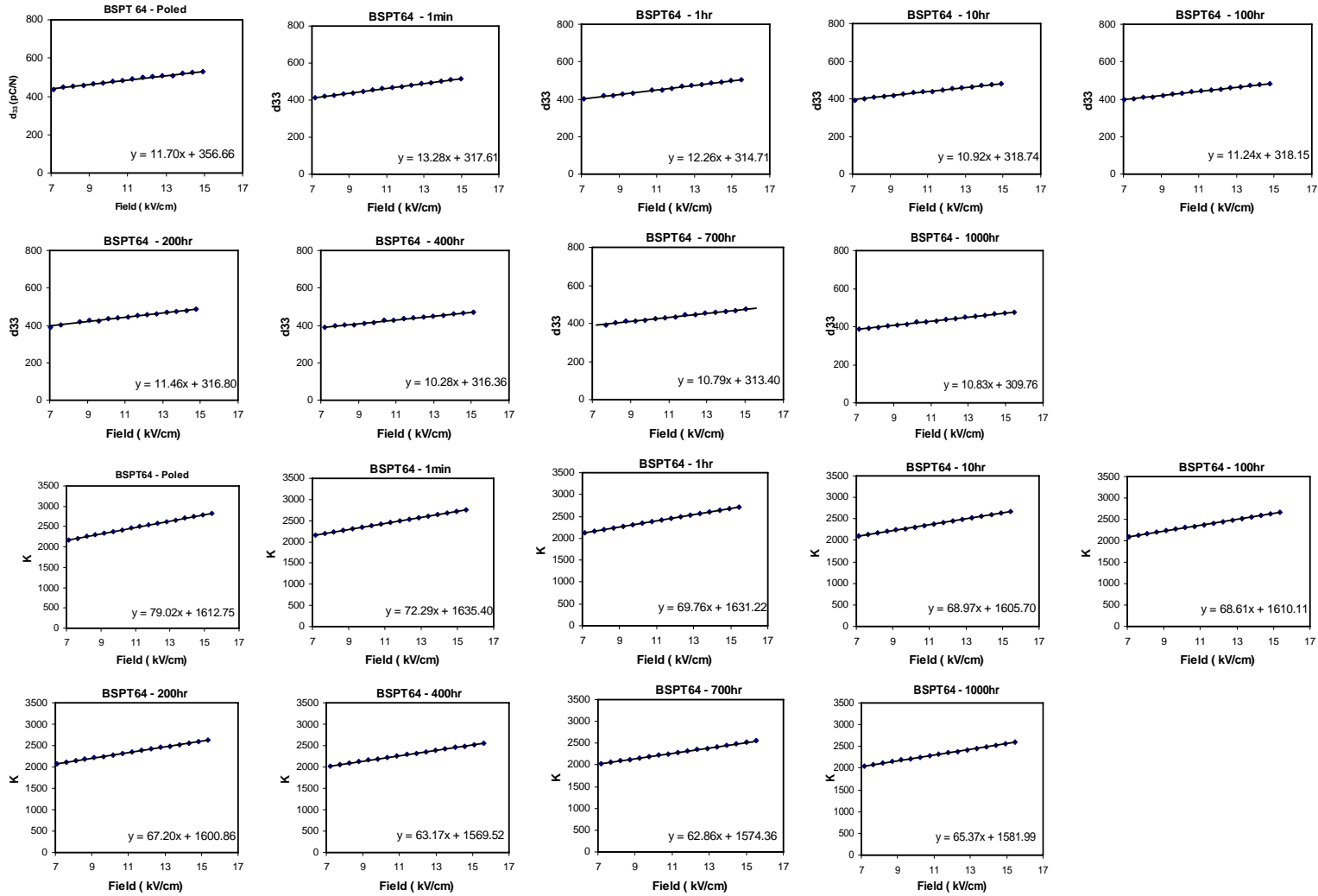
Material: PZT ($x=0.48$)



Material: PZT (x=0.48) + Fe

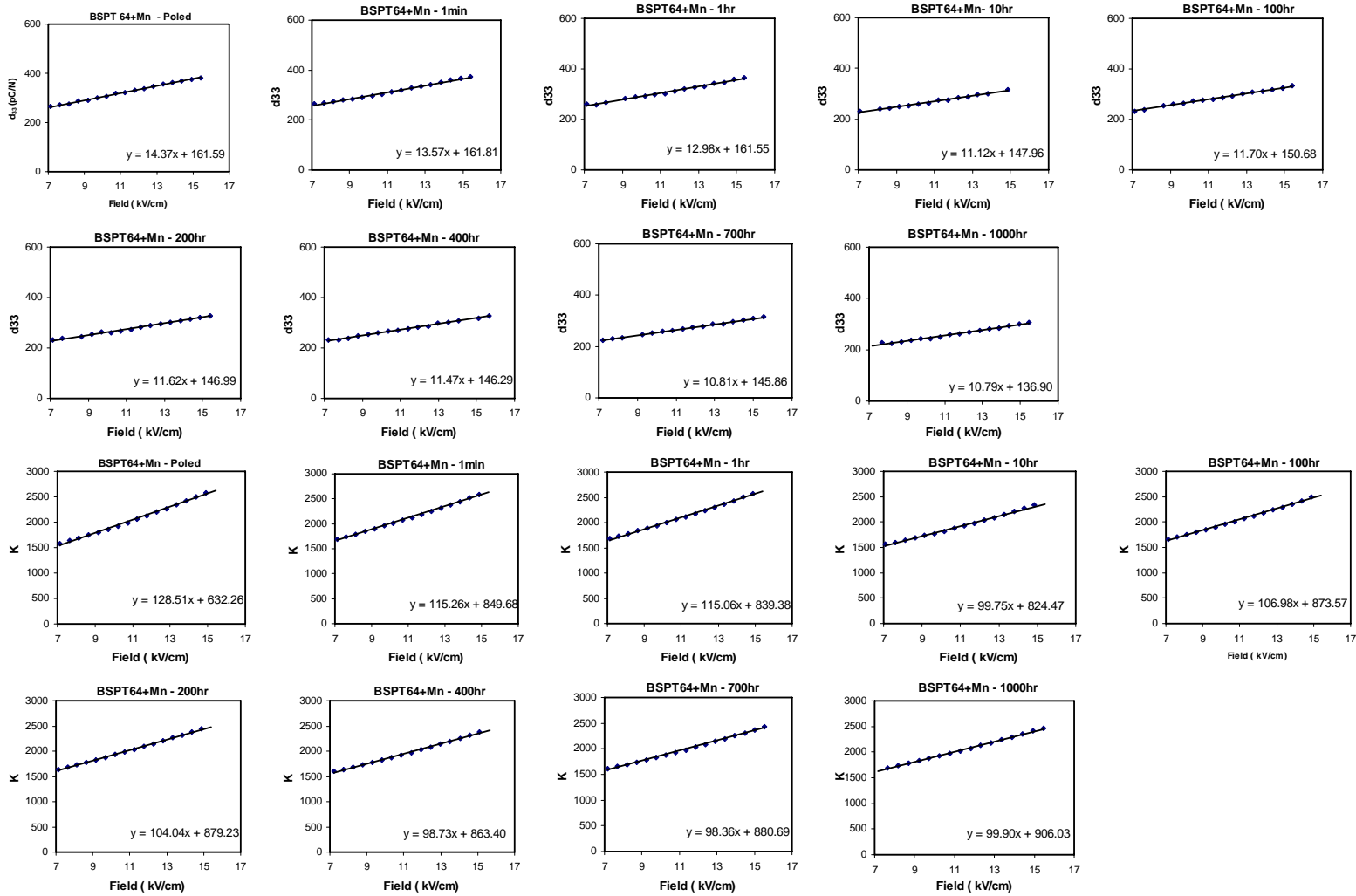


Material: BSPT (x=0.64)



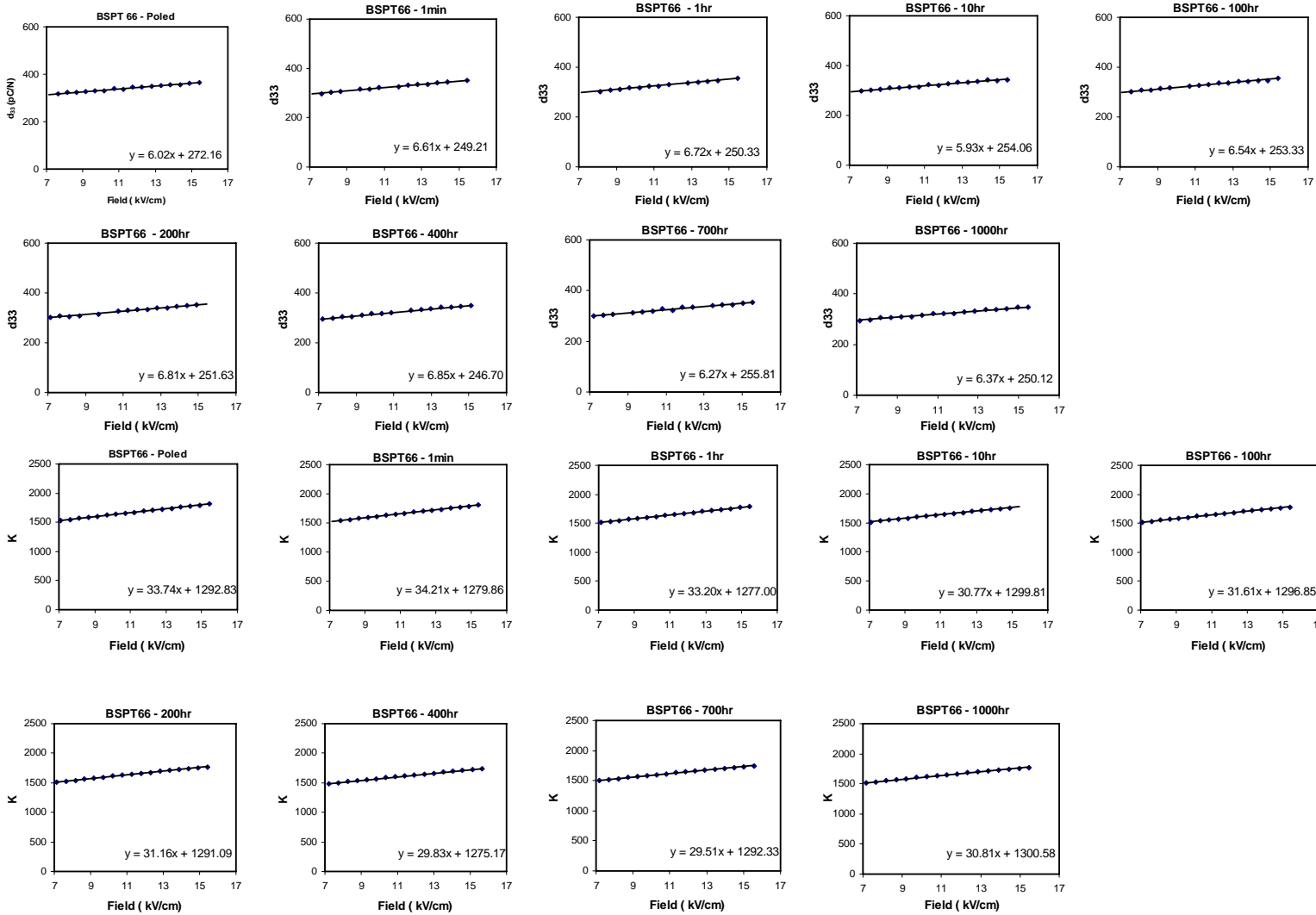
Material: BSPT (x=0.64) + Mn

86



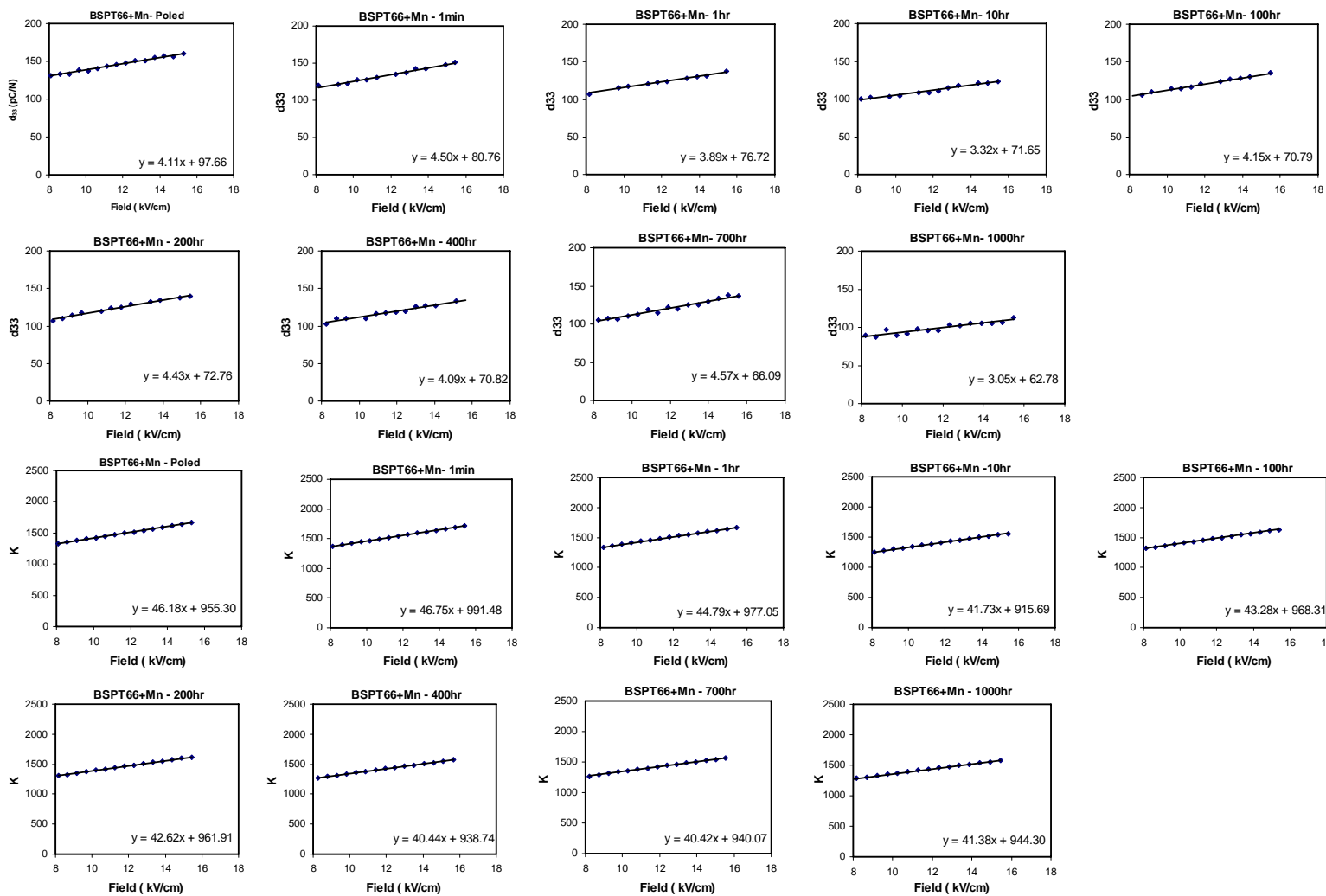
Material: BSPT (x=0.66)

66



Material: BSPT (x=0.66) + Mn

001



References :

1. A. Barzegar, R. Bagheri, and A. K. Taheri, "Aging of piezoelectric composite transducers," *Journal of Applied Physics*, **89**, (2001)
2. B. Guiffard, E. Boucher, L. Lebrun, and D. Guyomar, Characteristics of F doped PZT ceramics using different fluorine sources," *Material Science and Engineering*, **137**, (2007)
3. B. Jaffe, W. R. Cook, and H. Jaffe, *Piezoelectric ceramics* (Academic Press, New York, 1971)
4. B. Jaffe, R. S. Roth, and Marzullo, "Piezoelectric properties of lead zirconate – lead titanate solid-solution ceramics," *Journal of Applied Physics*, **25**, (1954)
5. B. Jaffe, and D. A. Berlincourt, "Piezoelectric transducer materials," *Proceeding of the IEEE*, **53**, (1965)
6. B. Noheda, "Structure and high piezoelectricity in lead oxide solutions," *Current Opinion in Solid State and Materials*, **6**, (2002)
7. B. Noheda, and J. A. Gonzalo, "Tetragonal-to-monoclinic phase transition in ferroelectric perovskite : The structure of $\text{PbZr}_{0.52}\text{Ti}_{0.48}\text{O}_3$," *Physical Review*, **61**, (2000)
8. B. S. Li, G. Li, Z. Xu, Q. Yin, and A. Ding, "Relaxation process of defect dipoles in ferroelectric ceramics," *Integrated Ferroelectric*, **71**, (2005)
9. C. A. Randall, N. Kim, J.P. Kucera, W, Cao, and T. R. Shrout, "Intrinsic and extrinsic size effect in fine grained morphotropic phase boundary lead zirconate titanate ceramics," *Journal of American ceramic society*, **81**, (1998)
10. C. B. Carter, and M. G. Norton, *Ceramic material science and engineering*, (Springer New York 2007)
11. C. Sawyer, and C. Tower, "Rochelle salt as a dielectric," *Physical Review*, **35**, (1930)
12. D. A. Hall, " Review: Non linearity in piezoelectric ceramics," *Journal of Material Science*, **36**, (2001)
13. D. Berlincourt, "Piezoelectric ceramic compositional development," *Journal Acoustic Society of America*, **91**, (1992)
14. D. Berlincourt, and H. Krueger, "Domain Processes in lead titanate zirconate and barium titanate ceramics ," *Journal of Applied Physics*, **30**, (1959)
15. D. Damjanovic, "Ferroelectric, dielectric and piezoelectric properties of ferroelectric thin films and ceramics," *Prog Phys*, **61**, (1998)
16. D. Damjanovic, and M. Demartin, "The Rayleigh law in piezoelectric ceramics," *Journal of Physics*, **29**, (1996)
17. D. Damjanovic, and M. Demartin, "Contribution of the irreversible displacement of domain walls to the piezoelectric effect in barium titanate and lead zirconate titanate ceramics," *Journal of Physics: Condens. Matter*, **9**, (1997)
18. D. Damjanovic, "Stress and frequency dependence of the direct piezoelectric effect in ferroelectric ceramics," *Journal of Applied Physics*, **82**, (1994)
19. D. Wang, Y. Fotinich, and P. Carman, "Influence of temperature on the electromechanical and fatigue behavior of piezoelectric ceramics," *Journal of Applied Physics*, **83**, (1998)

20. G. H. Haertling, "Ferroelectric ceramics: History and technology," *Journal of American Ceramic Society*, **82**, (1992)
21. G.H.L. Wong, B.W. Chua, L. Li, and M.O. Lai, "Processing of thermally stable doped perovskite PZT ceramics," *Journal of Materials Processing Technology*, **113**, (2001)
22. F. Jona, and G. Shirane, *Ferroelectric crystals* (Dover Publications, Inc., New York, 1993)
23. J. E. Garcia, R. Perez, D. A. Ochoa, A. Albareda, M. H. Lente, and J. A. Eiras, "Evaluation of domain wall motion in lead zirconate titanate ceramics by nonlinear response measurements," *Journal of Applied Physics*, **103**, (2008)
24. J. F. Shepard Jr., "Characterization and aging response of the d31 piezoelectric coefficient of lead zirconate titanate thin films," *Journal of Applied Physics*, **85**, (1999)
25. J. Koh, S. Jeong, M. Ha, J. Song, "Aging of piezoelectric properties in Pb(MgNb)O₃-Pb(ZrTi)O₃ multilayer ceramic actuators," *Journal of Applied Physics*, **96**, (2004)
26. J. S. Reed, *Introduction to the principle of ceramic processing*, (John Wiley & Sons, New York 1998)
27. K. Uchino, and S. Hirose, "Loss mechanisms in piezoelectrics : How to measure different losses separately," *IEEE Transactions on Ultrasonics, Ferroelectrics and Frequency Control*, **48**, (2001)
28. M. A. Meyers, and K. K. Chawla, *Mechanical behavior of materials*, (Prentice Hall, New Jersey 1999).
29. M. K. Zhu, P. X. Lu, Y. D. Hou, H. Wang, and H. Yan, "Effect of Fe₂O₃ addition on microstructure and piezoelectric properties of 0.2PZN-0.8PZT ceramics," *Journal of Material Research Society*, **20**, (2005).
30. M. N. Rahaman, *Ceramic processing and sintering*, (CRC Taylor & Francis, Boca Raton, 2003)
31. N. J. Donnelly, T. R. Shrout, and C. A. Randall, "Addition of a Sr, K, Nb (SKN) combination to PZT(53/47) for high strain applications," *Journal of American ceramic society*, **90**, (2007)
32. N. Izyumskaya, Y. I. Alivov, S. J. Cho, H. Morkoc, H. Lee, and Y. S. Kang, "Processing, structure, properties and applications of PZT thin films," *Critical Reviews in Solid State and Materials Science*, **32**, (2007)
33. Pizoceram, <http://www.piezoceram.com/tmatprop.htm>
34. PI Ceramic, http://www.piceramic.com/site/piezo_002.html
35. P. M. Chaplya, and G. P. Carman, "Dielectric and piezoelectric response of lead zirconate – lead titanate at high electric and mechanical load in terms of non-1800 domain wall motion," *Journal of Applied Physics*, **90**, (2001)
36. P. Winotai, N. Udomkanb, S. Meejoo, "Piezoelectric properties of Fe₂O₃-doped (1-x)BiScO₃-xPbTiO₃ ceramics," *Sensors and Actuators*, **122**, (2005)
37. Q. A. Jiang, E. C. Subbarao, and L. E. Cross, "Effect of composition and temperature on electric fatigue of La-doped lead zirconate titanate ceramics," *Journal of Applied Physics*, **75**, (1994)

38. Q. M. Zhang, "Electromechanical properties of lead zirconate titanate piezoceramics under the influence of mechanical stresses," *IEEE Transactions on Ultrasonics, Ferroelectrics, and Frequency control*, **46**, (1999)
39. Q. M. Zhang, J. Zhao. And L. E. Cross, "Aging of the dielectric and piezoelectric properties of relaxor ferroelectric lead magnesium niobate – lead titanate in the electric field biased state," *Journal of Applied Physics* , **79**, (1996)
40. R.E. Eitel, C. A. Randall, T.R. Shrout, and P. W. Rehrig, "New high temperature morphotropic phase boundary piezoelectrics based on Bi(Me)O₃- PbTiO₃ ceramics," *Japanese Journal of Applied Physics*, **401**, (2001)
41. R. E. Eitel, C. A. Randall, T.R. Shrout, and S. E. Park, "Preparation and characterization of high temperature perovskite ferroelectrics in the solid solution (1-X)BiScO₃-(X)PbTiO₃," *Japanese Journal of Applied Physics*, **41**, (2002)
42. R.E. Eitel, S. J. Zhang, T.R. Shrout, and C. A. Randall, "Phase diagram of the perovskite system (1-x)BiScO₃- xPbTiO₃," *Journal of Applied Physics*, **96**, (2004)
43. R. Gerson, "Variation in ferroelectric characteristics of lead zirconate titanate ceramics due to minor chemical modifications," *Journal of Applied Physics*, **31**, (1960)
44. R. Perez, J. E. Garcia, and A. Albareda, "Relation between nonlinear dielectric behavior and alterations of domain structure in a piezoelectric ceramic," *Ferroelectrics*, **273**, (2002)
45. R. Torah, S.P. Beeby, and N.M. White, "An improved thick-film piezoelectric material by powder blending and enhanced processing parameters," *IEEE Transactions on Ultrasonics, Ferroelectrics, and Frequency Control*, **52**, (2005)
46. S. Chen, X. Dong, C. Mao, and F. Cao, "Thermal stability of (1-x) BiScO₃-xPbTiO₃ piezoelectric ceramics for high temperature sensor applications," *Journal of American Ceramic Society*, **89**, (2006)
47. S. F. Liu, S. E. Park, L.E. Cross, and T. R. Shrout, "Temperature dependence of electrostriction in rhombohedral Pb(Zn_{1/3}Nb_{2/3})O₃-PbTiO₃ single crystals," *Journal of Applied Physics* , **92**, (2002)
48. S. J. Zhang, R.E. Eitel, C. A. Randall, and T.R. Shrout, "Manganese-modified BiScO₃-PbTiO₃ piezoelectric ceramic for high temperature shear mode sensor," *Applied Physics Letters*, **96**, (2005)
49. S. Li, W. Cao, and L. E. Cross, "The extrinsic nature of nonlinear behavior in lead zirconate titanate ferroelectric ceramics," *Journal of Applied Physics*, **69**, (1991).
50. S. Zhang, C. A. Randall, and T.R. Shrout, "Dielectric and piezoelectric properties of BiScO₃-PbTiO₃ crystal with morphotropic phase boundary composition," *Japanese Journal of Applied Physics*, **43**, (2004)
51. S. Zhang, E. F. Alberta, R.E. Eitel, C. A. Randall, and T.R. Shrout, "Elastic, piezoelectric, and dielectric characterization of modified BiScO₃-PbTiO₃ ceramics," *IEEE Transactions on Ultrasonics, Ferroelectrics, and Frequency control*, **52**, (2005)
52. T. R. Shrout, and S. J. Zhang, "Lead free piezoelectric ceramics: Alternatives for PZT?," *Journal of Electroceramic*, **19**, (2007)
53. T. Yamamoto, "Ferroelectric properties of PbZrO₃-PbTiO₃ system," *Japanese Journal of Applied Physics*, **35**, (1996)

54. T. Zo, X. Wang, W. Zhao, and L. Li, "Preparation and properties of fine grain (1-x)BiScO₃-xPbTiO₃ ceramics by two step sintering," *Journal of American ceramic society*, **00**, (2007)
55. U. Robels, and G. Arlt, "Domain wall clamping in ferroelectrics by orientation of defects," *Journal of Applied Physics*, **73**, (1993)
56. W. A. Schulze, "Review of literature on aging of dielectrics," *Ferroelectrics*, **87**, (1988)
57. W. Pan, S. Sun, and P. Fuierer, "Effect of ferroelectric switching on the dielectric and ferroelectric properties in lead zirconate titanate ceramics and their modeling," *Journal of Applied Physics*, **74**, (1993)
58. W. Zhao, X. Wang, J. Hao, H. Wen and L. Li, "Preparation and characterization of nanocrystalline (1-x)BiScO₃-xPbTiO₃ powder," *Journal of American ceramic society*, **89**, (2006)
59. Y. Chen, D. Lan, Q. Chen, D. Xiao, X. Yue and J. Zhu, "Stability of the perovskite structure in BSPT based ferroelectric ceramics," *Key Engineering Materials*, **336-338** (2007)
60. Z. Surowiak, D. Bochenek, D. Czekaj, S. Gavriyachenko, and M. Kupriyanov, "Piezoceramic transducers with high thermal stability of the resonance frequency," *Ferroelectrics*, **273**, (2002)

Vita

Name : Sunil Wasudeo Gotmare

Date of birth : 02 July 1975

Place of birth : Nagpur, India

Educational institutions:

1. College of Engineering, Pune, India
Bachelors of Engineering – Metallurgy (1996)

Professional positions:

1. Senior Engineer (Quality) – M/s Choksi Tubes, Ahmedabad, India
2. Executive (S.C.M.) – M/s Dresser Rand, Ahmedabad, India
3. Surveyor (Quality) – M/s Bureau Veritas, Pune, India

Professional honors:

1. Certified Welding Inspector – American Welding Society
2. IRCA certified Lead Auditor in ISO 9001: 2000 QMS